

**SUB-RECORDER  
RECEIVED**  
FEB 20 1992  
M.R. # ..... \$.....  
VANCOUVER, B.C.

**REPORT ON THE DIAMOND DRILLING  
AND DOWNHOLE GEOPHYSICS ON THE  
MGM PROPERTY**

Golden Mining Division  
NTS 83 D/1 & 82M/16  
Lat: 52°02' Long: 118°14'

Owner: John Leask; White Knight Resources  
Suite 922 - 510 West Hastings St.,  
Vancouver, B.C.  
V6B 1L8

Operator: Teck Exploration Ltd.  
960 - 175 Second Avenue  
Kamloops, B.C.  
V2C 5W1

LOG NO:	FEB 26 1992	RD.
ACTION:		
FILE NO:		

**GEOLOGICAL BRANCH** Craig Alford  
**ASSESSMENT REPORT** Carol Lormand

22,149

## TABLE OF CONTENTS

	<b>Page</b>
Summary .....	i
Recommendations .....	i
1. Introduction .....	1
2. Location and Access .....	1
3. Physiography and Vegetation .....	1
4. Claim Status .....	2
5. Previous Work .....	3
6. 1991 Program .....	4
7. Geology .....	5
8. Drilling .....	7
9. Geophysics .....	11
10. Discussions .....	12
11. Conclusions .....	13
12. References .....	14
13. Appendices	
A) Statement of Qualifications	
B) Cost Statement	
C) Certificate of Analysis	
D) Analytical Procedures	
E) Drill Logs	
F) Geophysical Report	

## TABLES

	<b>Page</b>
Table 1	Claim Records ..... 2
Table 2	New Claims ..... 3
Table 3	Diamond Drill Hole Data ..... 7

## LIST OF FIGURES

Figure 1	Location Map ..... Following Page 1
Figure 2	Road Access Map (1:20,000) ..... Following Page 2 (N. Side of Cummins River)
Figure 3	Claim Map ..... Following Page 3
Figure 4	Drill Hole Location Map (1:5,000) ..... In Pocket
Figure 5	Drill Hole Section ..... In Pocket (TK-91-01)
Figure 6	Drill Hole Section ..... In Pocket (TK-91-02)
Figure 7	Drill Hole Section ..... In Pocket (TK-91-03)
Figure 8	Drill Hole Section ..... In Pocket (TK-91-04)
Figure 9	Zn/Pb Ratio Map (1:5,000) ..... In Pocket
Figure 10	Three Dimensional Drill Hole Plot ..... In Pocket

## SUMMARY

Results from the 1991 drilling program were encouraging.

A crudely strata-bound sulphide horizon was intersected in drill holes TK-91-1, TK-91-3 and TK-91-4.

Intersections of the sulphide horizon are generally of sub-economic width. Best intersections include:

	<i>grams</i>	
Hole TK-91-1	2.2m of 2.78 <del>oz</del> /t Ag, 0.18% Pb, 0.88% Zn from 269.0-272.0 metres	
	0.5m of 65.6 <del>oz</del> /t Ag, 4.22% Pb, 9.36% Zn from 272.0-272.5 metres	
Hole TK-91-3	0.4m of 34.6 <del>oz</del> /t Ag, 3.06% Pb, 4.44% Zn from 332.3-332.7 metres	
	1.3m of 9.27 <del>oz</del> /t Ag, 0.45% Pb, 2.01% Zn from 387.1-388.4 metres	
Hole TK-91-4	0.5m of 8.0 <del>oz</del> /t Ag, 0.76% Pb, 5.82% Zn from 441.3-441.8 metres	

No significant base metal sulphides were encountered in hole TK-91-2.

Drilling confirmed the presence of the sulphide horizon, similar to that observed within the canyon showing, from the Cummins River, south to Line 20+00S, a strike length of 3 kilometres.

The sulphide horizon initially exhibits characteristics of a large, mineralized basinal environment, with generally decreasing width and increasing Zn/Pb ratios toward grid south.

Broad, weakly conductive horizons were recognized by the downhole UTEM survey of holes TK-91-2 and TK-91-4. No indication of large, strong conductors was exhibited.

With a large prospective area yet to be tested, the potential for the discovery of a Pb-Zn-Ag deposit is considered good.

## RECOMMENDATIONS

Further drilling with an emphasis on areas of low Zn/Pb ratios.

Attempt to locate wide basinal sequences within the Tsar Creek Formation which may reflect sub basins or structural thickening.

A combined surface and borehole survey with different loop configurations (drill holes TK-91-1 and TK-91-2 could be filled with PVC pipe and surveyed).

Grid extension. Soil sampling of areas both north and south of Cummins River (Mn, Zn and Pb key elements).

## 1. INTRODUCTION

During June to September 1991, a program consisting of property mapping, lithochemistry, soil sampling and HLEM geophysics on the MGM and TSAR claim groups located a geological sequence similar to that which hosts the Cummins River massive sulphide occurrence (covered by the Cominco Bend claim group).

This report encompasses a four hole (1873.8m) diamond drill program and down hole geophysical surveys completed on the MGM and TSAR claim groups from October 7 to November 14, 1991. The drilling program was designed to assess the depth potential and *continuity of mineralization*. This report describes the program's results and presents an interpretation of the results.

## 2. LOCATION AND ACCESS

The property lies on the east side of the Rocky Mountain Trench approximately 100km northwest of Golden, B.C. (Figure 1), located both north and south of the confluence of Cummins River and Columbia Reach (Kinbasket Lake). The property is located on NTS map sheet 83D1 and 82M/16, bounded by latitude's 51°59' to the south and 52°05' to the north and longitude's 118°04' to the east and 118°17' to the west.

The property is not road accessible. Helicopter services out of Golden or Revelstoke or a float plane service from Golden are available. Large freight may be brought in by a barge service out of Bush Harbour, located 50km southeast of the claim area.

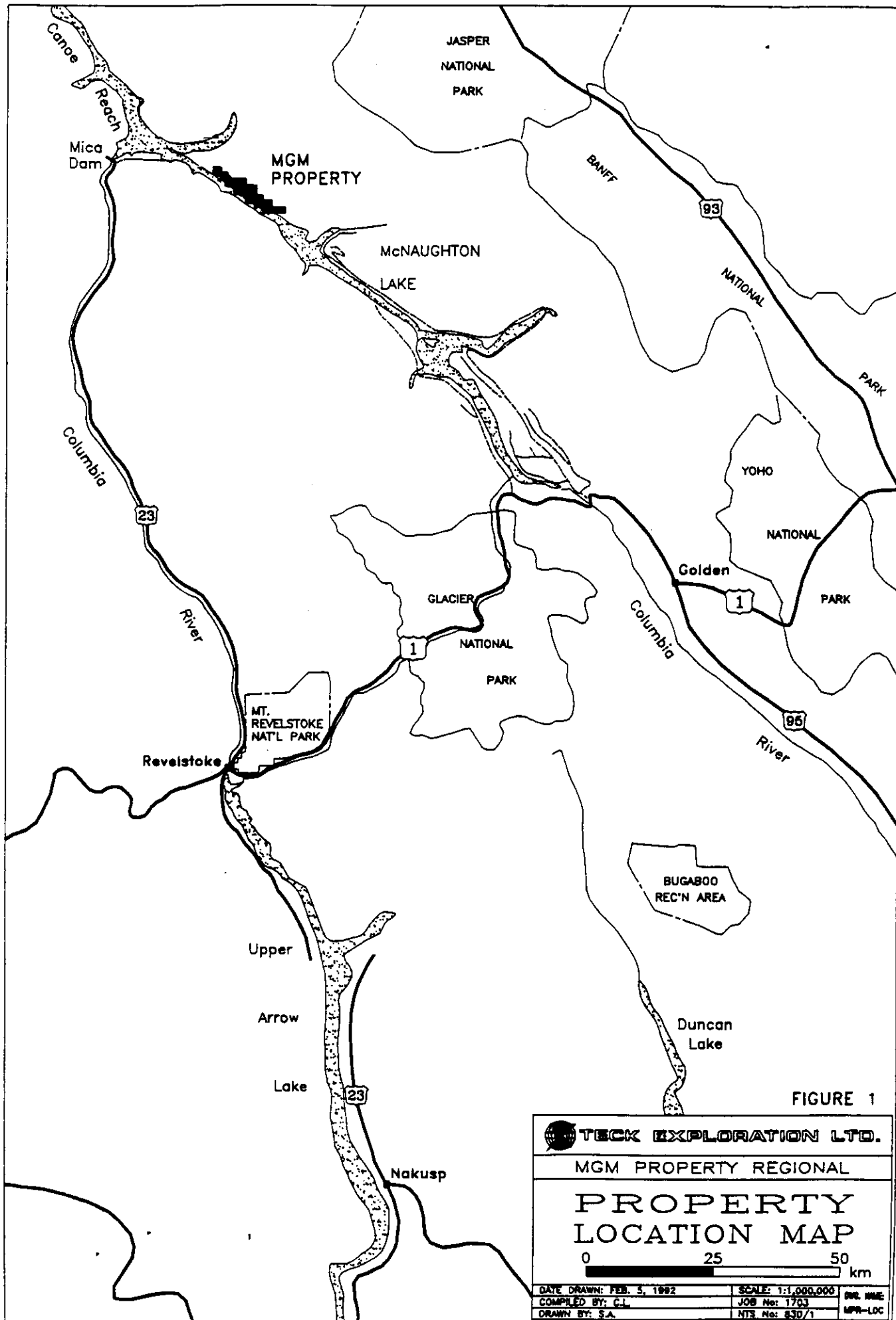
The property itself is well covered by recent clear cut logging areas and logging roads which are in good driveable condition. Several are present between Cummins River and Tsar creek. The portion of the property lying to the north of Cummins River is crossed by one main logging road and plans for new road to be constructed in 1992 are displayed on Figure 2.

## 3. PHYSIOGRAPHY AND VEGETATION

Elevations across the property range between lake level at approximately 762m, to the top of the property boundary at 1,800m. The entire property is below the treeline which is approximately at 1,970 metres. Slopes are moderate to steep.

The property lies within the Interior Wet Belt where precipitation can exceed 100 centimetres per year. Winters in the area are usually long and severe with snowfall often exceeding 9 metres. Water line of the Columbia Reach varies seasonally from approximately 730-765 metres ( $\approx$ 2400-2500 ft).

Vegetation consists of thick stands of cedar, douglas fir and hemlock at lower elevations giving way to lodgepole pine and balsam fir above 1370 metres. For the most part the property is covered by alluvial sediments ranging in thickness from 1 to 20 metres.



#### 4. CLAIM STATUS

The property is located in the Golden mining division. The following claims are registered in the name of Teck Corporation currently held in trust for White Knight Resources Ltd.

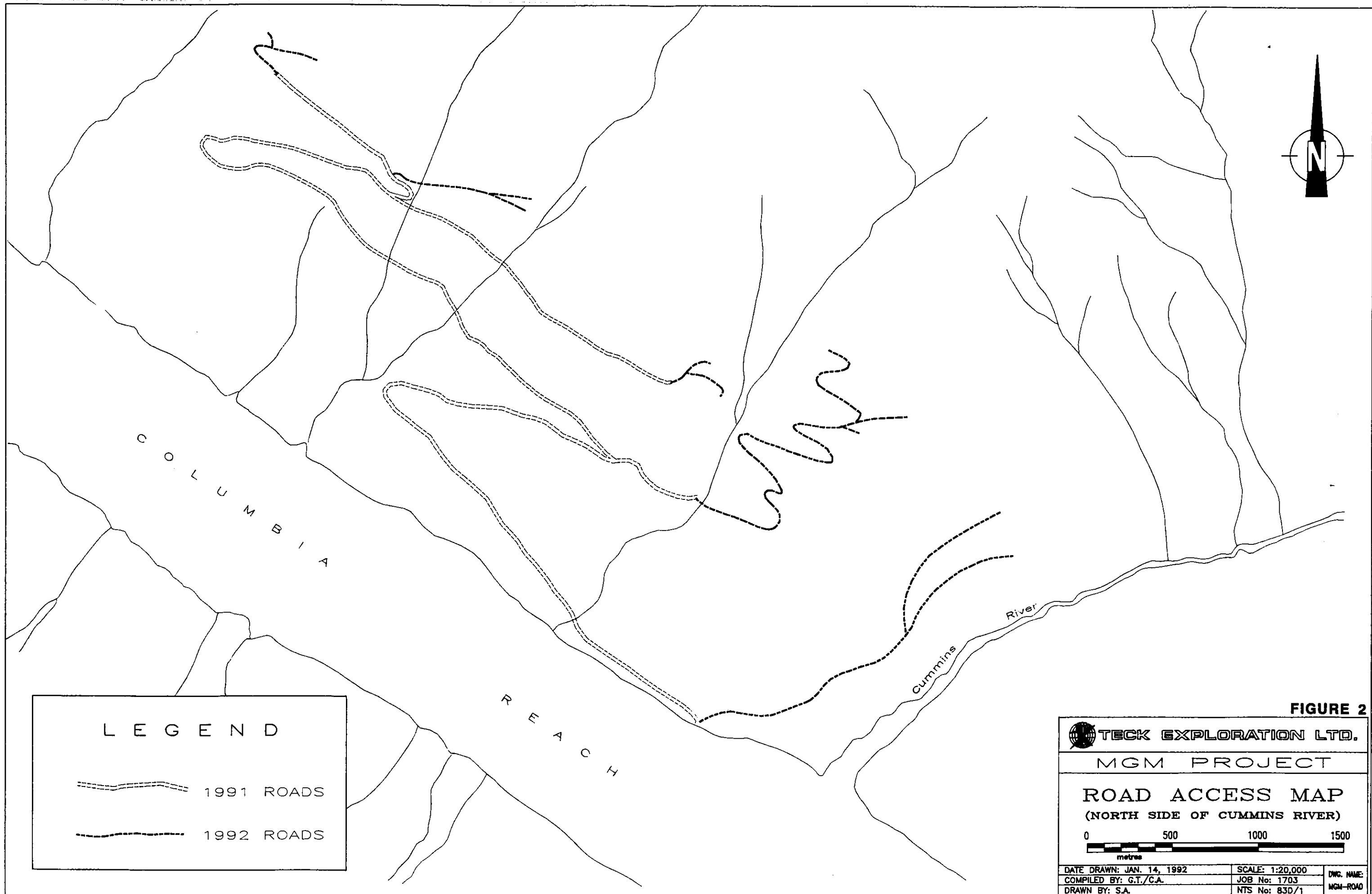
Table 1

#### CLAIM RECORDS

Claim Name	Record No.	Units	Record Date	Expiry Date
MGM	373	9	AUG/20/79	AUG/20/2000
MGM 2	422	2	SEPT/19/79	SEPT/19/2000
MGM 3	423	6	SEPT/19/79	SEPT/19/2000
MGM 4	1004	20	AUG/4/82	AUG/4/2000
MGM 5	1130	5	JAN/28/83	JAN/28/2000
MGM 8	2156	6	MAY/27/90	MAY/27/2000
TSAR 1	2323	16	FEB/17/91	FEB/17/2000
TSAR 2	2324	20	FEB/17/91	FEB/17/98
TSAR 3	2325	12	FEB/18/91	FEB/18/98
TSAR 4	2326	12	FEB/18/91	FEB/18/98
TSAR 5	2327	6	FEB/16/91	FEB/16/98
TSAR 6	2328	12	FEB/18/91	FEB/18/98
TSAR 7	2329	6	FEB/16/91	FEB/16/98
TSAR 8	2330	18	FEB/17/91	FEB/17/98
ARM	2331	1	FEB/17/91	FEB/17/98
<b>Total: 152 Units</b>				

The MGM, MGM 2-5, MGM 8 and TSAR 1 (totalling 65 units) are grouped as the MGM Group. The TSAR 2-8 and ARM claims (totalling 87 units) are grouped as the TSAR Group.

After the initial 1991 field exploration program was completed, 42 additional units, the TSAR 9-21 claims, were staked to cover the area of possible down dip extension of the sulphide horizon. The Tsar 9-21 units are 100% owned by Teck Corporation.



LEGEND

1991 ROADS

1992 ROADS

FIGURE 2

TECK EXPLORATION LTD.  
MGM PROJECT

ROAD ACCESS MAP  
(NORTH SIDE OF CUMMINS RIVER)



DATE DRAWN: JAN. 14, 1992	SCALE: 1:20,000	DWG. NAME:
COMPILED BY: G.T./C.A.	JOB No: 1703	MGM-ROAD
DRAWN BY: S.A.	NTS No: 830/1	



**Table 2**  
**NEW CLAIMS**

<b>Claim Name</b>	<b>Record No.</b>	<b>Units</b>	<b>Record Date</b>	<b>Expiry Date</b>
TSAR 9	306069	6	Nov/8/91	Nov/8/92
TSAR 10	306070	5	Nov/8/91	Nov/8/92
TSAR 11	306071	2	Nov/8/91	Nov/8/92
TSAR 12	306072	2	Nov/8/91	Nov/8/92
TSAR 13	306073	2	Nov/8/91	Nov/8/92
TSAR 14	306074	2	Nov/8/91	Nov/8/92
TSAR 15	306075	3	Nov/8/91	Nov/8/92
TSAR 16	306076	2	Nov/8/91	Nov/8/92
TSAR 17	306077	3	Nov/8/91	Nov/8/92
TSAR 18	306078	3	Nov/8/91	Nov/8/92
TSAR 19	306079	6	Nov/8/91	Nov/8/92
TSAR 20	306080	2	Nov/8/91	Nov/8/92
TSAR 21	306081	4	Nov/8/91	Nov/8/92
<b>Total: 42 Units</b>				
<b>Property Total: 194 Units</b>				

The current claim configuration for the property is shown on Figure 3.

## 5. PREVIOUS WORK

Refer to the Teck 1991 Report on the Geology, Geochemistry and Geophysics of the MGM Property for a full description of previous work in the property area.

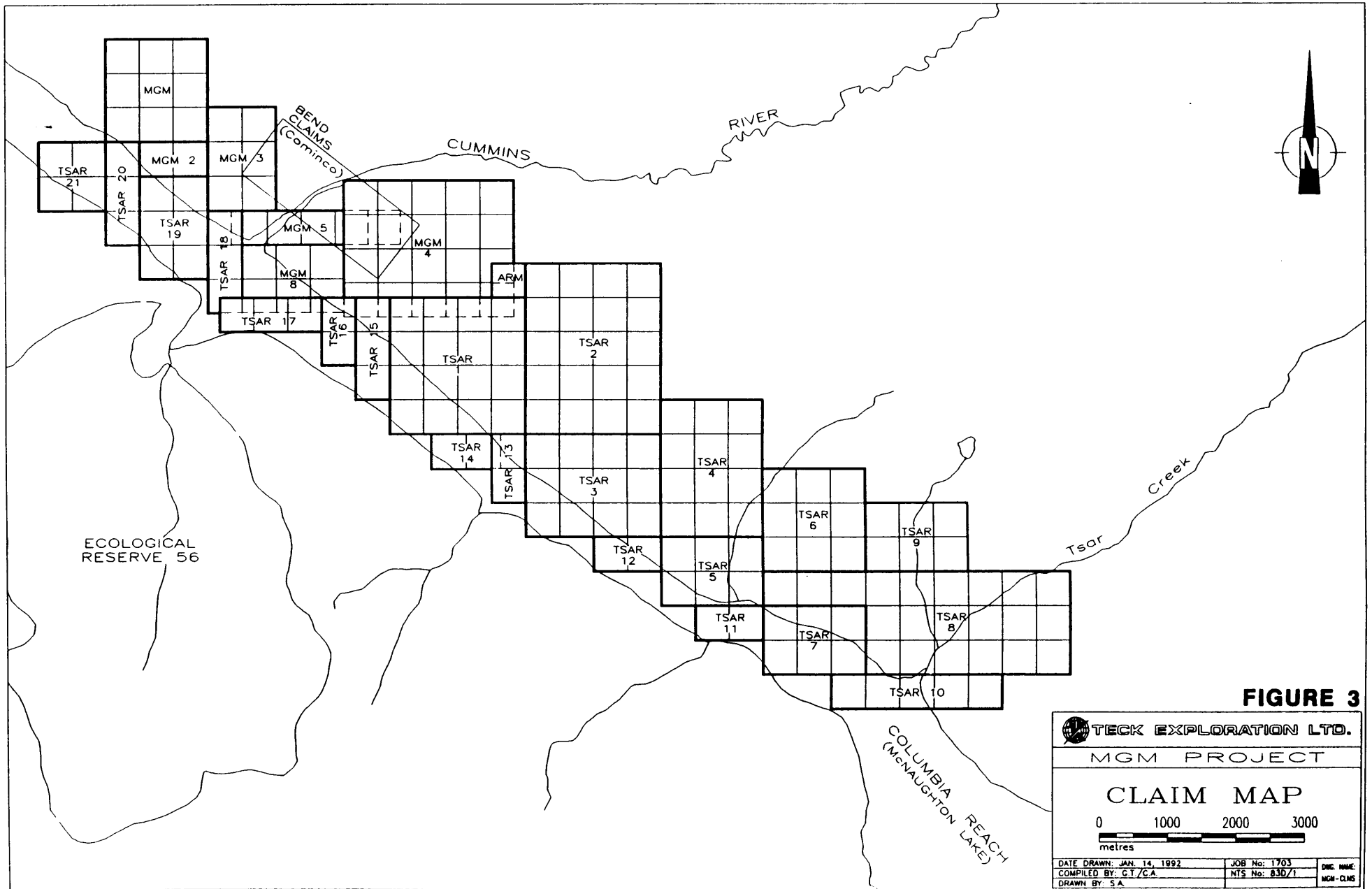


**FIGURE 3**

## 6. 1991 PROGRAM

From June 14 to August 25, 65 field days were spent on the MGM property. The program consisted of geologic mapping (at 1:10,000 and 1:5,000), rock sampling, stream silt sampling, soil sampling, trenching and a HLEM survey. In addition on-site drill core from previous workers was relogged.

The drill program, described in this report, was a continuation of Teck's 1991 exploration program.

Objectives of the drill program were:

- 1) To trace Cominco's Bend massive sulphide horizon southeast onto the MGM property.
- 2) To trace the down dip extension of the sulphide horizon off the southwest corner of the Bend claims.
- 3) To test a geophysical and soil geochemical target observed on Line 20+00S.

A total of 1873.8 metres were diamond drilled in four holes. Grid lines, extended by hip chain and slope corrected, were used to site the drill holes. Drill hole locations are shown on Figure 4.

Drill core samples were analyzed by Eco-Tech Labs of Kamloops, B.C.

A down hole UTEM (University of Toronto Electromagnetometer) survey was conducted between November 9-14 on two drill holes by Syd Visser of SJ Geophysics Ltd. Two insulated copper wire loop arrays were laid out for the survey.

Down hole surveys were attempted on TK-91-1, TK-91-2 and TK-91-4. Hole TK-91-3 was not attempted due to a broken and blocky section within the hole. Hole TK-91-1 proved unusable as the borehole instrument was impeded by excessive grease.

Down hole surveys were completed on TK-91-2 and TK-91-4.

## 7. GEOLOGY

Regionally, the property lies on the west limb of a major anticlinorium and is bounded to the west by the Purcell Thrust Fault.

The property is in an area of dominantly Lower to Mid Cambrian miogeosynclinal rocks represented by three main lithological elements: the Mid to Upper Cambrian Kinbasket Limestones and the Mid to Lower Cambrian Tsar Creek metapelites of the Chancellor Group and the Lower Cambrian Quartzites of the Gog Group. All lithologies have been metamorphosed to middle and upper greenschist assemblages.

### Gog Group

The Lower Cambrian Gog Group consists of three formations, from youngest to oldest: Mahto, Mural and McNaughton. For the purpose of this investigation Gog Group lithologies have not been subdivided according to formational boundaries.

*In the property area this sequence consists of milky to greyish white quartzite, light grey to pale pink micaceous quartzite, thinly laminated light grey to pink quartzofeldspathic (psammitic) schists, chert, interbedded biotite and garnet schists and a greyish white to light buff coloured marble.*

The Gog Group quartzites conformably overlie Upper Proterozoic Miette Group metasediments which were not observed in outcrop on the property. The overall thickness of the Gog Group is estimated to be slightly greater than 1,000 metres.

### Chancellor Group

The Tsar Creek and Kinbasket Formations of the Chancellor Group are documented as Middle Cambrian. Due to structural thickening, stratigraphic thicknesses are hard to establish. The upper Tsar Creek-lower Kinbasket contact is gradational and thus its placement is very much subjective.

### Tsar Creek Formation

The Tsar Creek Formation is dominantly a pelitic schist of variable metamorphic grade and argillaceous component. Lithological units recognized within this formation were muscovite and biotite schists, garnet-mica and garnet-staurolite-mica schists, greywacke turbidites, micaceous limestone and argillite.

Metamorphic grade throughout the property ranges from lower and upper greenschist facies to amphibolite or garnet-staurolite-kyanite grade. Muscovite, biotite and almandine garnet are common metamorphic minerals. Kyanite and sillimanite were observed in a few localities.

The Tsar Creek Formation hosts a crudely stratabound sulphide horizon of variable width bounded by distinct hanging and foot wall lithologies. The sulphide mineralogy is simple with pyrite, sphalerite and galena predominating. Lithologies associated with the mineralization are quartz sericite schists, manganiferous dolomites, argillaceous garnet schists and micaceous quartzites. Such lithologies may relate to metamorphosed cherts, carbonates and argillites deposited within a cratonic margin basin.

### **Kinbasket Formation**

The Kinbasket Formation is dominated by pale grey to grey, thinly laminated, sandy to silty limestones with interlaminated pelitic sediments. Interstratified beds of pelitic sediments from 2-30m in thickness occur within the limestones. Thinly bedded, grey micritic limestones with thin graphitic laminae are also recognized within the formation.

The limestones have been metamorphosed to impure marbles and pelitic material within the limestones have formed micaceous and garnetiferous horizons. Similarly, the interstratified pelitic layers have been metamorphosed to mica schists and garnet mica schists. Under the local metamorphic grade the Kinbasket Limestones generally appear as a rusty to buff weathered, biotitic and locally garnet bearing grey unit.

Lithologies of the Kinbasket and Tsar Creek Formations generally strike northwest-southeast and dip  $50^{\circ}$ - $60^{\circ}$  southwest in the area between Cummins River and Tsar Creek. A thrust fault bounded sequence of similar lithologies occurs mainly in the area north of the Cummins River, with a portion occurring south of the Cummins toward Columbia Reach.

The dominant structures within the Kinbasket and Tsar Creek rocks are the second phase ( $F_2$ ) tight to isoclinal asymmetric step-like folds with an associated axial planar cleavage ( $S_2$ ) near parallel with the average long limb orientation.

## 8. DIAMOND DRILLING

Four diamond drill holes were cored for a total of 1873.8 metres. Drilling was carried out between October 5th and November 13th 1991 by Falcon Drilling Ltd. of Prince George, B.C. Selected portions of the NQ (1 7/8") core were split and sent to Eco-Tech Labs in Kamloops for analysis. A total of 39 samples were collected and analyzed; all for 30 element by ICP; 26 were assayed for Ag, Pb and Zn, 28 for Ba; 3 assayed for Au and a total of 3 for whole rock analysis. Best sample intervals are located on the drill sections (Figures 5-8), and complete results are listed on the certificates of analyses in Appendix C.

Drill hole locations are plotted on Figure 4 and Table 3 summarizes all pertinent drill data. Core is currently being stored on the property. Core recovery averaged 90%-100%.

**TABLE 3**

**Diamond Drill Hole Data**

Hole No.	Grid Location	Elevation	Azimuth	Dip	Length	No. of Samples
TK-91-1	5+00S, 3+05W	1039.4 m	035°	-70°	319.1 m	15
TK-91-2	1+00N, 5+90W	950.9 m	---	-90°	572.0 m	7
TK-91-3	10+00S, 5+95W	947.9 m	035°	-70°	462.4 m	16
TK-91-4	18+75S, 7+06W	911.3 m	035°	-70°	520.3 m	1
<b>Total</b>					1873.8 m	39

The target stratigraphy, the Kinbasket and Tsar Creek Formations were intersected within all drill holes.

Where the mineralized dolomite horizon occurred, a hanging wall sequence of calcareous garnet schists, quartz-sericite schists and cherts and a foot wall sequence of argillaceous garnet schists and micaceous quartzites was observed.

Numerous minor folds were observed within all horizons.

Complete drill logs are included in Appendix E. A brief description of each drill hole with best mineralized intersections follows.

**1) Hole TK-91-1 (Figure 5)**

**Objective:** To test the strike extension of Cominco's Bend sulphide horizon onto the MGM ground.

**Result:** 0-18.3m; Overburden.

18.3m-224.8m; Fine grained, grey to dark grey, occasionally garnet bearing, micaceous limestone with locally numerous quartz (minor carb) bands.

224.8m-236.1m; Fine grained, light grey to grey, weakly calcareous garnet schist with minor cordierite and staurolite. This unit grades into a cordierite-muscovite schist with elliptical cordierite (see Appendix F for thin section description) from 233.4-236.1m.

236.1m-267.7m; A sequence of grey cherts and quartz-sericite schist often with minor interbeds of pelitic schists. Thinly laminated pyrite and sphalerite occur locally.

267.7m-275.3; Fine to medium grained, light grey manganese dolomite. Thinly laminated to massive sulphides.

275.3m-285.5m; Fine grained, banded, grey to black argillaceous garnet schist.

285.5m-287.7m; Grey chert.

287.7m-E.O.H.; Garnet-staurolite schist with interbedded muddy chert horizons.

**Best results include:**

Sample No.	From	To	Length(m)	Ag	Pb%	Zn%
114202	246.2	246.7	0.5	0.5	8.6	0.76
114208	269.8	270.0	0.2	5.2	0.39	1.12
114209	270.0	271.1	1.1	2.5	0.19	0.98
114210	271.1	272.0	0.9	2.6	0.13	0.71
114211	272.0	272.5	0.5	65.6	4.22	9.36

**2) Hole TK-91-2 (Figure 6)**

**Objective:** To test the down dip expression of the Bend sulphide horizon, drilled vertical to remain off of the Cominco's Bend claim Group.

**Result:** 0-6.1m; Overburden.

6.1m-295.1m; A sequence of cherts and argillaceous schists grading to quartzofeldspathic schists, garnet schists and garnet-staurolite schists. This sequence is bounded by a thrust fault to the sequence below.

295.1m-435.8m; Fine grained, grey, micaceous limestone with interbedded and intercalated mica schist and garnet-mica schists.

435.8m-484.8m; Fine grained, grey to grey-brown, garnet-mica schist with intercalated limestone. Garnets often are of large size (0.5cm-3.0cm in diameter).

484.8m-485.6m; Quartz-sericite schist.

485.6m-523.8m; Light grey to white marble. Thin bands of pyrite occur locally.

523.8m-561.3m; Interlayered quartz-sericite schists, chert and garnet schists.

Repetitions of units is probably due to folding.

561.3-E.O.H.; Garnet-staurolite schist.

Hole TK-91-2 continued.

Best results include:

Thin laminations of pyrite and pyrrhotite were observed within cherts and quartz-sericite schist of the Tsar Creek Formation, however, no significant base metals were observed within the hole. The massive sulphide horizon likely tapered out prior to the targeted depth.

### 3) Hole TK-91-3 (Figure 7)

Objective: To test the strike and down-dip extension of the sulphide horizon observed in Hole TK-91-1.

Result: 0-6.0m; Overburden.

6.0m-23.5m; Grey to black banded graphitic limestone.

23.5m-174.7m; A sequence of grey, fine grained, micaceous limestones. Rubbly, broken rock occurs from 38.0m-122.4m.

174.7m-290.9m; Fine grained, grey limestones with interbedded and intercalated fine grained, light grey, garnet mica schists.

290.9m-293.3m; Grey to black banded graphitic limestone.

293.3m-294.7m; Fine grained dark grey cordierite schist with  $\approx 3\%$  pyrrhotite.

294.7m-441.7m; Folded sequence of mica schists, quartz-sericite schists, cherts, weakly brecciated dolomite, siliceous pelitic schists and argillaceous garnet schists (See enlarged portion of drill hole section, Figure 7).

441.7m-448.3m; Grey opalescent chert.

448.3m-E.O.H.; Fine grained, dark grey, garnet-staurolite schist.

Best results include:

Sample No.	From	To	Length(m)	Ag	Pb%	Zn%
114227	324.1	350.0	0.9	21.1	2.16	1.32
114228	325.5	326.2	0.7	3.3	0.41	1.54
114230	332.3	332.7	0.4	34.6	3.06	4.44
114233	387.1	387.9	0.8	10.7	0.51	2.26
114234	387.9	388.4	0.5	7.0	0.35	1.60
114236	396.2	396.6	0.4	6.2	0.38	3.52



**4) Hole TK-91-4 (Figure 8)**

**Objective:** This hole 'stepped out' 1Km toward the southeast from TK-91-3 in order to test the Line 20+00S area defined by soil and HLEM anomalies, where trenching unearthed lithologies similar to hanging and foot wall units observed in Cummins River.

**Result:** 0-6.1m; Overburden.

6.1m-127.1m; A series of fine grained, well foliated garnet biotite schists interbedded with light grey to creamy white cherty layers. The rocks appear similar to those contained within the thrust section of hole TK-91-2.

127.1m-378.5m; Fine grained, light grey to grey micaceous limestones with minor interbeds of mica schists and garnet-mica schists.

378.5m-423.5m; Intercalated micaceous limestone and garnet-mica schists grading into garnet biotite schist with minor cordierite porphyroblasts.

423.5m-428.5m; Garnet-mica schist with zoned cordierite porphyroblasts.

428.5m-494.8m; Quartz-sericite schists with 1-2m beds of dolomite from 462.4m-464.6m and 469.7m-471.4m. Interbedded saccharoidal, limy dolomite/limestone and garnet schists from 471.4m-477.8m. Trace to thinly laminated sulphides.

494.8m-E.O.H.; Garnet-staurolite schist.

Best results include:

Sample No.	From	To	Length(m)	Ag	Pb%	Zn%
114239	441.3	441.8	0.5	8.0	0.76	5.82

## 9. GEOPHYSICS

A downhole UTEM survey was employed in an attempt to locate thick sections of mineralization. The association of pyrite-pyrrhotite with the lead-zinc mineralization was inferred to indicate areas of increased base metal accumulations.

Two boreholes, TK-91-2 and TK-91-4 were surveyed with the BH-UTEM system utilizing two separate loop configurations. Obstructions encountered in holes TK-91-1 and TK-91-3 prevented those holes from being surveyed.

Two insulated copper wire loop arrays were laid out for the survey (see Figure 4). Both loops were run along the baseline; Loop 1 encompassed lines 3+00S and 14+00S; Loops 2 included lines 14+00S and 20+00S for loop 2. Both loops were closed along the lower main logging road.

The survey was conducted by Syd Visser of SJ Geophysics Ltd. and Lamontagne Geophysics Ltd. from November 9-14.

The data from borehole TK-91-2 indicates a conductive zone with a conductivity of  $\approx 10$  mhos near the bottom of the hole at a depth of 460 to 550 metres. This conductor correlates well with thin bands of graphite and pyrite observed in drill core. The major part of this anomaly is off-hole toward the east and north, as shown on the model FIG-1 and FIG-2. The same response is seen from both loop 1 and 2.

A weak extensive conductor, with a conductivity of  $\approx 10$  mhos, was located within TK-91-4 between 480 to 500m depth. The sign of the secondary field from the anomaly is the same as the primary field outside loop 1 and opposite in sign from loop 2, therefore, the conductor must be located toward the loop in the northeast direction. A sharp return on the lower end of the anomaly from loop 1 may suggest that the conductor is dipping toward the north.

The data from loop 2 confirms the large anomaly in TK-91-4, but further indicated a small but very strong off-hole anomaly located at a depth of  $\approx 460$  m.

A full report and interpretation of the geophysics is included in Appendix G.

## 10. DISCUSSIONS

A summary of some geological characteristics of 'Sedex' deposits (after Large 1980) follows;

Deposits exist in sub (second or third order) basins within large first order epicratonic and intracratonic basins of Middle Proterozoic and Lower-Middle Palaeozoic age.

The lateral dimensions are an order of magnitude greater (several hundreds to thousands of metres) than the thickness. Ore bodies are concordantly interbedded in marine sediments and may be distributed through stratigraphic intervals of 1000m or more.

Deposits usually occur close to fault controlled margins of first or second order basins. Reactivation of such zones comprise excellent pathways for the rise of hydrothermal solutions.

The stratiform sulphides may, in part, be texturally massive or commonly and characteristically occur as laterally persistent beds of fine-grained sulphides from 1mm to 1m in thickness. Brecciation and/or stockwork, disseminated or cross-cutting vein-type mineralization is commonly found under-lying or adjacent to the stratiform mineralization. Hydrothermal alteration (usually silicification) is commonly found associated with the cross-cutting mineralization.

Mineralogy is relatively simple, containing fine grained pyrite and/or pyrrhotite, sphalerite and galena with minor chalcopyrite.

Lateral and/or vertical zonation of Pb-Zn may exist as a result of rapid cooling and dilution of the hydrothermal solution by sea water near the discharge zone and the consequent precipitation of minerals in a sequence according to their solubilities. Subsequently, a lateral zonation of Cu-Pb-Zn-(Ba) and a vertical zonation of Cu-Zn-Pb-(Ba) away from the discharge zone is observed. The Zn/Pb ratio gradually increases distally.

Very fine grained, opalescent chert is commonly found interbedded within the stratiform sulphide mineralization. The chert is spatially restricted to the ore deposits and it probably represents an exhalative hydrothermal silica phase that was deposited as a gel on the sea floor.

Similar characteristics to those listed above are exhibited within the MGM property.

Figure 10 displays a composite three-dimensional plot of results from drilling and surface mapping. TK-91-1 and TK-91-3 as well as the 1991 Cominco drill holes and TK-91-2 are plotted on common planes. Best results are displayed for the 1991 Teck drill holes. Several lithologies within the Tsar Creek Formation are displayed in order to observe facies thickness changes.

Mineralization is contained within quartz-sericite schist and manganiferous dolomite horizons. The lateral extent of the sulphide zone is much greater than its width.

Within first order basins, abrupt changes in sedimentary facies and thicknesses reflect the presence of sub basins. Typically, within Sedex deposits, the whole sequence containing the stratiform mineralization is typically thickest at a point adjacent to the massive sulphide ore. Shelf facies may be characterized as sequences of pelagic limestone and basinal facies by siltstones and shales.

Individual facies thicknesses for most of the Tsar Creek Formation prove to be constant over the investigated area. Greater study of the facies within the Tsar Creek is necessary before sub basins can be defined.

To date, evidence for faults associated with the massive sulphide mineralization has not been observed.

Zn/Pb ratios determined from the massive sulphide horizons encountered within the Teck drill holes 1-4, along with ratios from surface sampling of the sulphide horizon near the Cummins canyon showing and the Line 20+00S trenches are displayed on Figure 9. Higher ratios reflect a distal environment, low ratios (approaching zero) reflect a proximal environment. Results indicate a general increase of ratio values toward grid south and a decrease toward grid north.

## 11. CONCLUSIONS

Results from the 1991 drilling program were encouraging.

Drilling confirmed the presence of the sulphide horizon, similar to that observed within the canyon showing, south from Cummins River to Line 20+00S a strike length of approximately 3.0 kms.

The geological characteristics of the sulphide horizon are consistent with a large, basin controlled style of mineralization with generally decreasing width and increasing Zn/Pb ratios toward grid south.

Additional geophysical and drilling programs are warranted.

## 12. REFERENCES

Dodson, E.D., 1971. Report on a Geochemical Survey on the Bend No.1 Mineral Claim. Golden Mining Division. MacDonald Consultants Ltd. Assessment Report 2991.

Dodson, E.D., 1971. Report on a Geochemical Survey on the Bend 17-26 Mineral Claims. Golden Mining Division. MacDonald Consultants Ltd. Assessment Report 2992.

Jenks, J., 1985. Drilling report - MGM Property. Golden Mining Division. Esso Minerals Canada. Assessment Report 15251.

Large, D.E., 1980. Geological Parameters Associated with Sediment-Hosted, Submarine Exhalative Pb-Zn Deposits: An Empirical Model for Mineral Exploration, Geol. Jb. D40, p. 59-129.

Large, D.E., 1983. Sediment-Hosted Massive Sulphide Lead-Zinc Deposits: An Empirical Model in Short Course in Sediment hosted stratiform lead-zinc deposits, Mineralogical Association of Canada Short Course Handbook, v.8, p.1-29.

Leask, J.M., 1981. Geology of the MGM Property, Big Bend District, East Central British Columbia. Assessment Report No. 9994.

Marr, J.M., Oliver, J.L. and Melnyk, W.D., 1986. MGM Project 1985. Esso Minerals of Canada Ltd. (in house report)

Mawer, A.B., 1987. Geological - Access road and Drill site construction report. Bend Group, Golden Mining District, Cummins River Area. Cominco Ltd. Assessment Report No. 16544.

Reddy, D.G. and Godwin, C.I. 1986. Geology of the Bend Zinc-Lead-Silver Massive Sulphide Prospect Southeastern British Columbia, British Columbia Ministry of Energy, Mines and Resources, Geological Fieldwork, Paper 1987-1, p.47-52.

Simony, P.S., Ghent, E.D., Craw, D., Mitchell, W. and Robbins, D.B., 1980. Structural and metamorphic evolution of the northeast flank of Shuswap complex, southern Canoe River area, British Columbia: Geological Survey of America, Memoir 153, p.445-461.

Spence, C.D., 1983. Geophysics and Geochemistry. Riocanex. Assessment Report 12155.

Walcott, P.E. and Associates, 1983. A Geophysical Report on Electromagnetic and Magnetic Surveys. McNaughton Lake, British Columbia. Riocanex Inc. Assessment Report 11565.

**APPENDIX A**

**Statement of Qualifications**

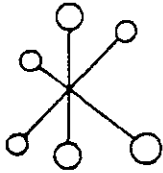
**APPENDIX B**  
**Cost Statement**

**EXPLORATION COSTS**  
(October 6 - November 13, 1991)

<b>A) SALARIES</b>		
Geology		
G. Thomson (Project Geologist)		
40 days @ \$271.92	\$10,876.80	
C. Alford (Geologist)		
71.5 days @ \$232.00	16,588.00	
C. Lormand (Geologist)		
48.5 days @ \$232.00	11,252.00	
Drafting	<u>1,144.47</u>	
		\$39,861.27
<b>B) LIVING EXPENSES</b>		
Camp Rental (Evan's Forestry Camp)	\$6,631.47	
Motel, Meals (Oct 1-6, Nov 13-Dec 14)		
C. Alford (5 wks) 35 x \$84.00/day	2,940.00	
G. Thomson (2 wks) 14 x \$84.00/day	1,176.00	
C. Lormand (5 wks) 35 x \$39.20/day	<u>1,372.00</u>	
		\$12,119.47
<b>C) TRANSPORTATION</b>		
Barge Service (Mica Marine Ltd.)	\$6,133.42	
Truck Rentals (2 - 4x4 Trucks)		
Cana Rentals (2 mos. @ \$1148.00)	2,296.00	
Canex Rentals (2 mos. @ \$1075.20)	2,150.40	
Gas	<u>504.00</u>	
		\$11,083.82
<b>D) CHARTERED AIRCRAFT</b>		
Amiskwi Air, Canadian Helicopters (6 hrs.)		
Tundra Helicopters (5.8 hrs.)		\$11,882.04
<b>E) CONTRACTORS</b>		
Falcon Drilling (1,184 m)	\$141,013.66	
SJV Geophysics	<u>13,632.37</u>	
		\$154,646.03
<b>F) GEOCHEMICAL ANALYSES (Eco-Tech Labs)</b>		
39 Core Samples with 30 Element I.C.P. and Specific Pb, Zn, Ag, Au and Ba assays		\$1,306.29
<b>G) FIELD EXPLORATION COSTS</b>		
		\$70.41
<b>H) MAPS AND PRINTS</b>		
		\$63.84
<b>I) TELEPHONE</b>		
		\$120.04
<b>J) PETROGRAPHIC STUDY</b>		
		\$103.32
<b>K) RENTALS (Radiotelephone, Core Splitter)</b>		
		<u>\$493.88</u>
	<b>TOTAL</b>	<b>\$231,750.41</b>



**APPENDIX C**  
**Certificates of Analyses**



# ECO-TECH LABORATORIES LTD.

ASSAYING - ENVIRONMENTAL TESTING

10041 East Trans Canada Hwy., Kamloops, B.C. V2C 2J3 (804) 573-5700 Fax 573-4557

OCTOBER 18, 1991

CERTIFICATE OF ASSAY ETK 91-828

=====

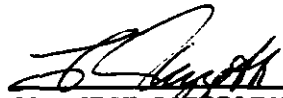
TECK EXPLORATION LTD.  
960 - 175 2nd. AVE.  
KAMLOOPS, B.C.  
V2C 5W1

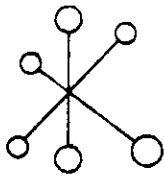
ATTENTION: FRED DALEY

SAMPLE IDENTIFICATION: 14 ROCK SAMPLES RECEIVED OCTOBER 16, 1991  
----- PROJECT: 1703

ET#	Description	AG (g/t)	AG (oz/t)	PB (%)	ZN (%)
1 -	114201	<.1	<.01	<.01	.01
2 -	114202	8.6	.25	.76	2.24
3 -	114203	1.1	.03	.09	.52
4 -	114204	.4	.01	.04	.08
5 -	114205	.1	<.01	.03	.28
6 -	114206	2.4	.07	.17	.31
7 -	114207	.1	<.01	.03	.05
8 -	114208	5.2	.15	.39	1.12
9 -	114209	2.5	.07	.19	.98
10 -	114210	2.6	.08	.13	.71
11 -	114211	65.6	1.91	4.22	9.36
12 -	114212	4.6	.13	.20	.73
13 -	114213	.5	.02	.04	.07
14 -	114214	<.1	<.01	.01	.01

NOTE: < = LESS THAN

  
\_\_\_\_\_  
ECO-TECH LABORATORIES LTD  
FRANK J. PEZZOTTI  
B.C. CERTIFIED ASSAYER



# ECO-TECH LABORATORIES LTD.

ASSAYING - ENVIRONMENTAL TESTING

10041 East Trans Canada Hwy., Kamloops, B.C. V2C 2J3 (604) 573-5700 Fax 573-4557

OCTOBER 18, 1991

CERTIFICATE OF ANALYSIS ETK 91-828  
=====

TECK EXPLORATION LTD.  
960 - 175 2nd. AVE.  
KAMLOOPS, B.C.  
V2C 5W1

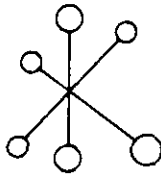
ATTENTION: FRED DALEY

SAMPLE IDENTIFICATION: 14 ROCK SAMPLES RECEIVED OCTOBER 16, 1991  
----- PROJECT: 1703

ET#	Description	BA (ppm)
1 -	114201	3380
2 -	114202	170
3 -	114203	150
4 -	114204	840
5 -	114205	650
6 -	114206	200
7 -	114207	210
8 -	114208	240
9 -	114209	340
10 -	114210	210
11 -	114211	300
12 -	114212	610
13 -	114213	230
14 -	114214	70

NOTE: < = LESS THAN

ECO-TECH LABORATORIES LTD  
FRANK J. PEZZOTTI  
B.C. CERTIFIED ASSAYER



# ECO-TECH LABORATORIES LTD.

ASSAYING - ENVIRONMENTAL TESTING

10041 East Trans Canada Hwy., Kamloops, B.C. V2C 2J3 (604) 573-5700 Fax 573-4557

NOVEMBER 22 , 1991

CERTIFICATE OF ANALYSIS ETK 91-828B

=====


TECK EXPLORATION LTD.  
960 - 175 2nd. AVE.  
KAMLOOPS, B.C.  
V2C 5W1

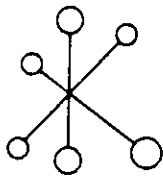
ATTENTION: FRED DALEY

SAMPLE IDENTIFICATION: 14 ROCK SAMPLES RECEIVED OCTOBER 16, 1991  
----- PROJECT: 1703  
TELEPHONE REQUEST NOVEMBER 19, 1991

ET#	Description	BA (ppm)
1 -	114201	3773

NOTE: < = LESS THAN

  
\_\_\_\_\_  
ECO-TECH LABORATORIES LTD  
*Per* FRANK J. PEZZOTTI  
B.C. CERTIFIED ASSAYER



# ECO-TECH LABORATORIES LTD.

ASSAYING - ENVIRONMENTAL TESTING

10041 East Trans Canada Hwy., Kamloops, B.C. V2C 2J3 (604) 573-5700 Fax 573-4557

NOVEMBER 22 , 1991

CERTIFICATE OF ASSAY ETK 91-828B

=====

TECK EXPLORATION LTD.  
960 - 175 2nd. AVE.  
KAMLOOPS, B.C.  
V2C 5W1

ATTENTION: FRED DALEY


SAMPLE IDENTIFICATION: 14 ROCK SAMPLES RECEIVED OCTOBER 16, 1991

----- PROJECT: 1703

TELEPHONE REQUEST NOVEMBER 19, 1991

ET#	Description	AU (g/t)	AU (oz/t)
2 -	114202	.10	.003
8 -	114208	.22	.006
11 -	114211	.18	.005

NOTE: < = LESS THAN

  
\_\_\_\_\_  
ECO-TECH LABORATORIES LTD  
*Per* FRANK J. PEZZOTTI  
B.C. CERTIFIED ASSAYER

ECO-TECH LABORATORIES LTD.  
 10041 EAST TRAMS CANADA HWY.  
 KAMLOOPS, B.C. V2C 2J3  
 PHONE - 604-573-5700  
 FAX - 604-573-4557

TECK EXPLORATIONS LTD.- ETK 91-828  
 960, 175 SECOND AVENUE  
 KAMLOOPS, B.C.  
 V2C 5W1

OCTOBER 18, 1991

ATTENTION: FRED DALEY

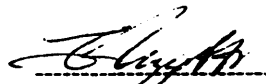
VALUES IN PPM UNLESS OTHERWISE REPORTED

PROJECT NUMBER: 1703  
 14 ROCK SAMPLES RECEIVED OCTOBER 16, 1991

RT#	DESCRIPTION	AG	AL(t)	AS	B	BA	BI	CA(t)	CD	CO	CR	CU	FE(t)	K(t)	LA	MG(t)	MN	MO	NA(t)	NI	P	PB	SB	SN	SR	TI(t)	U	V	W	Y	ZN
1-	114201	<.2	6.52	<5	4	100	<5	7.26	<1	20	66	23	3.35	.01	<10	2.05	218	1	.24	36	320	48	15	<20	257	.07	<10	24	<10	<1	84
2-	114202	8.4	.29	40	<2	45	<5	5.93	29	9	17	48	10.18	.11	10	3.04	>10000	3	<.01	4	570	6292	25	<20	30	.02	20	<1	30	<1	>10000
3-	114203	1.2	.16	20	4	30	<5	6.48	6	3	30	11	4.26	.06	<10	2.52	8220	2	<.01	<1	980	654	15	<20	8	.01	<10	<1	20	1	5105
4-	114204	.6	.17	5	4	30	<5	.58	1	3	47	2	1.22	.10	10	.19	1107	2	<.01	4	390	312	<5	<20	5	<.01	<10	<1	10	1	603
5-	114205	<.2	.27	25	4	40	<5	11.90	2	5	11	2	4.34	.08	<10	4.11	>10000	<1	<.01	1	1010	316	10	<20	45	<.01	10	<1	<10	<1	2286
6-	114206	2.2	.49	65	6	80	<5	10.39	4	11	9	54	13.79	.14	20	4.09	>10000	2	<.01	5	940	1610	20	<20	46	.02	50	<1	10	<1	2804
7-	114207	<.2	.05	25	4	20	<5	>15.	<1	3	4	1	4.91	<.01	<10	6.26	>10000	<1	<.01	<1	700	294	10	<20	<1	<.01	10	<1	<10	<1	319
8-	114208	5.4	.11	45	<2	25	<5	14.45	16	5	8	9	7.33	.01	10	4.94	>10000	1	<.01	<1	1210	3474	20	<20	1	<.01	10	<1	20	<1	>10000
9-	114209	2.2	.10	65	2	45	<5	14.45	11	6	9	8	8.06	.01	10	5.78	>10000	1	<.01	<1	860	1200	15	<20	<1	<.01	20	<1	10	<1	8749
10-	114210	2.4	.04	30	2	25	<5	>15.	9	3	5	3	5.34	<.01	<10	6.42	>10000	<1	<.01	<1	320	930	10	<20	<1	<.01	10	<1	10	<1	6825
11-	114211	>30.	.36	200	<2	70	<5	3.41	183	16	29	34	>15.	.19	<10	2.04	>10000	7	<.01	4	1610	>10000	40	<20	17	.03	80	<1	30	<1	>10000
12-	114212	4.4	.65	205	4	60	<5	6.40	6	10	32	19	12.10	.33	20	3.00	>10000	2	<.01	6	1370	1968	20	<20	81	.06	40	3	10	<1	6483
13-	114213	.4	.09	40	4	30	<5	>15.	<1	3	13	9	5.17	<.01	10	7.20	>10000	1	<.01	<1	760	358	10	<20	167	<.01	10	<1	<10	<1	675
14-	114214	<.2	.05	15	6	15	<5	>15.	<1	1	25	2	3.07	<.01	<10	9.43	>10000	1	<.01	<1	430	18	5	<20	100	<.01	<10	<1	<10	<1	88

NOTE: < = LESS THAN  
 > = GREATER THAN

TECK/SCS

  
 ECO-TECH LABORATORIES LTD.  
 FRANK J. PESSOTTI  
 B.C. CERTIFIED ASSAYER

ECO-TECH LABORATORIES LTD.  
 10041 EAST TRANS CANADA HWY.  
 KAMLOOPS, B.C. V2C 2J3  
 PHONE - 604-573-5700  
 FAX - 604-573-4557

TECK EXPLORATIONS LTD.- RTK 91-059  
 960, 175 SECOND AVENUE  
 KAMLOOPS, B.C.  
 V2C 5W1

NOVEMBER 7, 1991

ATTENTION: FRED DALEY


VALUES IN PPM UNLESS OTHERWISE REPORTED

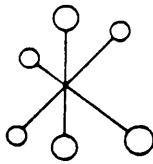
PROJECT NUMBER: 1703  
 7 CORE SAMPLES RECEIVED OCTOBER 29, 1991

ET#	DESCRIPTION	AG	AL(%)	AS	B	BA	BI	CA(%)	CD	CO	CR	CU	FE(%)	K(%)	LA	MG(%)	MN	MO	NA(%)	NI	P	PB	SB	SN	SR	TI(%)	U	V	W	Y	ZN
1-	114215	<.2	1.47	<5	10	40	<5	.21	<1	20	52	41	2.50	.62	20	.87	136	8	.01	43	450	16	5	<20	6	.07	<10	11	<10	4	38
2-	114216	<.2	1.92	<5	8	230	<5	.60	<1	14	61	7	2.72	1.23	10	1.37	548	2	.01	18	90	18	10	<20	5	.14	<10	27	<10	2	56
3-	114217	<.2	3.65	5	10	165	<5	.41	<1	40	305	82	4.83	2.24	<10	2.92	315	2	.07	141	1110	26	15	<20	4	.24	<10	118	<10	8	71
4-	114218	<.2	3.26	5	8	95	<5	.34	<1	51	287	129	4.89	1.94	<10	2.44	251	3	.05	144	850	24	15	<20	3	.21	<10	102	<10	5	31
5-	114219	<.2	.06	<5	6	<5	<5	>15	<1	1	4	<1	.29	.03	<10	.52	626	<1	<.01	<1	740	2	5	<20	<1	<.01	<10	<1	<10	2	64
6-	114220	<.2	1.29	<5	8	30	<5	.50	<1	19	72	32	1.97	.66	30	.70	155	3	.02	35	480	8	5	<20	9	.06	<10	7	<10	3	43
7-	114221	.2	.25	5	10	10	<5	2.24	<1	3	169	10	1.63	.08	20	.61	1867	6	<.01	4	2350	14	5	<20	28	.02	<10	3	<10	9	29

NOTE: < = LESS THAN

TECKS/SCS

  
 ECO-TECH LABORATORIES LTD.  
 FRANK J. PAVESOTTI  
 B.C. CERTIFIED ASSAYER



# ECO-TECH LABORATORIES LTD.

ASSAYING - ENVIRONMENTAL TESTING

10041 East Trans Canada Hwy., Kamloops, B.C. V2C 2J3 (804) 573-5700 Fax 573-4557

NOVEMBER 7, 1991

**CERTIFICATE OF ANALYSIS ETK 91-859W**

---

TECK EXPLORATION  
960-175 2ND AVE.  
KAMLOOPS, B.C.  
V2C 15W

ATTENTION: FRED DALEY

SAMPLE IDENTIFICATION: 7 CORE samples received OCTOBER 29, 1991

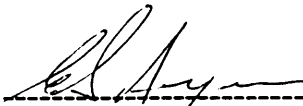
-----PROJECT#: 1703

SAMPLES SUBMITTED BY CRAIG ALFORD

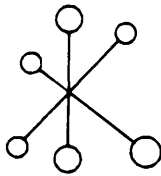
ET#	Description	BaO	P2O5	SiO2	MnO	Fe2O3	MgO	Al2O3	CaO	TiO2	NaO2	K2O	L.O.I.
5-	114219	.01	.35	11.69	.10	.71	1.11	1.89	45.32	.10	.08	.56	38.09
6-	114220	.05	.21	63.13	.12	6.32	1.64	19.53	.93	.86	.64	4.68	2.48
7-	114221	.01	.54	87.89	.24	2.59	.94	1.36	2.71	.27	.01	.42	3.08

NOTE: VALUES EXPRESSED IN PERCENT

SC91/TECK5

  
-----  
ECO-TECH LABORATORIES LTD.  
*P.J.P.* FRANK J. PEZZOTTI  
B.C. CERTIFIED ASSAYER





# ECO-TECH LABORATORIES LTD.

ASSAYING - ENVIRONMENTAL TESTING

10041 East Trans Canada Hwy., Kamloops, B.C. V2C 2J3 (604) 573-5700 Fax 573-4557

NOVEMBER 22, 1991

CERTIFICATE OF ASSAY ETK 91-866B

=====

TECK EXPLORATION LTD.  
960 - 175 2nd. AVE.  
KAMLOOPS, B.C.  
V2C 5W1

ATTENTION: FRED DALEY

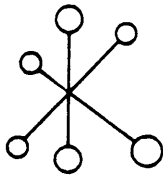
SAMPLE IDENTIFICATION: 16 CORE SAMPLES RECEIVED NOVEMBER 4, 1991  
----- PROJECT: 1703  
TELEPHONE REQUEST NOVEMBER 19, 1991

ET#	Description	AG (g/t)	AG (oz/t)	PB (%)	ZN (%)
4 -	114225	1.4	.04	.08	.54
8 -	114229	1.9	.06	.17	.26
14 -	114235	1.3	.04	.04	.31

  
ECO-TECH LABORATORIES LTD

*Pro* FRANK J. PEZZOTTI

B.C. CERTIFIED ASSAYER



# ECO-TECH LABORATORIES LTD.

ASSAYING - ENVIRONMENTAL TESTING  
10041 East Trans Canada Hwy., Kamloops, B.C. V2C 2J3 (804) 573-5700 Fax 573-4557

NOVEMBER 5, 1991


CERTIFICATE OF ASSAY ETK 91-866  
=====

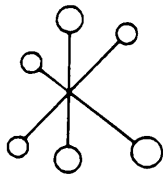
TECK EXPLORATION LTD.  
960 - 175 2nd. AVE.  
KAMLOOPS, B.C.  
V2C 5W1

ATTENTION: FRED DALEY

SAMPLE IDENTIFICATION: 16 CORE SAMPLES RECEIVED NOVEMBER 4, 1991  
----- PROJECT: 1703

ET#	Description	AG (g/t)	AG (oz/t)	PB (%)	ZN (%)
6 -	114227	21.1	.62	2.16	1.32
7 -	114228	3.3	.10	.41	1.54
9 -	114230	34.6	1.01	3.06	4.44
12 -	114233	10.7	.31	.51	2.26
13 -	114234	7.0	.20	.36	1.60
15 -	114236	6.2	.18	.38	3.52
16 -	114237	.7	.02	.03	.26

  
-----  
ECO-TECH LABORATORIES LTD  
FRANK J. PEZZOTTI  
B.C. CERTIFIED ASSAYER



# ECO-TECH LABORATORIES LTD.

ASSAYING - ENVIRONMENTAL TESTING

10041 East Trans Canada Hwy., Kamloops, B.C. V2C 2J3 (604) 573-5700 Fax 573-4557

NOVEMBER 22, 1991

CERTIFICATE OF ANALYSIS ETK 91-866B  
=====

TECK EXPLORATION LTD.  
960 - 175 2nd. AVE.  
KAMLOOPS, B.C.  
V2C 5W1

ATTENTION: FRED DALEY

SAMPLE IDENTIFICATION: 16 CORE SAMPLES RECEIVED NOVEMBER 4, 1991  
----- PROJECT: 1703  
TELEPHONE REQUEST NOVEMBER 19, 1991

ET#	Description	BA (ppm)
4 -	114225	1221
5 -	114226	225
6 -	114227	252
7 -	114228	119
8 -	114229	53
9 -	114230	186
10 -	114231	650
11 -	114232	769
12 -	114233	610
13 -	114234	676
14 -	114235	795
15 -	114236	1331
16 -	114237	66

*Pro*

ECO-TECH LABORATORIES LTD  
FRANK J. PEZZOTTI  
B.C. CERTIFIED ASSAYER

SC91/TECK2

ECO-TECH LABORATORIES LTD.  
 10041 EAST TRANS CANADA HIGHWAY  
 KAMLOOPS, B.C. V0E 2P0  
 PH - 604 -573-5700  
 FAX - 604 - 537-4557

TECK EXPLORATIONS LTD. - ETX 91-866  
 960, 175 SECOND AVENUE  
 KAMLOOPS, B.C.  
 V2C 5W1

NOVEMBER 5, 1991

ATTENTION: FRED DALEY

VALUES IN PPM UNLESS OTHERWISE REPORTED


PROJECT NUMBER: 1703  
 16 CORE SAMPLES RECEIVED NOVEMBER 4, 1991

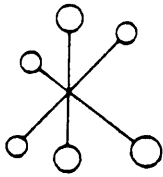
ET#	DESCRIPTION	AG	AL(%)	AS	B	BA	BI	CA(%)	CD	CO	CR	CU	FE(%)	K(%)	LA	MG(%)	NH	NO	NA(%)	NI	P	PB	SB	SE	SR	TI(%)	U	V	W	Y	SM
1-	114222	.2	.16	25	12	20	<5	1.85	<1	8	115	8	2.11	.05	<10	.54	1377	5	<.01	8	1510	106	5	<20	27	<.01	<10	<1	<10	5	177
2-	114223	.2	2.18	<5	6	20	<5	7.53	<1	20	33	28	3.04	.15	<10	1.24	333	3	<.01	39	420	210	10	<20	58	<.01	<10	8	<10	<1	71
3-	114224	.2	.28	15	8	10	<5	2.18	<1	7	83	32	2.81	.14	<10	.66	1866	3	<.01	13	1340	78	5	<20	17	<.01	<10	<1	<10	<1	79
4-	114225	1.0	.20	20	8	10	<5	2.26	6	6	98	14	2.96	.06	<10	.96	3033	6	<.01	9	1090	592	5	<20	1	<.01	<10	<1	<10	1	3865
5-	114226	.8	.27	20	10	35	<5	.41	<1	6	141	19	3.82	.10	<10	.47	3183	5	<.01	6	830	430	5	<20	8	.02	<10	<1	<10	<1	142
6-	114227	16.8	.31	25	<2	35	<5	1.44	17	6	88	30	4.43	.15	<10	.78	2912	6	<.01	7	960	>10000	20	<20	8	.01	<10	<1	<10	<1	>10000
7-	114228	3.2	.16	25	2	15	<5	3.67	18	4	83	22	4.21	.05	<10	1.56	4609	4	<.01	3	1000	3172	15	<20	21	<.01	<10	<1	<10	<1	>10000
8-	114229	1.6	.28	15	10	20	<5	4.34	2	3	82	11	2.86	.14	<10	1.79	4727	5	<.01	2	960	1286	15	<20	30	.02	<10	<1	<10	1	1574
9-	114230	26.2	.07	315	<2	5	<5	2.67	55	5	99	20	2.25	<.01	<10	.99	2599	6	<.01	6	770	>10000	60	<20	13	<.01	<10	<1	<10	<1	>10000
10-	114231	.4	.17	95	8	25	<5	.94	<1	3	65	1	2.64	.06	<10	.29	810	4	<.01	5	620	338	5	<20	4	<.01	<10	<1	<10	<1	923
11-	114232	.6	.17	185	8	25	<5	1.08	<1	4	85	2	4.67	.01	<10	.33	1121	3	<.01	8	520	294	10	<20	1	<.01	<10	<1	<10	<1	270
12-	114233	9.2	.18	170	2	35	<5	5.37	16	8	42	9	8.18	.02	<10	1.67	>10000	4	<.01	1	1020	4670	5	<20	51	.01	10	<1	<10	<1	>10000
13-	114234	8.2	.42	150	8	55	<5	8.65	13	8	42	15	8.23	.21	<10	2.72	>10000	4	<.01	3	1570	2770	25	<20	70	.03	20	<1	20	<1	>10000
14-	114235	1.2	.15	85	8	35	<5	14.08	1	7	21	3	2.25	.04	<10	2.69	4749	1	<.01	7	2670	294	15	<20	99	<.01	<10	<1	<10	6	1884
15-	114236	6.4	.35	100	<2	45	<5	6.55	25	19	23	23	6.98	.12	<10	1.91	>10000	4	<.01	7	2790	3074	15	<20	75	<.01	10	<1	10	<1	>10000
16-	114237	1.0	.03	230	8	20	<5	13.11	<1	10	3	94	10.54	<.01	<10	5.38	>10000	<1	<.01	7	320	182	15	<20	53	<.01	20	<1	<10	<1	2394

NOTE: < = LESS THAN  
 > = GREATER THAN

c.c. Greg Thomson/ C. Alford

TECK5/8C5

  
 ECO-TECH LABORATORIES LTD.  
 Per FRANK J. PRESOTTI  
 B.C. CERTIFIED ASSAYER



# ECO-TECH LABORATORIES LTD.

ASSAYING - ENVIRONMENTAL TESTING  
10041 East Trans Canada Hwy., Kamloops, B.C. V2C 2J3 (604) 573-5700 Fax 573-4557

NOVEMBER 19, 1991


CERTIFICATE OF ASSAY ETK 91-884  
=====

TECK EXPLORATION LTD.  
960 - 175 2nd. AVE.  
KAMLOOPS, B.C.  
V2C 5W1

ATTENTION: GREG THOMSON

SAMPLE IDENTIFICATION: 2 CORE SAMPLES RECEIVED NOVEMBER 18, 1991  
----- PROJECT: NONE GIVEN

ET#	Description	AG (g/t)	AG (oz/t)	PB (%)	ZN (%)
1 -	114328	.6	.02	<.01	.05
2 -	114329	8.0	.23	.76	5.82

  
\_\_\_\_\_  
ECO-TECH LABORATORIES LTD  
FRANK J. PEZZOTTI  
B.C. CERTIFIED ASSAYER

ECO-TECH LABORATORIES LTD.  
 10041 EAST TRANS CANADA HIGHWAY  
 KAMLOOPS, B.C. V0E 2P0  
 PH - 604 -573-5700  
 FAX - 604 - 537-4557

TECK EXPLORATIONS LTD.- ETK 91-884  
 960, 175 SECOND AVENUE  
 KAMLOOPS, B.C.  
 V2C 5W1

NOVEMBER 19, 1991

ATTENTION: GREG THOMSON

VALUES IN PPM UNLESS OTHERWISE REPORTED

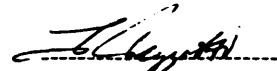
PROJECT NUMBER: NONE GIVEN

2 CORE SAMPLES RECEIVED NOVEMBER 18 , 1991

ET#	DESCRIPTION	AG	AL(%)	AS	B	BA	BI	CA(%)	CD	CO	CR	CU	FE(%)	K(%)	LA	MG(%)	MM	MO	NA(%)	NI	P	PB	SB	SN	SR	TI(%)	U	V	W	Y	ZN
1-	114328	1.0	.07	25	4	10	<5	13.16	<1	4	9	10	5.32	<.01	<10	5.64	>10000	1	<.01	<1	490	14	<5	<20	8	<.01	<10	<1	<10	<1	218
2-	114329	7.4	.06	20	<2	10	<5	4.62	63	4	73	22	4.54	<.01	<10	1.95	5104	5	<.01	3	690	6982	5	<20	26	<.01	<10	<1	<10	<1	>10000

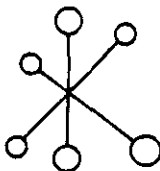
NOTE: < = LESS THAN  
 > = GREATER THAN

TECK5/SC5

  
 ECO-TECH LABORATORIES LTD.  
 FRANK J. PEISOTTI  
 B.C. CERTIFIED ASSAYER

**APPENDIX D**

**Analytical Procedures**



# ECO-TECH LABORATORIES LTD.

ASSAYING - ENVIRONMENTAL TESTING

10041 East Trans Canada Hwy., Kamloops, B.C. V2C 2J3 (604) 573-6700 Fax 573-4657

## GEOCHEMICAL LABORATORY METHODS

### SAMPLE PREPARATION (STANDARD)

1. Soil or Sediment: Samples are dried and then sieved through 80 mesh sieves.
2. Rock, Core: Samples dried (if necessary), crushed, riffled to pulp size and pulverized to approximately -140 mesh.
3. Humus/Vegetation: The dry sample is ashed at 550 C. for 5 hours.

### METHODS OF ANALYSIS

All methods have either canmet certified or in-house standards carried through entire procedure to ensure validity of results.

#### 1. MULTI ELEMENT ANALYSES

(a) ICP Packages (6,12,30 element).

Digestion	Finish
-----	-----
Hot Aqua Regia	ICP

(b) ICP - Total Digestion (24 element).

Digestion	Finish
-----	-----
Hot HClO <sub>4</sub> /HNO <sub>3</sub> /HF	ICP

(c) Atomic Absorption (Acid Soluble)

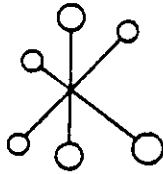
Ag\*, Cd\*, Cr, Co\*, Cu, Fe, Pb\*, Mn, Mo, Ni\*, Zn.

Digestion	Finish
-----	-----
Hot Aqua Regia	Atomic Absorption
	* = Background corrected

(d) Whole Rock Analyses.

Digestion	Finish
-----	-----
Lithium Metaborate fusion	ICP





# ECO-TECH LABORATORIES LTD.

ASSAYING - ENVIRONMENTAL TESTING

10041 East Trans Canada Hwy., Kamloops, B.C. V2C 2J3 (804) 573-5700 Fax 573-4557

## 2. Antimony

Digestion

Finish

Hot aqua regia

ICP

## 3. Arsenic

Digestion

Finish

Hot aqua regia

Hydride generation - A.A.S.

## 4. Barium

Digestion

Finish

Lithium Metaborate

ICP

## 5. Beryllium

Digestion

Finish

Hot aqua regia

Atomic Absorption

## 6. Bismuth

Digestion

Finish

Hot aqua regia

Atomic Absorption  
(Background Corrected)

## 7. Chromium

Digestion

Finish

Sodium Peroxide  
Fusion

Atomic Absorption

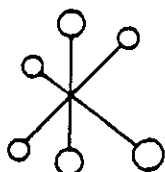
## 8. Fluorine

Digestion

Finish

Lithium Metaborate  
Fusion

Ion Selective Electrode



# ECO-TECH LABORATORIES LTD.

ASSAYING - ENVIRONMENTAL TESTING

10041 East Trans Canada Hwy., Kamloops, B.C. V2C 2J3 (604) 573-5700 Fax 573-4557

## 9. Gallium

Digestion  
-----

Finish  
-----

Hot HClO<sub>4</sub>/HNO<sub>3</sub>/HF

Atomic Absorption

## 10. Germanium

Digestion  
-----

Finish  
-----

Hot HClO<sub>4</sub>/HNO<sub>3</sub>/HF

Atomic Absorption

## 11. Mercury

Digestion  
-----

Finish  
-----

Hot aqua regia

Cold vapor generation -  
A.A.S.

## 12. Phosphorus

Digestion  
-----

Finish  
-----

Lithium Metaborate  
Fusion

ICP finish

## 13. Selenium

Digestion  
-----

Finish  
-----

Hot aqua regia

Hydride generation -  
A.A.S.

## 14. Tellurium

Digestion  
-----

Finish  
-----

Hot aqua regia  
Potassium Bisulphate  
Fusion

Hydride generation - A.A.S.  
Colorimetric or I.C.P.

**APPENDIX E**

**Drill Hole Logs**





DEPTH (meters) FROM/TO	G R A P H I C	DESCRIPTION	R E C O V E R Y	STRUCTURE			METALLIC MINERALS (%)	SAMPLE DATA				RESULTS			
				ANGLES	VEINS	ALTERATION		SAMPLE NO.	FROM	TO	LENGTH	Ag g/t	Pb %	Zn %	Ba ppm
224.8 - 233.4		- light grey to grey fine grained garnet schist red to red-brown 0.5 - 2.0 cm garnets compose 5-20 % of unit - 1-4 mm anhedral staurolites occur within the schist from 226.3 m - from 225.2 - 225.9 numerous rounded elliptical inclusions are observed (cordierite) chloritized rims		- Minor field axis at 227.4 m		- weak chlorite	- minor pyrrhotite and pyrite	4201	225.0	225.2	0.2	< 0.1	< 0.01	0.01	3380
233.4 - 236.1		- fine grained grey to dark grey cordierite-muscovite schist - rounded elliptical cordierite with preferred dimensional orientation (P.D.D.) parallel to the foliation - garnets compose only 1-3 % of the unit - the core is broken and rubbly from 235.7 - 236.1 m		- Foliation at 38° to core axis		- chlorite (weak to moderate)	- pyrite occurs in stringers and 1-4 cm subhedral to euhedral crystals along fractures that parallel the core axis								
236.1 - 248.0		- banded very fine grained grey chert with alternating 1-15 cm interbeds of mica and garnet mica schist (chert dominant) core broken from 236.6 - 237.7 and 241.2 - 242.7 m		- Minor fold axis at 247.9 m			- laminate to massive bed of pyrrhotite, pyrite and sphalerite thinly laminated sulphides at 247.5 - 247.8 m	4202	246.2	246.7	0.5	8.6	0.76	2.24	
248.0 - 264.2		- quartz-sericite schist - fine grained waxy light grey to pale yellow - highly siliceous with sericitic partings - foliation defined by sericite, graphite and pyrite smears and bedding - 0.5 - 1.0 cm thick beds with greater percentage micaceous material towards top		- Foliation at 42°			- thinly laminated pyrite and sphalerite	4203	248.3	248.5	0.2	1.1	0.09	.52	
264.2 - 267.7		- fine grained grey siliceous unit (originally massively bedded chert) correlates with siliceous pyrite unit observed in cummins canyon showing					- 1-3 % pyrite	4204	264.2	264.7	0.5	0.4	0.04	0.08	

DEPTH (meters) FROM/TO	G R A P H I C	DESCRIPTION	R E C O V E R Y	STRUCTURE		ALTERATION	METALLIC MINERALS (%)	SAMPLE DATA				RESULTS				
				ANGLES	VEINS			SAMPLE NO.	FROM	TO	LENGTH	Ag g/t	Pb %	Zn %		
267.7 - 275.3		- mineralized dolomite horizon - fine to medium grain light grey dolomite - from 274.3 - 275.3 m increased silica and micaceous percentage				- weak silica	- thinly laminated to massive sections of sphalerite and pyrite with minor magnetite, pyrrhotite and galena	4205 4206 4207 4208 4209 4210 4211 4212 4213 4214	267.7 268.5 269.0 269.8 270.0 271.1 272.0 272.5 273.0 273.6	268.5 269.0 269.8 270.0 271.1 272.0 272.5 273.0 273.6 274.4	0.8 0.5 0.8 0.2 1.1 0.9 1.1 0.5 0.5 0.6 0.8	0.1 2.4 0.1 5.2 2.5 2.6 65.6 4.6 0.5 < 0.1	0.03 0.17 0.03 0.39 0.19 0.13 4.22 0.2 0.04 0.01	0.28 0.31 0.05 1.12 0.98 0.71 9.36 0.73 0.07 0.01		
275.3 - 285.5		- banded grey to black garnet-biotite schist (argillaceous) 1-3 cm beds (younging uphole) 2nd foliation expressed by preferred orientation of 1-3 mm dark rhombal 'booklets' of biotite (possibly phlogopite)				- Foliation at 50° to core axis - 2nd foliation at 10° to core axis										
285.5 - 287.7		- fine grained siliceous layer (quartzite) originally muddy (1-5 %) chert layer					= 1-2 % pyrite									
287.7 - 300.7		- banded siliceous garnet-staurolite schist - 5-10 cm quartz bands locally				- Minor fold axis at 295.1 m										
300.7 - 307.7		- staurolite-garnet schist - fine grained grey matrix with abundant subhedral staurolite - quartz veins most likely originally cherty horizons														
307.7 - 312.8		- siliceous schist - cherty layers alternating with bands of garnet schist														
312.8 - 319.1		- garnet-staurolite schist with bronzy mica					- thinly laminated pyrrhotite	4215	313.7	314.3	0.6					









DEPTH (meters)	G R A P H I C	DESCRIPTION	R E C O V E R Y	STRUCTURE		ALTERATION	METALLIC MINERALS (%)	SAMPLE DATA			RESULTS				
				ANGLES	VEINS			SAMPLE NO.	FROM	TO	LENGTH				
435.8 - 484.4		- fine grained grey to grey-brown large garnet-mica schist with interbedded and intercalated very fine grained to fine grained limestone - numerous foliation parallel milk white quartz band occur through unit - thicker limestone sequences occur from 436.4 - 441.8, 441.1 - 446.5, 454.2 - 457.0 m - garnets are pink to red-brown and 0.5 - 2.5 cm in diameter - larger fold axis at 473.9 - 475.7 m		- Foliation at 40° to core axis - Minor fold axis at 446.1, 456.8, 477.0, 479.7, 480.5			- Minor pyrite								
484.4 - 485.6		- waxy yellowish-grey quartz sericite schist with thin foliation parallel laminations of graphite, pyrite and magnetite		- Foliation at 20° to core axis											
485.8 - 523.8		- light grey to white marble 0.5 - 3.0 cm biotite rich bands occur locally		- Foliation at 20° to core axis - Foliation at 45° from 504 m		- weak silica (<10%)	- subhedral to euhedral pyrite occurs in thin bands	4219	514.2	514.5	0.3				
523.8 - 561.3		- Interlayered quartz sericite schist - garnet schist and chert quartz sericite schist from 523.8 - 526.3, 530.7 - 532.6, 542.7 - 546.7 m - garnet-mica schist from 526.3 - 530.4 - chert-schist interbed 533.1 - 542.7, 546.7 - 561.3 - marble from 530.4 - 530.7, 532.6 - 533.1		- Foliation at 30° - Foliation at 20° at 546.5 m - Foliation at 15° at 558.0 m - Minor fold axis at 543.3, 546.5, 554.1 m			- thin laminations of pyrite and pyrrhotite - parallel to foliation pyrite also occurs	4221 4222	555.0 560.3	555.3 561.3	0.3 1.0				
561.3 - 572.0		- garnet staurolite schist fine grained well foliated grey unit with 20 % 0.5 - 1.0 cm anhedral to subhedral pink garnets - 5-10 % anhedral brown-yellow staurolites - possible phlogopite (? bronze mica)		- Foliation at 28° at 561.3 m - Foliation at 5° from 571.0 m				4220	566.1	566.4	0.3				



DEPTH (meters) FROM/TO	G R A P H I C	DESCRIPTION	R E C O V E R Y	STRUCTURE		ALTERATION	METALLIC MINERALS (%)	SAMPLE DATA			RESULTS						
				ANGLES	VEINS			SAMPLE NO.	FROM	TO	LENGTH						
209.7 - 276.2		- interlayered and intercalated micaceous limestone and mica schist with greater percentage of limestone - 1-3 cm wide quartz-carbonate bands locally - brecciated sections from 211.9 - 212.3, 224.8 - 226.3, 273.4 - 273.9 (possibly a reef breccia) areas with greater percentage of mica schist to limestone 242.1 - 243.2, 267.3 - 269.3, 273.4 - 274.4		- Foliation at 35°-45°									Ag (ppm)	Pb (ppm)	Zn (ppm)		
275.2 - 290.9		- fine grained dark grey mica schist with 5-20 % calcareous material - 3-10 mm subhedral to anhedral red garnets often rotated and elongated along foliation - 0.5 - 1.0 cm elliptical dark grey to black fine grained round inclusions (cordierite ?) from 286.3 - 289.6 inclusions are moderately sericitic		- Foliation at 45° - Minor fold axis at 280.4 - numerous minor folds from 283.0 - 285.0 m - interlayered with graphitic limestone		- weak chlorite and sericitic altered											
290.9 - 293.3		- banded grey to black graphitic limestone with numerous minor folds throughout unit															
293.3 - 294.7		- fine grained dark grey cordierite schist - numerous fine grained elliptical cordierite porphyroblasts - 0.3 - 1.5 cm in diameter - elliptical clasts have long axis parallel to the foliation - matrix is weakly carbonaceous and mica rich		- Foliation at 37°			~6% pyrrhotite	4223	293.3	294.7	1.4	0.2	210	71			



DEPTH (meters) FROM/TO	G R A P H I C	DESCRIPTION	R E C O V E R Y	STRUCTURE			METALLIC MINERALS (%)	SAMPLE DATA				RESULTS				
				ANGLES	VEINS	ALTERATION		SAMPLE NO	FROM	TO	LENGTH	Ag g/t	Pb %	Zn %		
392.2 - 398.4		- light grey siliceous pelitic schist with inter bedded sugary white limestone - limestone layers from 394.6 - 394.8, 396.0 - 396.1, 396.6 - 396.9, 397.0 - 397.7m (interbedded with schist) - quartz band with galena in wisps and aggregates from 398.1 - 398.4 m		- Foliation at 30° - Minor fold axis at 392.4, 395.2m		- weak calcareous - weak sericitic		4236	396.2	396.6	0.4	6.2	0.38	3.52		
398.4 - 401.1		- mottled light grey weakly brecciated dolomite					- stockwork pyrrhotite	4237	399.7	400.3	0.6	0.7	0.03	0.26		
401.1 - 403.0		- sericitic siliceous pelitic schist much like unit from 392.2 - 398.4 m, however, slightly greater percentage of quartz sericitic schist		- Foliation at 40°												
403.0 - 404.6		- banded gray to black argillaceous garnet schist (footwall rock)		- Antiform axis at 403.6 m		- weak to moderate chlorite										
404.6 - 404.6		- sericitic siliceous pelitic schist same unit as 401.1 - 403.0 the unit is fold bounded to above unit with garnet schist in an antiformal axis with siliceous schist folded about it														
404.6 - 405.0		- mottled light grey weakly brecciated dolomite, ~ 5 cm of sericitic siliceous schist at bottom														
405.0 - 405.3		- banded gray to black argillaceous garnet schist - fold axis in center of unit														
405.3 - 407.2		- sericitic siliceous pelitic schist														
407.2 - 409.7		- mottled light grey weakly brecciated dolomite					- stockwork pyrrhotite	4238	407.9	408.5	0.6	0.6	< 0.01	0.05		

















**APPENDIX F**

**Thin sections**



# Vancouver Petrographics Ltd.

## RECEIVED

JAMES VINNELL, Manager  
JOHN G. PAYNE, Ph.D. Geologist  
CRAIG LEITCH, Ph.D. Geologist  
JEFF HARRIS, Ph.D. Geologist  
KEN E. NORTHCOTE, Ph.D. Geologist

FILE: \_\_\_\_\_  
NOV 25 1991  
COPIES TO: \_\_\_\_\_  
P.O. BOX 39  
8080 GLOVER ROAD,  
FORT LANGLEY, B.C.  
VOX 1J0  
PHONE (604) 888-1323  
FAX. (604) 888-3642

Report for: Greg Thomson,  
Teck Exploration Ltd.,  
968 - 175 2nd Avenue,  
KAMLOOPS, B.C., V2C 5W1

*Luq*  
\_\_\_\_\_  
Job 269  
November 1991

Sample: Cordierite-Muscovite Schist, Chancellor Group, MGM Property

### Summary:

Sample 1 is a cordierite-muscovite schist. Complex porphyroblasts of cordierite are set in a well foliated groundmass dominated by muscovite. Many porphyroblasts contain prominent relic textures of a tightly-folded rock. A few segregation lenses and patches are dominated by quartz with locally abundant biotite, ankerite, and/or muscovite. Minor minerals are biotite, pyrite, ankerite, Ti-oxide, and zoisite, and trace minerals are chlorite and tourmaline.

*John G. Payne*  
John G. Payne  
(604)-986-2928



**Sample 1      Cordierite-Muscovite-(Quartz-Biotite-Pyrite-Ankerite)  
Schist; Calcite Vein**

Complex, in part concentrically zoned porphyroblasts of cordierite are set in a well foliated groundmass dominated by muscovite. Many porphyroblasts contain patches with relic textures indicating replacement of a tightly-folded rock. A few segregation lenses and patches are dominated by quartz with locally abundant biotite, ankerite, and/or muscovite. Minor minerals are biotite, pyrite, ankerite, Ti-oxide, and zoisite, and trace minerals are chlorite and tourmaline. At one end of the hand sample is a calcite-(quartz) vein.

cordierite	50-55%
muscovite	30-35
quartz	4- 5
biotite	2- 3
pyrite	2- 3
ankerite/dolomite	1
Ti-oxide	0.5
zoisite	0.3
chlorite	trace
tourmaline	trace

Porphyroblasts averaging 2-5 mm in size are complex intergrowths of cordierite. Early-formed(?) patches averaging 0.2-1 mm in size and locally up to 2 mm across have finely laminated twins, and resemble plagioclase. Some of these form large cores of porphyroblasts. Many of these contain abundant equant inclusions averaging 0.02-0.03 mm in size of quartz. These are the paler colored cores of the "ovoid patches" seen in hand sample. In some porphyroblasts they are replaced irregularly by aggregates of fine to medium grained cordierite, commonly with strongly interlocking grain borders, and locally showing weak lamellar twinning. Elsewhere they are rimmed by similar material. Most of this "secondary" cordierite has a prominent, relic, tightly folded texture outlined by thin trains of semiopaque (Ti-oxide), which indicates that cordierite formed by replacement of a tightly folded rock rich in phyllosilicates. These inclusions give this cordierite a darker grey color. Cordierite is altered slightly to very fine to extremely fine grained muscovite/sericite. Some porphyroblasts contain moderately abundant disseminated flakes of muscovite averaging 0.1-0.15 mm long oriented parallel to foliation; this muscovite probably is of metamorphic rather than replacement origin.

Muscovite is concentrated in patches and seams between porphyroblasts, and shows a moderate to prominent foliation which is warped slightly around some porphyroblasts. It forms slightly interlocking aggregates of flakes averaging 0.1-0.2 mm in size, and a few up to 0.5 mm long.

Quartz is concentrated in a few lenses and seams averaging 0.5-1.0 mm wide as very fine to fine grained aggregates. Intergrown with quartz is minor to moderately abundant biotite, muscovite, and/or ankerite/dolomite.

Biotite is concentrated moderately in a few layers, mainly at one end of the section as ragged flakes averaging 0.1-0.3 mm in size interstitial to cordierite, and subhedral flakes intergrown with quartz. It forms a few porphyroblasts in cordierite, which appear to have formed after cordierite. Pleochroism is from pale to light yellowish brown.

Sample 1 (page 2)

Pyrite forms irregular patches up to 1.5 mm in size; in part it may have formed by replacement of Ti-oxide. It also occurs as discontinuous veinlets up to 0.07 mm wide in porphyroblasts.

Ti-oxide forms irregular to skeletal patches averaging 0.2-0.7 mm in size, commonly enclosed in porphyroblasts.

Ankerite forms ragged patches of very fine to fine grains concentrated in a quartz-ankerite segregation lens at one end of the section, and forms extremely fine grained seams and discontinuous veinlets elsewhere in the rock.

Zoisite forms a few ragged to subhedral grains averaging 0.3-0.6 mm in size.

Chlorite forms a few patches up to 0.3 mm across of pale green flakes.

Tourmaline forms scattered, subhedral, prismatic grains averaging 0.1-0.12 mm long. Pleochroism is from pale to light or medium yellowish green.

**APPENDIX G**  
**Geophysical Report**

**BOREHOLE UTEM SURVEY**

**ON THE**

**MGM PROPERTY**

**FOR**

**TECK EXPLORATION LTD.**

**SURVEY BY**

**SJ GEOPHYSICS LTD. AND LAMONTAGNE GEOPHYSICS LTD.**

GOLDEN M.D., B.C.

N.T.S. 83D/1

NOVEMBER 1991

REPORT BY

SYD J VISSER  
SJ GEOPHYSICS LTD.

## TABLE OF CONTENTS

	PAGE
INTRODUCTION	1
DESCRIPTION OF UTEM SYSTEM	1
FIELD WORK	2
DATA PRESENTATION	4
SURVEY PREPARATION	5
MODELING	5
<i>VECTOR PLOTS</i>	
<i>MULTILOOP MODELS</i>	
INTERPRETATION	7
<i>TK-91-04</i>	
<i>TK-91-02</i>	
RECOMMENDATIONS	8
CONCLUSION	9
APPENDIX I	Statement of Qualifications
APPENDIX II	Legend
APPENDIX III	A time domain EM system measuring the step response of the ground
APPENDIX IV	Data sections

## INTRODUCTION

A large loop time domain electromagnetic (UTEM-3) Borehole survey was completed by SJ Geophysics Ltd. and Lamontagne Geophysics Ltd., for Teck Exploration Ltd. on the MGM Property. The MGM property is located north of Golden, B.C., on the east side of Columbia Reach and south of Cummings Arm in the Golden M.D., of B.C. (N.T.S. 83D/1).

The purpose of the survey was to search for massive sulphide.

## DESCRIPTION OF UTEM SYSTEM

UTEM is an acronym for "University of Toronto ElectroMagnetometer". The system was developed by Dr. Y. Lamontagne (1975) while he was a graduate student of that University.

The following is a short description of the UTEM system used in the field. A paper (A time-domain EM system measuring the step response of the ground) by G.F. West, J.C. Macnae and Y. Lamontagne, giving a more complete description with an overview of interpretations is located in Appendix III.

The field procedure consists of first laying out a large loop, which can vary in size from less than 100M X 100M to more than 2Km X 2Km, of single strand insulated wire and energizing it with current from a transmitter which is powered by a 2.2 kW motor generator. During a surface survey the lines are generally oriented perpendicular to one side of the loop and surveying can be performed both inside and outside the loop. For Borehole survey the sensor coil is placed down the borehole measuring the axial component of the electromagnetic field from a minimum of 2 separate loops.

The transmitter loop is energized with a precise triangular current waveform at a carefully controlled frequency (30.97 Hz for

this survey). The receiver system includes a sensor coil and backpack portable receiver module which has a digital recording facility. The time synchronization between transmitter and receiver is achieved through quartz crystal clocks in both units which are accurate to about one second in 50 years.

The receiver sensor coil measures the vertical horizontal, or axial magnetic component of the electromagnetic field and responds to its time derivative. Since the transmitter current waveform is triangular, the receiver coil will sense a perfect square wave in the absence of geologic conductors. Deviations from a perfect square wave are caused by electrical conductors which may be geologic or cultural in origin. The receiver stacks any preset number of cycles in order to increase the signal to noise ratio.

The UTEM receiver gathers and records 10 channels of data at each station occupied. The higher number channels (7-8-9-10) correspond to short time or high frequency while the lower number channels (1-2-3) correspond to long time or low frequency. Therefore, poor or weak conductors will respond on channels 10, 9, 8, 7 and 6. Progressively better conductors will give responses on progressively lower number channels as well. For example, massive, highly conducting sulfides or graphite will produce a response on all ten channels.

The Borehole system consists of a normal surface UTEM-3 transmitter and receiver along with special receiver coil (1 1/4" in diameter). The coil is connected to the receiver through a controller and fibre optic cable.

## **FIELD WORK**

Syd Visser (chief geophysicist), Chris Basil, (operator), both with SJ Geophysics Ltd., and the equipment were mobilized from Cranbrook through Golden to Columbia Reach and by barge to the property, on November 8, 1991. The work on the MGM property was completed between November 8, 1991 and November 14, 1991. The survey area were accessed daily by truck with chains on all 4

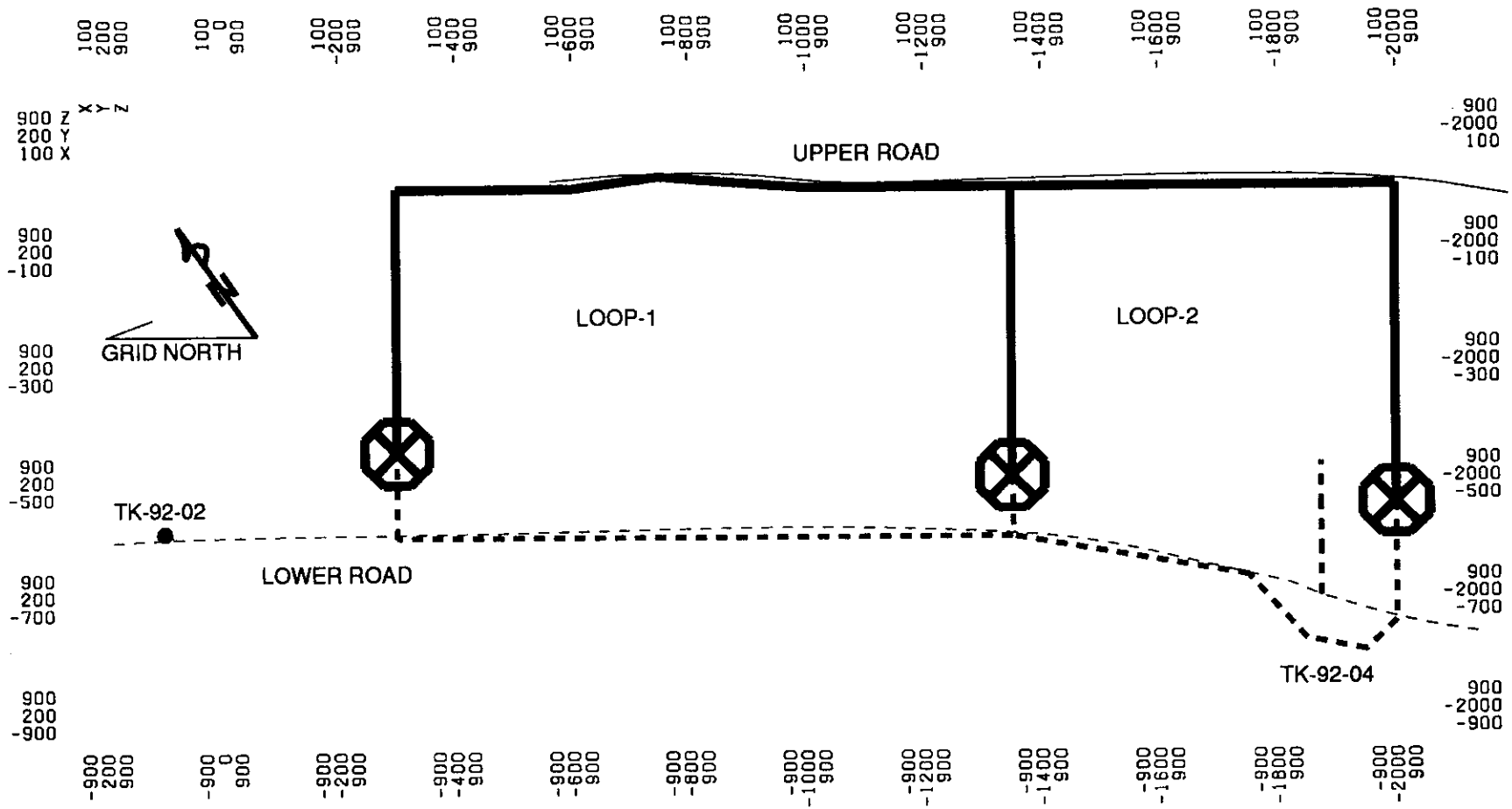
wheels because of the wet snow. The crew and equipment was demobilized on November 13, 1991 by barge to a landing near Mica Dam and then by road through Revelstoke to Vancouver on November 14, 1991.

The field parameters and local geology were discussed in the field with geologist (Gregg Thomson, Carol Lormand and Craig Alford) employed by Teck Exploration Ltd., before commencing the survey and during the survey period.

All the personal helped to lay out the two loops required for the Borehole survey. The snow conditions and steep topography forced us to locate the loops between two accessible logging roads. Teck personal agreed to take responsibility of the removal of the wire at a later date since it was almost impossible to recover due to the present weather conditions. The wet weather, near freezing temperatures along with the barge ride and damp propane heating in the accommodations were the likely cause for the majority of the equipment problems causing the loss of approximately one-half day production and long work days. Even the computer did not operate properly until it was dried for 3 days.

The first production day November 9, 1991 was used to lay out the two loops and prepare the equipment. Boreholes TK-91-01 (BH-1) and TK-91-02 (BH-2) were dummy probed on the second day. BH-1 was blocked due to excessive grease in the hole. An additional attempt was made by adding weight to the dummy probe with little success. BH-2 was surveyed on November 11, 1991. Borehole TK-91-04 (BH-4) was dummy probed before moving the drill and successfully surveyed that evening after repairing the equipment. Fuel oil was pored down BH-1 and attempts were made to enter the hole again on November 13, 1991 with no success. The diamond drillers informed us that borehole TK-91-03 was blocked therefore no attempts were made to survey it.





GOLDEN MINING DISTRICT  
 N.T.S. 83D/1  
 COLUMBIA REACH  
 CUMMINGS ARM

# LOOP LOCATION MAP MGM PROPERTY

BY: SJ GEOPHYSICS LTD  
 FOR: TECK EXPLORATION LTD.

**MAP-1**

## DATA PRESENTATION

The results of the 1991 UTEM survey are presented on 4 data sections along with 3 computer generated models (FIG-1 to FIG-3) and 2 vector plots (FIG-4 and FIG-5)

Legends for the UTEM data sections are also attached (Appendix II).

In order to reduce the field data, the theoretical primary field of the loop must be computed at each station. The normalization of the data is as follows:

a) For Channel 1:

$$\% \text{ Ch.1 anomaly} = (\text{Ch.1} - \text{PC}) / \text{PT} \times 100$$

Where:

PC is the calculated primary field in the direction of the component (axial in borehole) from the loop at the occupied station

Ch.1 is the observed amplitude of Channel 1

PT is the calculated total field

b) For remaining channels (n = 2 to 9)

$$\% \text{ Ch.n anomaly} = (\text{Ch.n} - \text{Ch.1}) / \text{Ni} \times 100$$

where Ch.n = the observed amplitude of Channel n (2 to 9)

N = Ch.1 for Ch1 normalized

N = PT for primary field normalized

i is the data station for continuous normalized (each reading normalized by different primary field)

i is the station below the arrow on the data sections for point normalized (each reading normalized by the same primary field)

Subtracting channel 1 from the remaining channels eliminates the topographic (loop and borehole location) errors from all the data except ch.1. If there is a response in channel 1 from a conductor (due to a very good or very large conductor) then this value must be added to do a proper conductivity determination from the decay curves. Therefore channel 1 should not be subtracted indiscriminately.

The axial component of the primary field is also plotted on the sections (the curve without symbols) to determine the direction of the field in the borehole.

## **SURVEY PREPARATION**

To prepare for the survey it is very important to maximize the coupling of the primary field, from at least one loop, with the possible location of the mineralized zone (conductor). The additional loops are to maximize coupling with other possible conductors or to change the coupling of the primary field with the conductor to aid in determining the location of the conductor with respect to the borehole. To determine the best location of the loops with respect to the hole and possible conductors a number of vector plots are generated. The drill holes and possible mineralized zones are drawn on the vector plots to determine the best loop location. On this property it was determined that placing the loops between the two logging roads was the best compromise between maximizing coupling and ability to lay out the loops due to the topography and snow conditions. The loops could likely have been better located with better weather conditions.

## **MODELING**

### **VECTOR PLOTS**

The vector plots are used both to determine the best loop locations for the borehole survey and to aid interpretation. The vector plots are generated on a computer and are a section, located

at any position or angle, that shows the direction and relative strength of the primary field in the section. The arrows are in the direction of the primary field and the length of the arrow is the strength ( $\log_{10}$ ), normalized by the current, of the primary field. The location of the section is marked along the edges of the section. The location of the loops and boreholes are projected on to the section with the solid lines showing the portion that is located to the front of the section and the dashed lines showing the portion located behind the section. The location of possible conductors are then drawn on the section by hand to determine the coupling and the direction of the secondary field. FIG-4 and FIG-5 are examples of vector plots. These plots are vertical sections through borehole TK-91-04, close to TK-91-02 and through loop-1 (FIG-4) and loop-2 (FIG-5).

#### **MULTILOOP MODELS**

Multiloop is a 3D electromagnetic (EM) computer modeling program developed by Lamontagne Geophysics Ltd. which models the EM response of an infinitely thin plate in free space (assuming and infinitely resistive ground) from a specified source. The thin plate is divided into a number of loops (usually 20) within the plate as shown in the models FIG-1 to 3. A large number of plates can be used in each model and the mutual inductance between all the loops are taken into account. This is a inductive response and any current channeling or response due to a conductive host rock is not taken into account. The computation time involved in computing a conductor in a conductive host rock is still prohibitive.

The programs outputs a 3D presentation showing the location of the loop, conductor, the survey line (or borehole) and the EM response from the conductor. The thin vertical lines projecting down from the loops and plate model indicates the distance to the zero elevation level. The direction shown on the models are grid north and grid east.

## INTERPRETATION

### BOREHOLE TK-91-04

There is a weak extensive conductor, with a conductivity of approximately 10mhos, located between a depth of 480 and 500m depth in borehole TK-91-04. The sign of the secondary field from the anomaly is the same as the primary field outside loop-1 and opposite in sign from loop-2 therefore conductor must be located towards the loop in the north east direction as shown in FIG-3. The sharp return on the lower end of the anomaly from loop-1 suggests that the conductor is dipping towards the north. The data from loop-2 confirms the large anomaly but also indicated a small but very strong off-hole anomaly located at a depth of approx. 460M. This has to be a small (at least in two dimensions) very good conductor located very close to the borehole and is likely not seen from loop-1 because of poor coupling. Both of these anomalies appear to correlate with weak mineralization located between a depth of 460 and 500M.

The background indicates that the background currents are past the holes on both loops.

### BOREHOLE TK-91-02

The data from the borehole Tk-91-02 indicates a conductive zone with a conductivity of approximately 10 mhos near the bottom of the hole at a depth of 460 to 550 m. This conductor correlates well with thin bands of graphite and pyrite in the drill hole. The major part of this anomaly is off-hole and likely to the east and north as shown on the model FIG-1 and FIG-2 . The same response is seen from both loop 1 and 2.

A surface calibration on borehole TK-91-01 from loop-2 indicated a positive response therefore this borehole is likely south of or near the southern edge of the conductive zone. The weak negative response along the length of the borehole is likely due to the currents flowing parallel to the borehole, along the southern edge of the dipping conductor. The negative response could also be due

to the conductor under the loops that is intersected in the borehole TK-91-04 but it is likely that this would also result in a negative surface calibration.

### **RECOMMENDATION**

It is recommended to survey the area from the surface with a time domain UTEM survey before attempting to survey the remaining two holes. With proper coupling, of the electromagnetic field with a conductor, a surface survey will be able to locate any conductors with dimension larger than the depth to the top of the conductor. The surface survey would also give a better indication of the edges of the weakly conductive horizon and locate areas of better conductivity within the weakly conductive horizon. The results from the surface survey would also be very beneficial in optimizing the loop locations for the borehole survey and to the interpretation of the borehole data.

The best location, in terms of good coupling of the possible conductors with the electromagnetic field, would be to place the loop above (to the east of) the surface trace of the prospective zone and survey to the west. The line spacing would depend somewhat on the size of conductor and depth of interest but should not be greater than 200m. Since the weak conductive plate appears to be terminated in all directions and the dip is close to the slope of the hill it can be viewed as a relatively flat lying plate. It is therefore not crucial to locate the loop on the top of the hill and survey down. A more cost effective method may be to survey parallel to the hill and therefore utilizing some of the existing roadways for survey lines. In this case a loop could be placed to the south of or surrounding the survey area. The direction of the survey could be crucial. If it is possible that the good mineralization could be elongated in one direction or the folding is predominately in one direction.

The results of the Max-Min survey should also be investigated to determine the conductivities of the near surface mineralization. These results along with all the geophysical and geological infor-

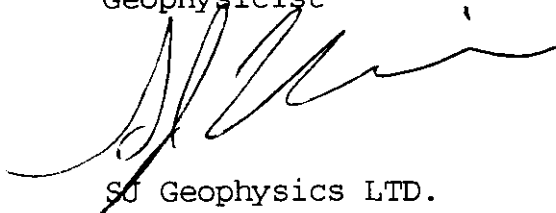
mation could be aided with modeling to determining the optimum loop and line locations locations.

### CONCLUSIONS

There is no indication of any large very good conductor in the borehole data. Both holes indicate that they are near the edges of large weakly conductive layers. It does not appear that the conductor is continuous between the holes although not enough information is available to confirm this. There is a strong but very small conductor located close to borehole TK-91-4.

It is recommended to combine a surface survey (the same equipment is used for both surveys) with any further borehole surveys in the area to located any good conductors from surface, to locate the edges of the weakly conductive zones, and to aid in the interpretation of the borehole data.

Syd Visser B.Sc., F.G.A.C.  
Geophysicist

A handwritten signature in black ink, appearing to read 'S. Visser', written over a horizontal line.

SG Geophysics LTD.

APPENDIX I

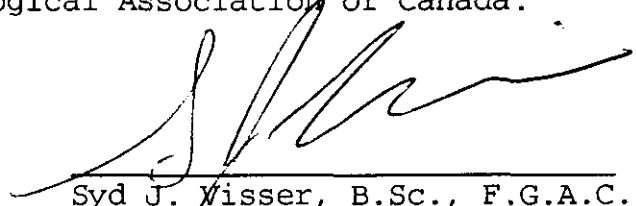
---



**STATEMENT OF QUALIFICATIONS**

I, Syd J. Visser, of 11762 94th Avenue, Delta, British Columbia, hereby certify that,

- 1) I am a graduate from the University of British Columbia, 1981, where I obtained a B.Sc. (Hon.) Degree in Geology and Geophysics.
- 2) I am a graduate from Haileybury School of Mines, 1971.
- 3) I have been engaged in mining exploration since 1968.
- 4) I am a Fellow of the Geological Association of Canada.



---

Syd J. Visser, B.Sc., F.G.A.C.  
Geophysicist

APPENDIX II



UTEM SYSTEM MEAN DELAY TIME

<u>Channel Number</u>	<u>Delay Time (msec)</u>	<u>Symbol</u>
1	12.8	
2	6.4	∖
3	3.2	/
4	1.6	□
5	0.8	∩
6	0.4	△
7	0.2	∇
8	0.1	×
9	0.05	△
10	0.025	◇

Base Frequency = 31 Hz

APPENDIX III

## A time-domain EM system measuring the step response of the ground

G. F. West\*, J. C. Macnae\*†, and Y. Lamontagne‡

### ABSTRACT

A wide-band time-domain EM system, known as UTEM, which uses a large fixed transmitter and a moving receiver has been developed and used extensively in a variety of geologic environments. The essential characteristics that distinguish it from other systems are that its system function closely approximates a step-function response measurement and that it can measure both electric and magnetic fields. Measurement of step rather than impulse response simplifies interpretation of data amplitudes, and improves the detection of good conductors in the presence of poorer ones. Measurement of electric fields provides information about lateral conductivity contrasts somewhat similar to that obtained by the gradient array resistivity method.

### INTRODUCTION

This article describes the design of the UTEM system and its development at the Geophysics Laboratory of the University of Toronto by Y. Lamontagne and G. F. West from 1971 to 1979. UTEM is a wideband, time-domain, ground EM system with a step-function system response. It was designed to try to achieve the sensitivity and interpretability necessary to handle problems of deep exploration, conductive environments, and a variety of terrain conditions, in an economically viable manner. As with most EM systems, effective exploration for massive sulfide ores was the principal objective. The method was conceived in 1971, and the first UTEM I instrument was operational in 1972. It was an analog electronic system, and was used in a number of surveys which have been described by Lamontagne (1975). An improved UTEM II which incorporated a digital recording system was then designed and constructed at the University of Toronto with financial aid from a consortium of mining companies. It was first used in 1976. To fall 1980, about 1000 line-km had been surveyed with the system from 144 loops in 35 areas. UTEM III, which is a microprocessor-controlled system with expanded capabilities, is now produced commercially by Lamontagne Geophysics Ltd. Some of the field results obtained using the UTEM II system have been described in Lamontagne et al. (1977, 1980), Macnae (1977, 1980, 1981), Lodha (1977), and Podolsky and Slankis (1979). Data from all

three UTEM systems are identical insofar as geophysical characteristics are concerned. The differences affect only data noise levels and operational convenience. Some of the noise rejection features of UTEM III are discussed by Macnae et al. (1984).

### THE UTEM SYSTEM

#### Design philosophy

UTEM uses a large, fixed, horizontal transmitter loop as its source. The field of the loop is mapped in the quasi-static zone with the receiver system; the vertical component of the magnetic field is always measured, and in some circumstances the horizontal magnetic and electric field components may be measured as well (Figure 1). The size of the transmitter loop depends on the prospecting problem; loops may range from about 2 km x 1 km in resistive terrain to 300 m x 300 m in a conductive area. Lines are typically surveyed to a distance of 1.5 to 2 times the loop dimensions.

The large loop transmitter-field mapping receiver configuration was chosen in order to give the system the deepest possible exploration for orebody sized conductors, without sacrificing the ability to resolve shallower structures (depth < 50 m). This dictates a very large transmitter moment, and makes an extended source desirable. The virtue of an extended source is that the coupling between the source and a receiver or the source and a nearby conductive zone is not so many orders of magnitude larger than the coupling to a distant receiver or deep target as is the case with a confined source.

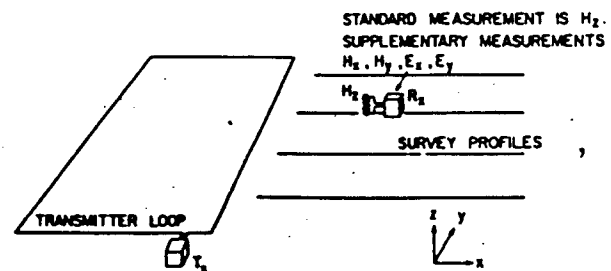


FIG. 1. Schematic layout of a UTEM survey.

Manuscript received by the Editor November 1983; revised manuscript received December 1983.  
 \*Geophysics Lab., Dept. of Physics, Univ. of Toronto, Ont., Canada M5S 1A7.  
 †Lamontagne Geophysics, 740 Spadina Ave., Toronto, Ont., Canada M5S 2J2.  
 © 1984 Society of Exploration Geophysicists. All rights reserved.



S. J. V. CONSULTANTS LTD.

SYD J. VISSER B.Sc. FGAC.

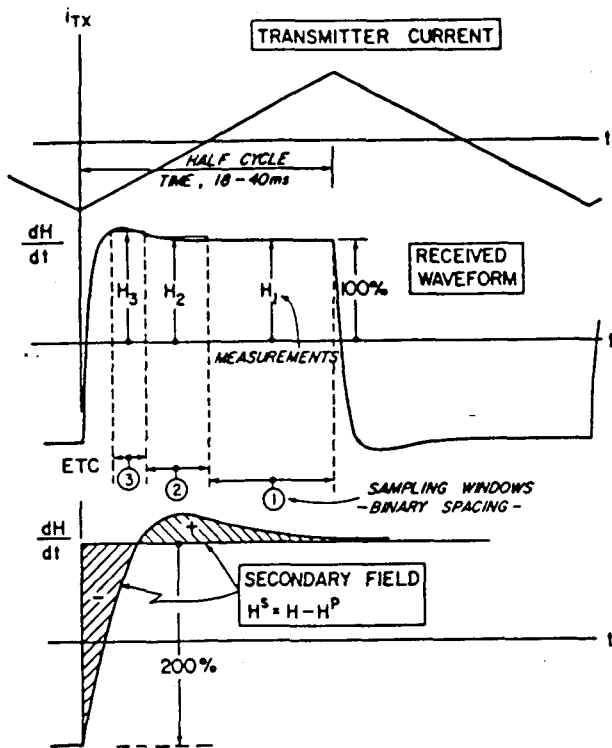


FIG. 2. Transmitted and received UTEM waveforms. Note that the measurement channels are numbered from the latest to the earliest. Sampling is repeated, with due regard to sign, in every half-cycle.

Given a large transmitter and a large Tx-Rx separation, it is inevitable that induction in extensive conductive overburden and in large formational conductors will contribute more to the response than with a small scale system. Also, as the separation becomes larger it becomes increasingly likely that the system will be responding to several nearby conductors at once. However, a fixed transmitter-moving receiver system offers a basis for separating the signal contributions from the various conductors and resolving the geometry of deep-seated conductors. At any time instant, the magnetic field of the current system induced in the ground is a potential field (within the quasi-static zone), and if it is mapped on a profile or over a surface, there is a firm theoretical basis for separating it into parts and estimating the current systems which caused it. When the transmitter and hence the eddy current system move for each observation, it is more difficult to find a theoretical basis for stripping of responses into component parts.

There are negative aspects to using a fixed transmitter method. In addition to the aforementioned enhancement of anomalies due to formational conductors, the transmitter can be positioned badly for induction in small plate-like conductors, and a large good conductor can screen a smaller, shorter time-constant conductor which lies behind it. For these reasons it may be desirable to have survey coverage from more than one transmitter location.

The UTEM II transmitter passes a low-frequency current of precise triangular waveform through the transmitter loop. The magnetic field is sensed with a coil, which responds to the time

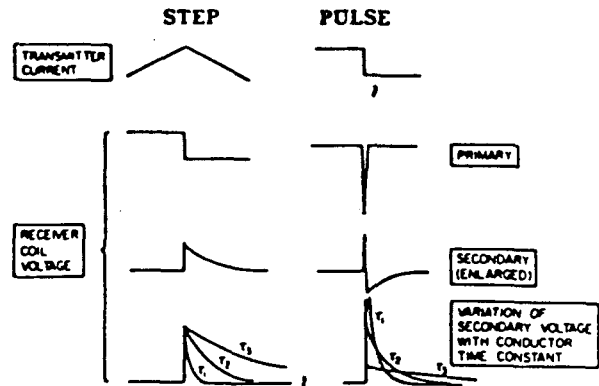


FIG. 3. Comparison of transient signals in step and pulse type systems.

derivative of the local magnetic field, so in "free space" a precise square-wave voltage would be induced in the receiver. In the presence of conductors the waveform is substantially distorted. The UTEM receiver measures this distortion by determining amplitudes at 10 delay times (actually, averages over time windows) which are spaced in a binary geometric progression between the waveform transitions. The sample scheme is shown in Figure 2. Note that the UTEM channel numbers are conventionally numbered in reverse order of time. This is because the latest time measurement often serves as a reference to which the other measurements are compared, whereas the number of earlier time measurements which can be made accurately may change if base period or instrument bandwidth is altered. The base frequency of the system is selectable, usually about 30 or 15 Hz (25 or 12.5 Hz in countries with 50 Hz power). A common practice is to set the base frequency (adjustable in 0.1 percent steps) about 0.5 Hz from a subharmonic of the power line in order that power line interference can be detected by slow beating in the data. The base frequency is usually set low enough that all ground response has nearly vanished by the end of the half-cycle. When this is the case, the UTEM system determines the step response of the ground in the time range  $25\mu\text{s}$  to 12.8 ms (30 Hz base frequency).

#### Time-domain systems

Time-domain systems have some advantage over frequency-domain systems in that simultaneous measurement is easier to achieve over the whole spectrum and, at the same time, it is possible to check the phase synchronization of the transmitter and receiver time bases. Most time-domain systems employ an on-off type of transmitter current and confine all measurements to the off-period, as this automatically separates the secondary from the primary field. However, when a coil is used as a sensor, the time derivative of the signal is observed. Thus, if the transmitter loop is energized with a step current, it is the impulse response of the ground which is observed.

When prospecting for conductive mineral deposits, it is generally more desirable for interpretation purposes to observe the step response than any other time response. The reason for this lies in the characteristics of eddy current decay. For the step

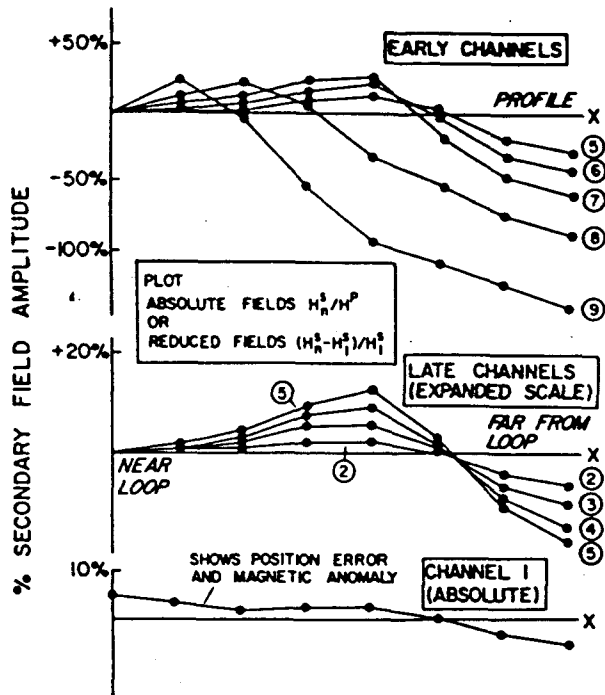


FIG. 4. Standard presentation of UTEM vertical component magnetic field data.

response, the early-time limit of response is identical to the frequency-domain inductive limit, and for a simple conductor in free space this is a function of geometry alone. For the impulse response, the early time limit is scaled from the step response limit by the inverse of the transient decay time constant (Figure 3). Thus, the decay rate must first be determined in order to interpret amplitude information in terms of geometry. This may present little difficulty in simple cases, but when complex or overlapping responses are observed it can be a serious problem. Also, even in the case of the step response, overburden anomalies which generally are of short time constant have early time amplitudes which are very much larger than the anomalies of target conductors with long time constant. Any further amplification caused by measuring the impulse rather than step response is clearly undesirable.

Although a system with a step response is usually desirable for interpretation purposes, the UTEM system is only one implementation of such a system. In fact a system using a magnetometer receiver with a square-wave transmitter instead of an induction coil (referred to as MSW system in the following sections) would have an identical system response. The foregoing rationale of the interpretational advantages of step response does not consider the other important factors which enter the design of actual systems such as signal-to-noise (S/N) efficiency and transmitter-sensor design constraints which in fact guide the choice of the actual transmitter waveform and sensor used. This is a complex topic discussed by Lamontagne et al. (1980). For example, the UTEM III system actually uses a modified triangular transmitter waveform and deconvolution in the receiver to improve its S/N performance but has a system response identical to the UTEM I and UTEM II systems (Macnae et al., 1984), i.e., a square-wave response. Thus the UTEM I/II systems, the conceptual MSW system, and the

UTEM III system all make identical measurements although they excite the ground differently. To avoid any confusion, discussions in this paper of actual induced current waveforms in the ground will be limited to the UTEM system with a purely triangular waveform and to the MSW system.

The sampling scheme of Figure 2 was chosen so that virtually all measuring time is utilized and time scaling of the measurements is permitted. In the frequency domain, inductive responses may be characterized by dimensionless parameters of the form

$$\theta_f = \sigma\mu\omega L^2,$$

which demonstrates that scale changes of conductivity, frequency or (length)<sup>2</sup> are equivalent to one another. The analogous parameter for the time domain is

$$\theta_t = \sigma\mu L^2/t.$$

In interpreting frequency-domain data, it is common to compare observed frequency response data with dimensionless model response data. This is convenient because it avoids the necessity of rescaling the model data for all frequencies and physical scale lengths that might be encountered in the field cases. The same sort of scaling is possible with time-domain data, but only if the system function of the apparatus is a pure discontinuity response. If this is not the case, for instance when the apparatus has a characteristic ramp shut-off time, model response curves cannot be rescaled in time to match field data as this would imply rescaling the shut-off time to a value different from that used by the apparatus.

To ensure that time scaling can readily be applied to data that have been sampled and averaged over a time window, it is also necessary that the window widths be proportional to time after the discontinuity. UTEM has such sampling. It should be noted that time scaling may only be applied to UTEM anomalous responses which are short enough so as to have vanished in the interval between the two successive transitions of the step which form the square wave.

#### Data presentation

Because the field intensity falls off rapidly with increasing distance from the transmitter loop, it is often desirable to normalize the secondary field observations in some manner. One suitable normalizing factor is the primary vertical magnetic field signal ( $H_1^p$ ). If the positions of the transmitter loop and the receiver are known reasonably accurately, a calculated value of  $H_1^p$  may be employed. If the ground response vanishes by late time, the channel 1 measurement is a direct measure of  $H_1^p$ . Normal survey data plotting practice encompasses both procedures.

Figure 4 is an example of a standard plot of UTEM secondary vertical magnetic field data ( $H_1^s$ ). Channel 1 is plotted as secondary field (Ch 1- $H_1^s/H_1^p$ ) (where  $H_1^p$  is the calculated primary field) and all other channels are normalized to Ch 1 [(Ch  $n$ -Ch 1)/Ch 1] to correct for any position error in calculation of  $H_1^p$  and also to remove the effect of induced magnetic anomalies (for further details see Lamontagne, 1975). The late channels on the example plot show a crossover type of anomaly, indicative of a concentration of (changing) induced current, as will be discussed. The amplitude variation with channel number indicates that these induced currents are decaying with

time. A small component of response appears to have persisted to Ch 1 and, for quantitative analysis, it should be remembered that the data reduction process will have caused subtraction of this amount from profiles of Ch 2-Chn. On the early-time channels, the migration of crossover location from one channel to another indicates that the secondary current flow at these times is not fixed in geometry, a characteristic which is indicative of an extensive conductor (here extensive overburden) rather than a localized conductor such as that responsible for the late time crossovers.

Since at any delay time, the secondary field is a potential field, interpretation of geometrically fixed current systems is best performed using absolute secondary fields normalized by the primary field intensity at a single point rather than continuously along the profile. Although only one case presented in this paper has this absolute or "point normalization," recent routine field practice is to point normalize all survey profiles exhibiting discrete anomalies, in order to simplify interpretation.

Horizontal magnetic field measurements may be made by

reorienting the receiver coil. Normalization is done using the vertical primary magnetic field (calculated or vertical Ch 1 measurement). Unfortunately, horizontal field measurements frequently suffer a somewhat higher noise level than vertical fields, due to the predominantly horizontal orientation of sferic interference.

The electric field waveform is, like the voltage from the coil sensor, a square wave if the ground is very resistive. It is distorted in much the same way as the coil signal when the ground is conductive. Electric field observations are usually plotted as  $E_i/E_T^p$ —the observed channel voltage between the electrodes divided by the maximum expected late time voltage between electrodes at the observation point in any horizontal direction, i.e.,  $E_T^p = (E_x^2 + E_y^2)^{1/2}$ . "Expected" here refers to the electric field produced by a loop on a laterally uniform, resistive half-space. This normalization facilitates intercomparison of x and y component data. The geologic noise level in electric field data is usually high, so plotting on expanded scales is rarely justified. All channel data are usually plotted on the same axes, as shown in Figure 5.

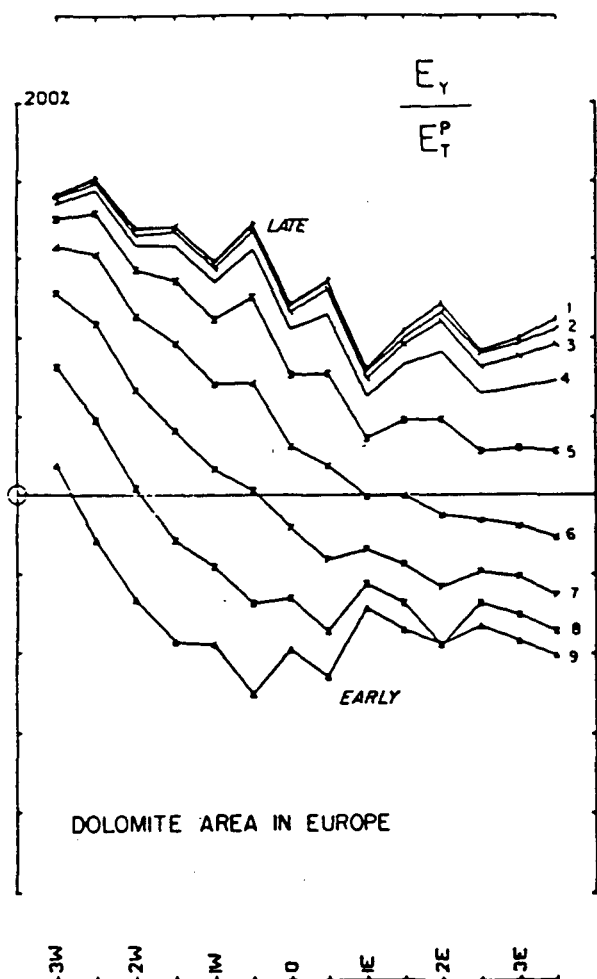


FIG. 5. Standard presentation of electric field data. The observed component is normalized to the total primary electric field of the transmitter loop.

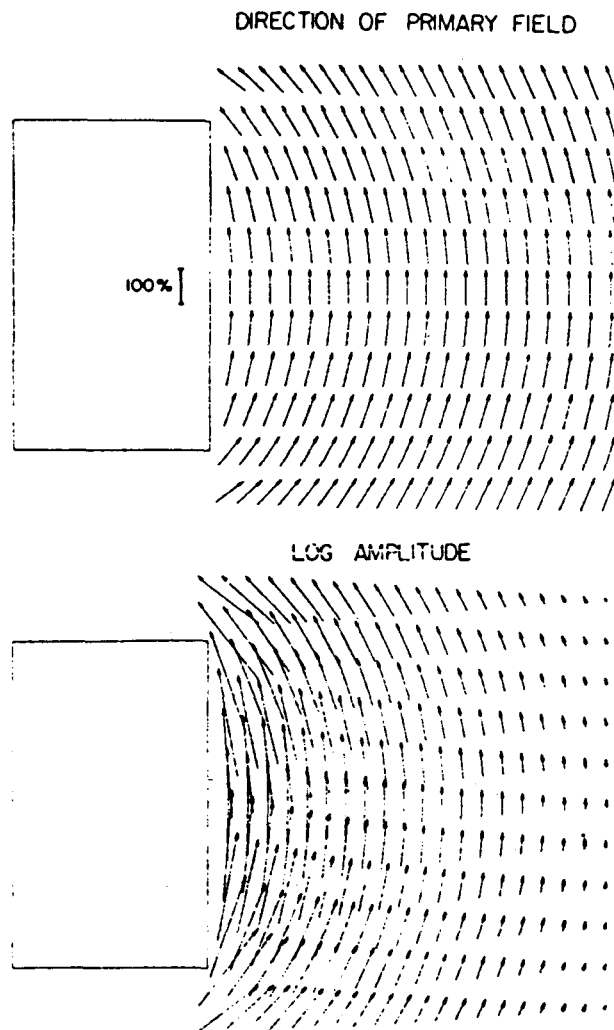


FIG. 6. Vector plots of late time electric field. (a) Direction information only. (b) Showing direction and intensity of the primary field.



The reference state for electric field data is usually described as a "laterally uniform, resistive half-space," rather than free space. By resistive is meant a case where all inductive transients have died out. The free-space electric field of a horizontal loop is horizontal, so introduction of a resistive half-space does not affect the field. However, for any other orientation of the transmitter loop or the earth-air interface, the free-space electric field will be directed across the interface and a strong distortion of the field will occur. Since the conductivity of air is virtually zero, the earth-air interface almost always has a high conductivity ratio, even if the earth is resistive in terms of induction. The charge which arises on the interface essentially doubles the vertical component of the  $E$  field in the air near the boundaries and annuls the vertical component in the ground. Thus the  $E$  field in the ground is (almost always) virtually horizontal. The nomenclature for the reference state serves to remind one that the earth-air interface has an important role in the physics of

the electric field and is always assumed to be present, but no lateral inhomogeneity or induction is permitted in the reference model.

The electric field of a heterogeneous, conductive earth does not normally become constant at late time, as the EM transients vanish. At the same time, the rate of change of magnetic field becomes constant. However, the observed late-time  $E$  limit is usually found to be different from the free-space or uniform resistive half-space value, due to lateral inhomogeneity of the earth's conductivity structure. The late-time electric field around a loop greatly resembles what might be seen in a gradient resistivity survey. The field weaves about, deflected around the more resistive areas and through the more conductive ones. A vector display of the late-time  $E$  field is an interesting reflection of the relative conductivity of various parts of the ground. It is impractical to plot the unnormalized  $E$  vectors, since the true field intensity falls off rapidly with increasing distance from the loop. The lengths of the plotted vectors are therefore proportioned to the normalized field of the loop, as for profile plots. Vector plots of the free-space field of a loop are shown in Figure 6. Examples of field data are given in the following section.

Errors caused by the presence of EM noise or by poor geometrical control are discussed for the magnetic ( $H$ ) field case in Lamontagne (1975). For the electric ( $E$ ) case, details of the measurement and sources of error are discussed in appendix G of Macnae (1981). As in the dc resistivity method, topographic features can seriously distort local electric fields, and local conductivity contrasts such as overburden patches and minor lithological changes can have quite large effects on the amplitude of measured  $E$  fields.

## INTERPRETATION

We shall describe briefly the responses from a number of simple geologic models and how these can be identified and interpreted.

### Layered earth responses

The problem of EM induction in a layered earth is very well treated in the literature, particularly for frequency-domain systems (e.g., Wait, 1962). Time-domain cases have also been studied for some specific problems, for example the infinite thin sheet was solved by Maxwell (1891) and the half-space response is discussed by Nabighian (1979). A general, layered earth solution for UTEM geometry and waveforms was given in Lamontagne (1975). Figure 7 shows three examples of computed responses for different layer conductivities. Figure 8 shows three examples of a thin layer at different depths. There are several common characteristics of layered earth responses. The shapes of the anomalous profiles are generally similar, becoming broader at later times. The migration of crossovers with time, with positive lobes toward the loop and negative lobes away from the loop, seems to indicate that the induced current system is migrating away from the loop. This is the type of behavior described by Nabighian (1979) as an expanding smoke ring.

If the UTEM system employed a magnetometer as receiver and a square current waveform in the transmitter, the smoke ring analogy would be exact, as the crossovers would indicate

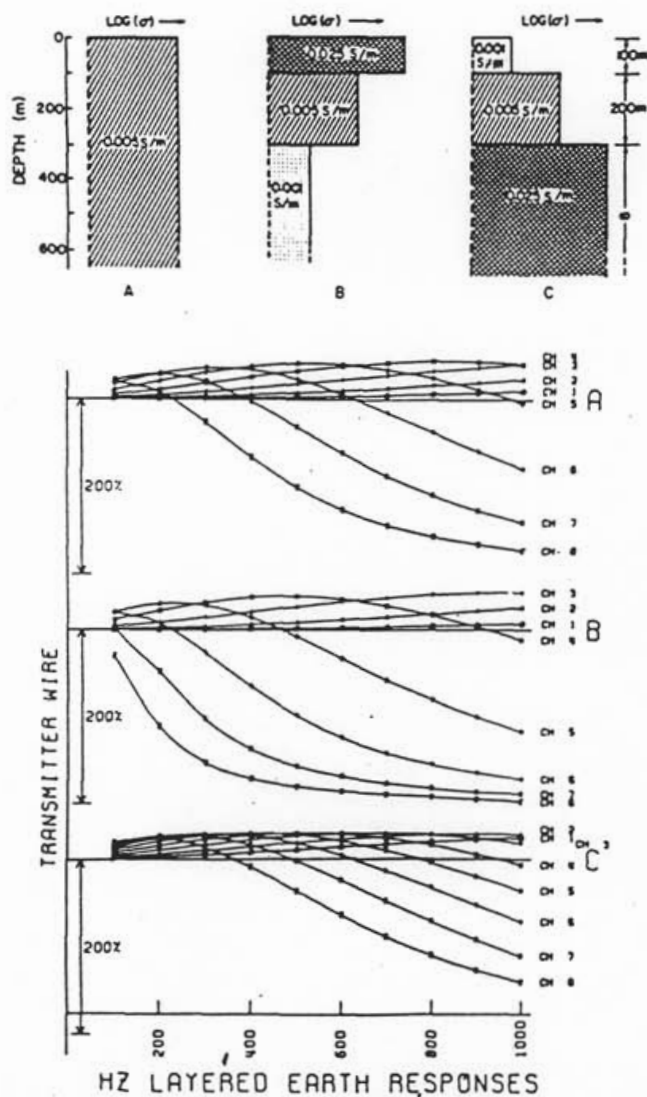


FIG. 7. UTEM layered earth response.

the position of the main current concentrations. However, the UTEM receiver is a coil which is sensitive only to  $dH/dt$ , and thus to the rate of change of induced and transmitter loop current. Thus the moving pattern of crossovers is actually indicating outward migration of changes in the induced current pattern. Toward the end of each half-cycle, the induced current system at any point in the survey area tends to a constant value, as indicated by the electric field measurements, but this steady current is invisible to the coil receiver.

When interpreting UTEM magnetic field data, it can often be simpler to think of the data in terms of the magnetometer receiver, square-wave transmitter current (MSW) analogy. Because the analogy is exact for a linear process like EM induction, there is no approximation in using it. It is very convenient to think of the field measurements of secondary signal at any delay time as describing the Biot-Savart magnetic field of a changing and decaying (analogous) induced current system. However, when electric field data are being analyzed and compared with magnetic field ( $dH/dt$ ) data, it is necessary to revert to the true picture of the induced currents (or take a time derivative of the  $E$  data) to maintain a consistent relationship. UTEM magnetic field data are usually symbolized as  $H_{zi}^p$  (alphabetic subscript = component direction, superscript =  $p$  primary,  $s$  secondary,  $T$  total, numeric subscript = channel number) to accord with the magnetometer analogy; and in most discussions of simple induction, it is the time history of the analogous induced current which is described.

An important feature of layered earth  $H_z^s$  data is the early-time limit of continuously normalized  $H_{zi}^s/H_z^p$  data. If the ground is sufficiently conductive near the surface, the early-time secondary field data at points remote from the transmitter loop will approach  $-200$  percent; i.e., one finds that the voltage in the receiver coil has had insufficient time to change from the steady value attained at the end of the previous half-cycle (Figure 2). This situation may be pictured in the magnetometer-square wave current analogy as an induced current system forming near the surface of the ground under the transmitter loop such as prevents the total (analogous) magnetic field from entering into the ground anywhere except very close to the transmitter wire. The  $-200$  percent anomaly thus represents response at the inductive limit.

Finite thin plate in free space

A convenient modeling method for thin finite plate conductors in free space is the integral equation solution of Annan (1974). Annan computed the best set of polynomial eigenpotentials of order 4, and used these to represent the induced current flow in the plate as a sum of 15 "eigencurrents." The solution for the eigencurrents themselves is quite complicated, but needs only to be done once for a plate of given width to length ratio. After that, any induced current system can be described in terms of 15 coefficients in the eigenpotential summation. The secondary field at a receiver can then be simply computed in terms of these induced eigencurrents. One great advantage of Annan's method is that each eigencurrent has a frequency or time-domain response identical to a simple loop circuit. Thus the solution for a broad frequency range or many time windows is very easy to calculate. Routines for simple, interactive application of Annan's algorithms to a number of EM systems have been programmed by Dyck (Dyck et al., 1980).

Examples of type curves generated with Annan's solution may be found in Lodha (1977) and Lamontagne et al. (1980). Figure 9 shows the results of a set of computed UTEM type curves for the geometry shown in Figure 10. Also shown in Figure 10 is the geometry of the primary magnetic field, which controls the nature of induction in the plate. For the zero dip case, the primary field is mostly perpendicular to the plate. The induction in the plate tends to cancel this field at early times, leading to a negative  $H_z$  anomaly directly over the plate. Positive shoulders on each side show the secondary magnetic field of the "forward (analogous) current" near the front edge of the plate nearest the loop and the "reverse current" near the rear edge. The normalization scheme used in plotting this data is to divide the total secondary field by the calculated primary field at the measuring point. It has the undesirable effect of making asymmetric a secondary anomaly that is symmetric in terms of absolute amplitude by increasing the relative amplitude away from the loop. In fact, the absolute secondary amplitude of the positive shoulder near the loop is usually larger than the one on the side away from the loop. As the dip of the plate is increased, the positive shoulder moves away, and by the time a 30-degree dip is reached the reverse crossover is off the end of the plotted line. From dips of 30 to 135 degrees, the anomaly maintains a basic shape in the form of a simple crossover. The amplitude

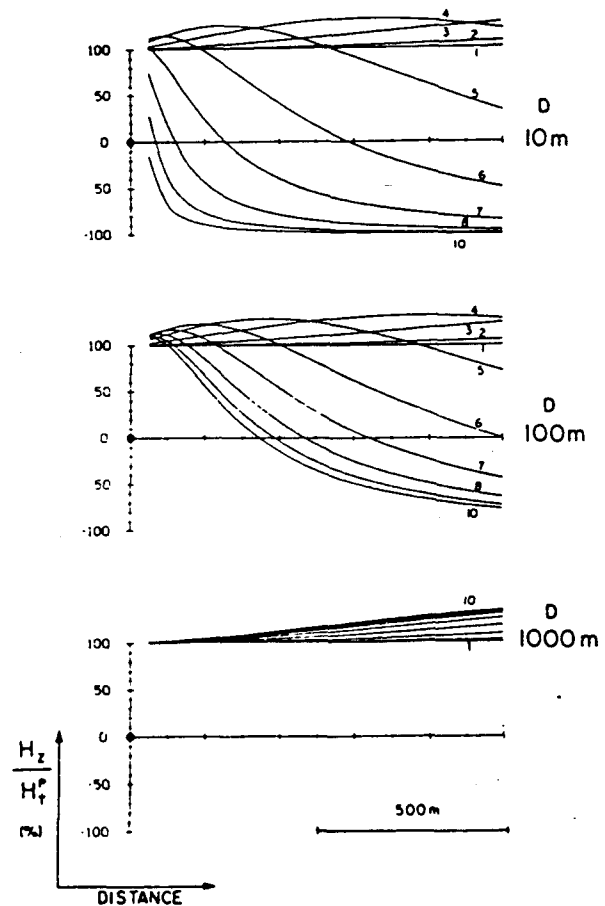


FIG. 8.  $H_z$  response of a thin horizontal sheet at various depths. The conductivity-thickness of the sheet is 2 S. The front of the transmitter loop is at the origin of coordinates.

does vary somewhat, however, being controlled by the primary field component normal to the plate which becomes a smaller and smaller fraction of the total field as the plate rotates from 30 to 150 degrees (Figure 10). The case at a dip of 150 degrees shows a very interesting behavior. The primary field can be seen to be *down* in the upper half of the plate and *up* in the lower half. The result of this is that the anomaly changes location and amplitude dramatically. For a very small plate, an anomaly could conceivably disappear completely. This phenomenon has been discussed by Bosschart (1964) for the Turam

method. For a large planar conductor, however, an anomaly is always present since a curving primary field must cut it somewhere, except in the special case when a vertical conductor is located directly under the center of a horizontal transmitting loop. The 165-degree dip case of Figure 9 shows a clear reverse crossover on the edge of the conductor far from the loop. The normal crossover is very small, due in part to the reduced induction at the near edge as shown in Figure 10, and also the large primary field used as a divisor for normalization.

The electric field anomaly generated by a plate conductor in

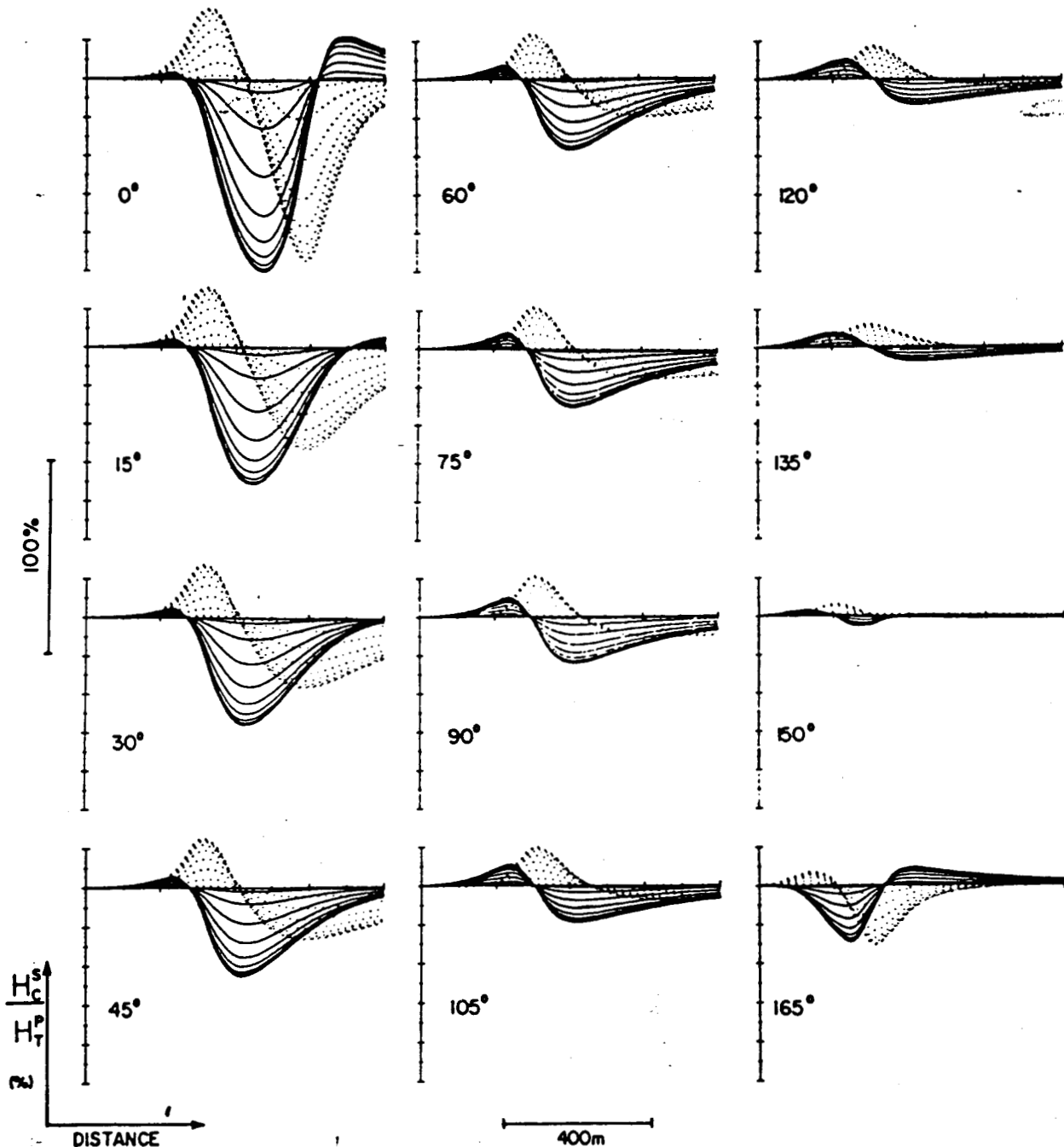


FIG. 9. UTEM  $H_x$  (solid) and  $H_z$  (dotted) profiles over a dipping plate (continuous normalization). (Geometry shown in Figure 10.)

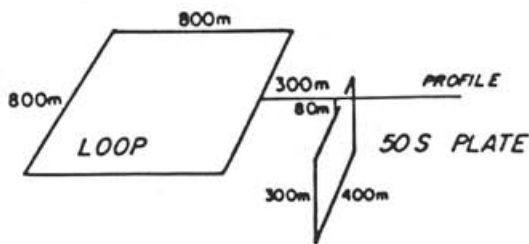
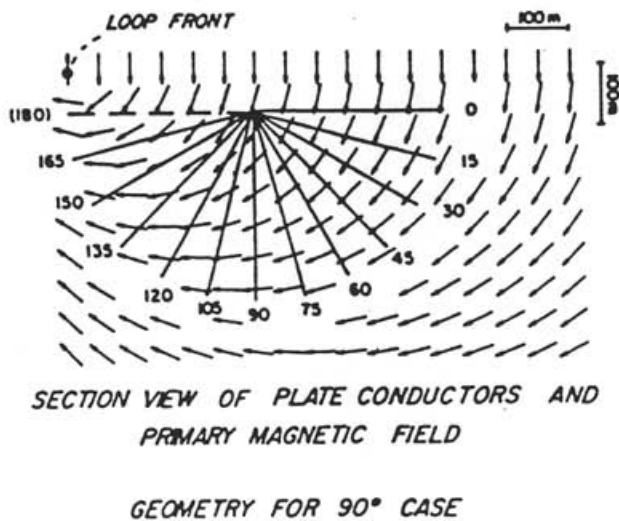


FIG. 10. Geometry and dimensions of the models shown in Figure 9. Also shown is the configuration of the primary field in the vicinity of the target conductor.

a resistive half-space is caused by charge on the plate as well as eddy currents flowing in it, and is affected by the earth-air interface. Annan's algorithm does not determine the charge distribution, so analog scale modeling methods were employed to produce type profiles. Figure 11 shows an example for a vertical plate. The longitudinal electric field is greatly reduced over the body at all times (i.e., there is a strong reduction in the late time limit). The dynamic (time-varying) part of the anomaly has the same time variation as the magnetic field but has a different geometrical pattern. The electric field is highly vulnerable to distortion by any conductivity contrast and the intensity of the static, late-limit anomaly over a conductor may therefore be reduced by any stratification between the conductor and the surface.

Other simple anomaly shapes

A set of simple schematic models is shown in Figure 12, for each of which the main features of the vertical magnetic field are sketched. The set of sketches was derived from quantitative scale model experiments by Lamontagne (1975). For the simple models illustrated where the host rock is completely non-conducting, the general anomaly shape for one body remains quite constant for the whole time range. The changes in anomaly from one channel to another are mostly in the amplitude and smoothness of the anomalies.

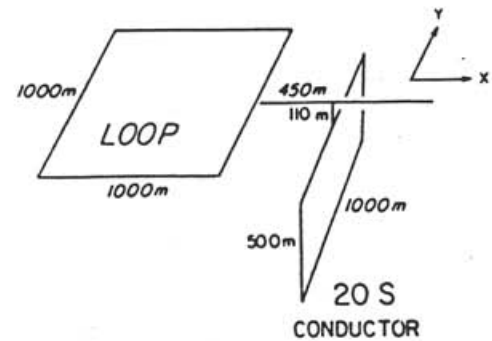
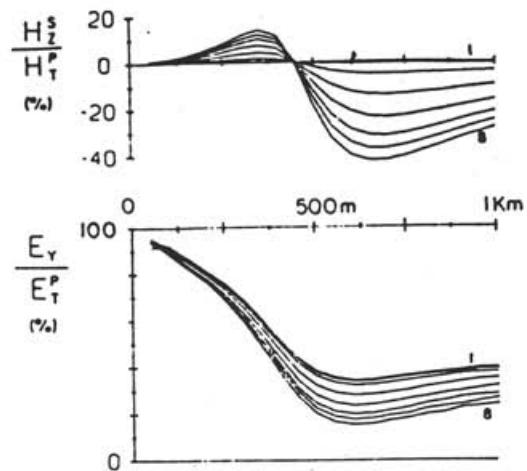


FIG. 11. Scale model UTEM secondary magnetic  $H_z^s$  and total electric  $E_y$  data over a vertical plate conductor.

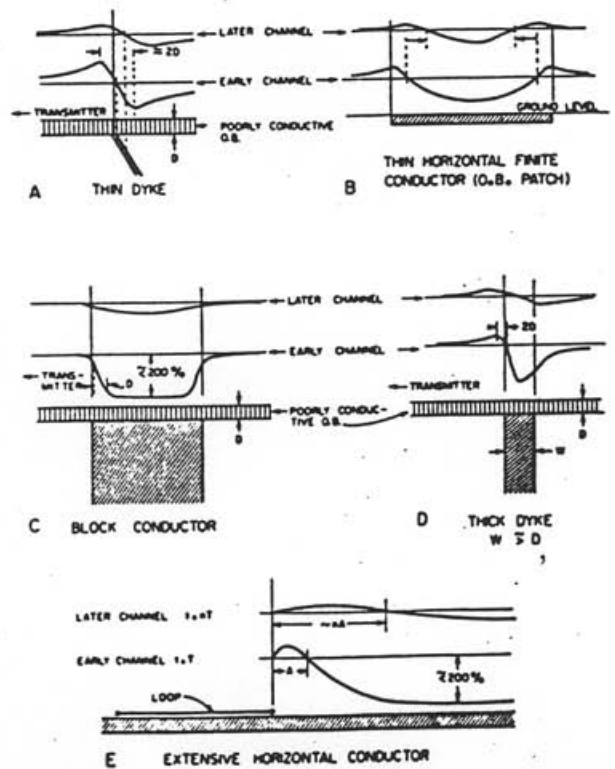


FIG. 12. The form of continuously normalized UTEM  $H_z^s$  anomalies over some simple shapes. All conductors are in free space.

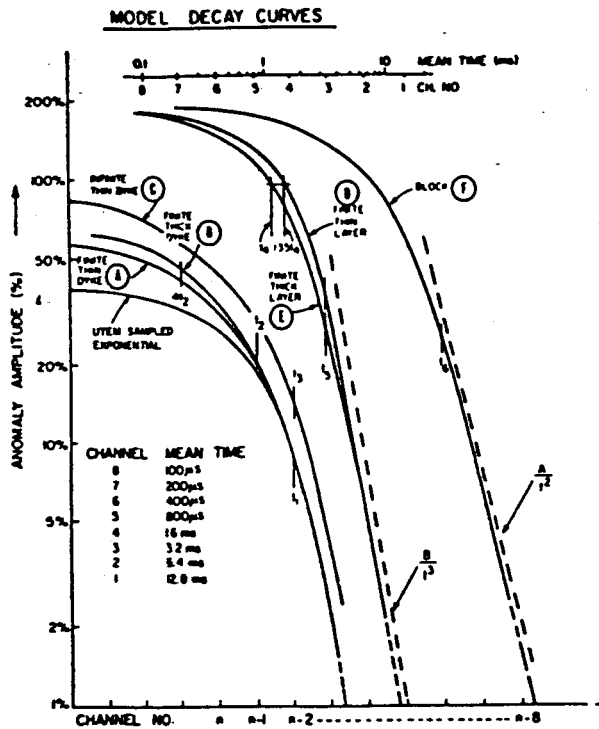


FIG. 13. The amplitude decay curves for the simple models of Figure 12. Mean sampling times are given for a base frequency of 30 Hz. The curve UTEM sampled exponential is a calculated function included for comparison. Lamontagne (1975) gives simple approximation formulas for interpreting target conductance from reference times  $t_1, \dots, t_6$  determined by translational curve matching.

**Thin dike.**—A conductive, steeply dipping body gives an  $H_z$  crossover shape similar to the plate model just discussed. The point where the anomaly changes sign indicates approximately the top edge of the conductor. The anomalies at later times tend to be broader and shifted slightly downdip from those at early times. The inductive decay rate of the anomalies will be discussed in a following section.

**Surface horizontal finite conductor.**—A thin horizontal conductor of limited dimensions (not extending under the loop) produces an anomaly consisting of a low over its central area, with large positive shoulders near its edge. The shoulders become rounded at later times and migrate towards the center of the conductor. Note that the thin horizontal plate shown in Figure 9 has a fairly deep location and thus the inward migration of the crossover points is less evident, although present.

**Shallow block conductor.**—This type of conductor produces a negative anomaly over its top having an amplitude of close to 200 percent at early times. An important characteristic of a block-like conductor is the absence of large positive flanking anomalies. The amplitude of the positive shoulders is less than 1/10 of the central negative, in contrast to the thin horizontal layer where the shoulders have amplitudes of order half the central negative. The sharpness of the crossovers at early time can be used as an indication of depth of burial. This type of anomaly is called a top anomaly and is due to a horizontal current pattern flowing around the top of the block.

**Thick dike.**—As might be expected, this is an intermediate case between a block and a thin dike where the width of a tabular body is of the same order as its depth of burial. In such cases the response is a combination of crossover and top anomaly due to vertical and horizontal current patterns, the top anomaly being more evident on the early-time channels and the crossover anomaly on later-time channels. The difference in decay rates results from the different scales of induced current flows, the top anomaly being controlled by the width of the dike, and the crossover by the depth extent.

**Extensive horizontal conductors.**—All the models with restricted lateral extent give rise to localized anomalies which simply change amplitude with time (approximately). The response of a very large conductor such as that shown in Figure 12e is included for comparison. In this case, the induced currents are not confined and they migrate horizontally with time.

**Time response of simple free-space models.**—Figure 13 shows example decay plots of log anomaly amplitude versus log time (channel number). The responses shown in Figure 13 are the UTEM sampled step responses that are only strictly valid for interpretation of actual field data when the observed anomalous response has effectively vanished at late times. Time scaling by lateral translation of the graphs is permitted for these cases, as previously discussed. The applicability of these time decays to interpretation is discussed by Lamontagne (1975), including the use of characteristic parameters to estimate conductance. A significant point to note is that simple induction in finite bodies eventually exhibits exponential decay at late time, whereas induction in infinite features takes the form of an inverse power law (Kaufman, 1978). Therefore, for models D, E, and F, the very late portion of the decay should ultimately show an exponential behavior if measured with sufficient sensitivity.

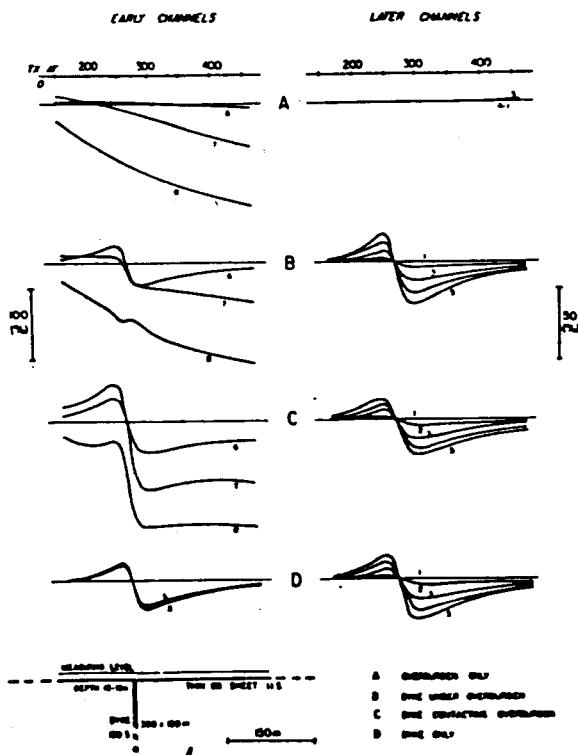


FIG. 14. Scale model UTEM  $H_z$  profiles over a conductive thin dike with overburden present.

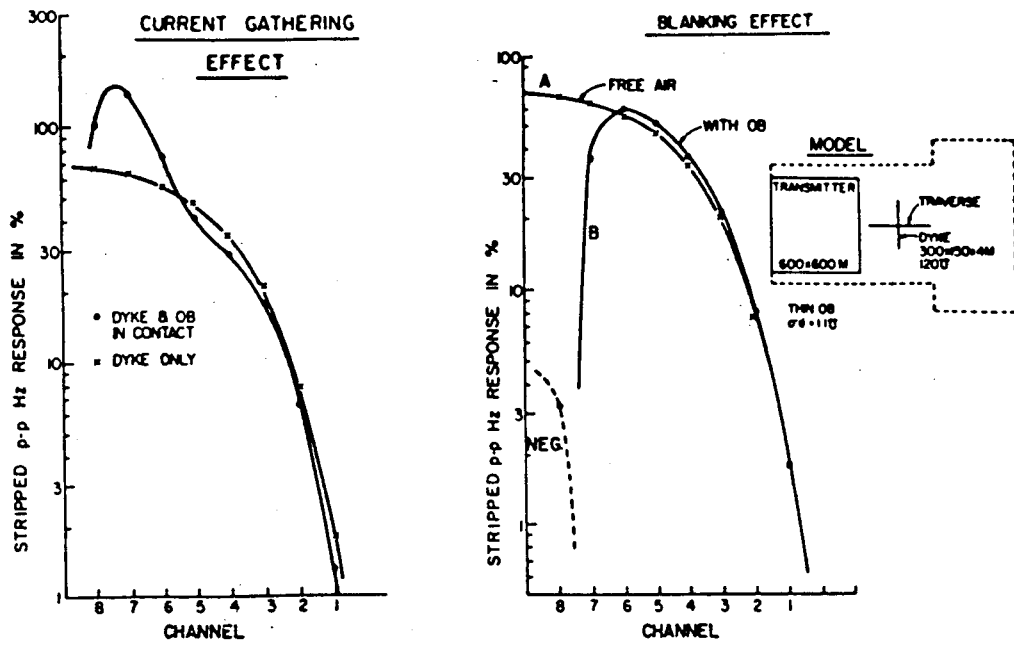


FIG. 15. Decay plots for the  $H_z$  anomalies of Figure 14.

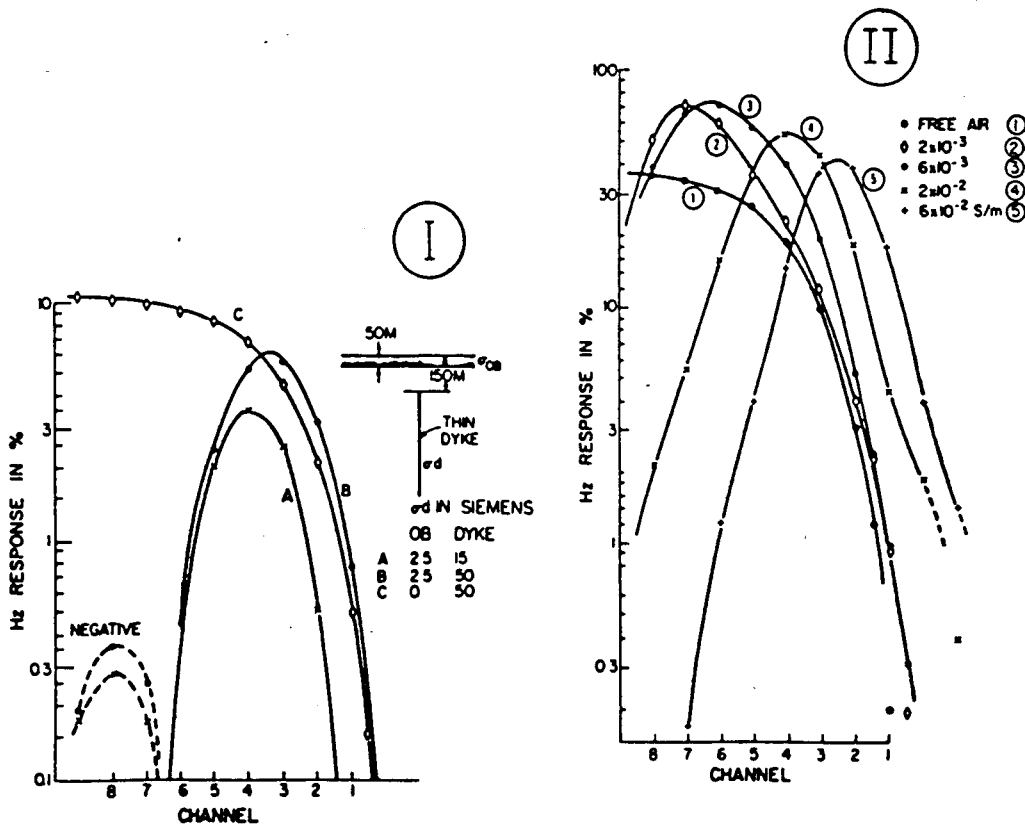


FIG. 16. Decay plots of  $H_z$  anomalies over a thin dike (I) under a conductive overburden and (II) in a conductive half-space.

Overburden effects

We will restrict the discussion of overburden and host-rock effects to the case of a simple vertical finite dike conductive target, which was studied by Lamontagne (1975) using a scale model. Conductive overburden cover can modify the responses of underlying conductors in two main ways. Let us consider a dike target whose response in free space is given in Figure 14d. If overburden is now placed over this target conductor, the resultant response (Figure 14b) is not just the sum of the overburden and dike response. At early times it can be seen that there is very little response from the dike. This is because the magnetic field (MSW analogy) has not yet penetrated the overburden, and it leads to the name "overburden blanking" for this characteristic. At later times (Ch 6-1), when we can see from Figure 14a that the field has completely penetrated the overburden layer, the dike and overburden response (14b) is virtually indistinguishable from that of the dike alone (14d). The time decay pattern of the peak-to-peak amplitude of the crossover is plotted in Figure 15. It clearly shows the blanking effect of the overburden at early times (right-hand figure). The minute negative response at earliest time is present only when the

overburden extends under the loop, and appears to result from the complicated way in which the field first reaches the hidden target.

A second effect occurs when the dike is in conductive contact with the overburden. The results are quite different from those where the dike was not in contact (Figure 14c). In this case, regionally induced (analogous) current flow in the overburden has been "gathered" or "channeled" into the dike which is of higher conductivity. This accounts for the large-amplitude crossover anomalies at early times. Because the conductance of the dike greatly exceeds that of the overburden, the amount of current gathering is virtually independent of the dike's depth extent. The gathering effect at early times of just a "line conductor" remaining attached to the overburden after most of the dike was removed was found to be over 80 percent of that of the complete dike. At later times, when the (analogous) current flow in the overburden has migrated away (i.e., the real overburden current is no longer time-varying), the response is again almost identical to that of the dike alone. The time decay of the response is plotted on Figure 15, and in addition to the enhancement at early times a slight attenuation of the response at intermediate times can be seen.

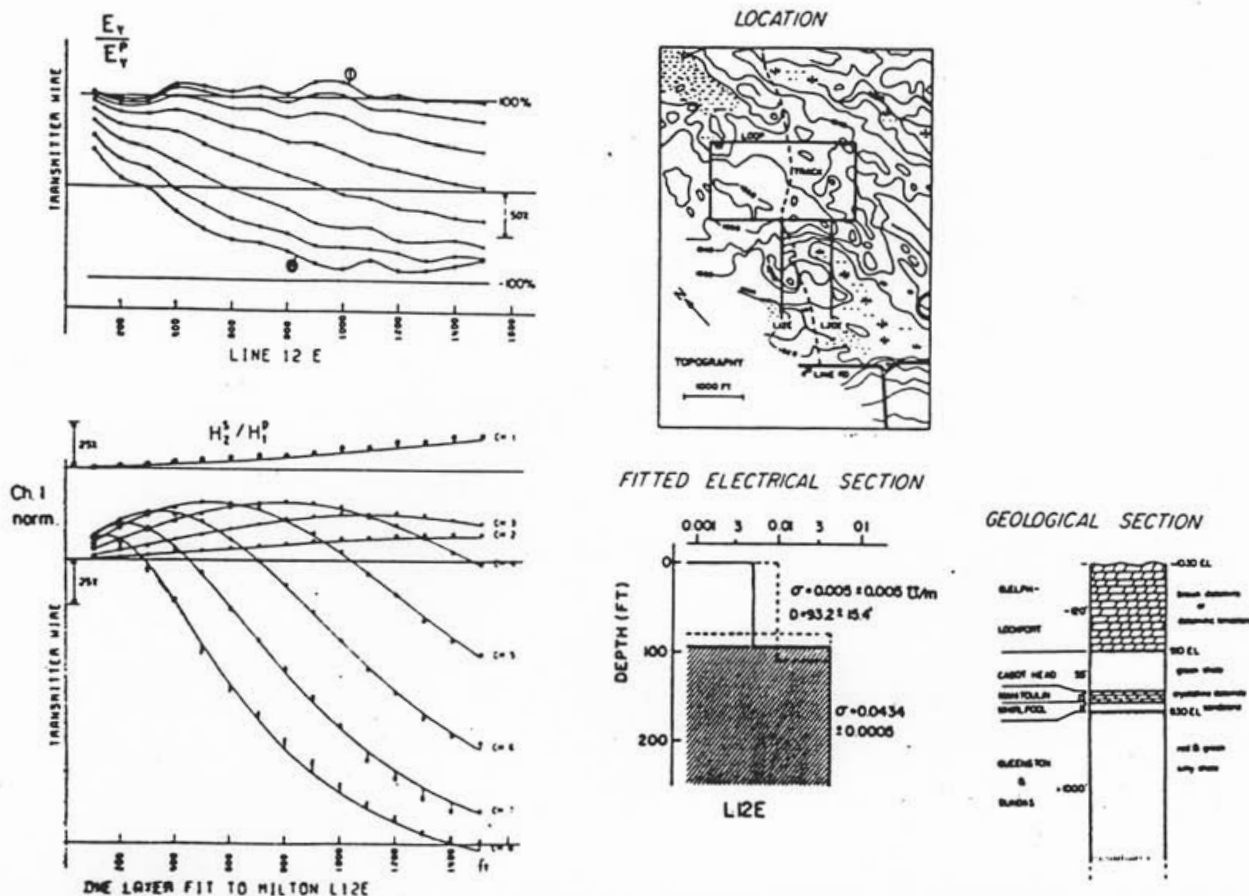


FIG. 17. Field example of  $E_v$  and  $H_z^2$  data from a well-stratified earth. The electrical section was obtained from inversion of the  $H_z^2$  data. The curves on the  $H_z^2$  graph are the theoretical model; the points are the field data. The bottom axis is at -150 percent. The geologic section is from nearby gas drilling exploration.

Host rock effects

Figure 16 II shows the time variation in response of a 60 S vertical plate located in a half-space. The results were calculated by Lamontagne (1975) by Fourier transformation of the frequency-domain numerical modeling of Lajoie and West (1976). At early times the response is reduced from the free-air response: this corresponds to blanking by the conductive region above the target. At later times the response is enhanced indicating that the regional (analogous) current in the host rock is being gathered into the plate at these times. For poorly conducting host rock, the response at late times is close enough to the free-space response that simple interpretation of the target using a plate in free-space model is valid. For the higher host conductivities (case 4, 5) this is no longer the case.

FIELD RESULTS

Milton, Ontario

This area was surveyed to demonstrate what data from a conductive, well-stratified earth looks like. The area is one where 650 m of flat-lying Paleozoic sediments overlie the Precambrian basement. The predominant member of the stratigraphy is a uniform and thick sequence of shale. Other beds are mostly resistive calcareous and sandstone formations. The survey area is covered by a mixed forest and marshy streams, with occasional outcrops. The top of the bedrock is a dolomite formation which is everywhere more than 20 m thick. Topographic relief is minor (< 10 m), with occasional rough spots near outcrop. Overburden is probably less than 10 m every-

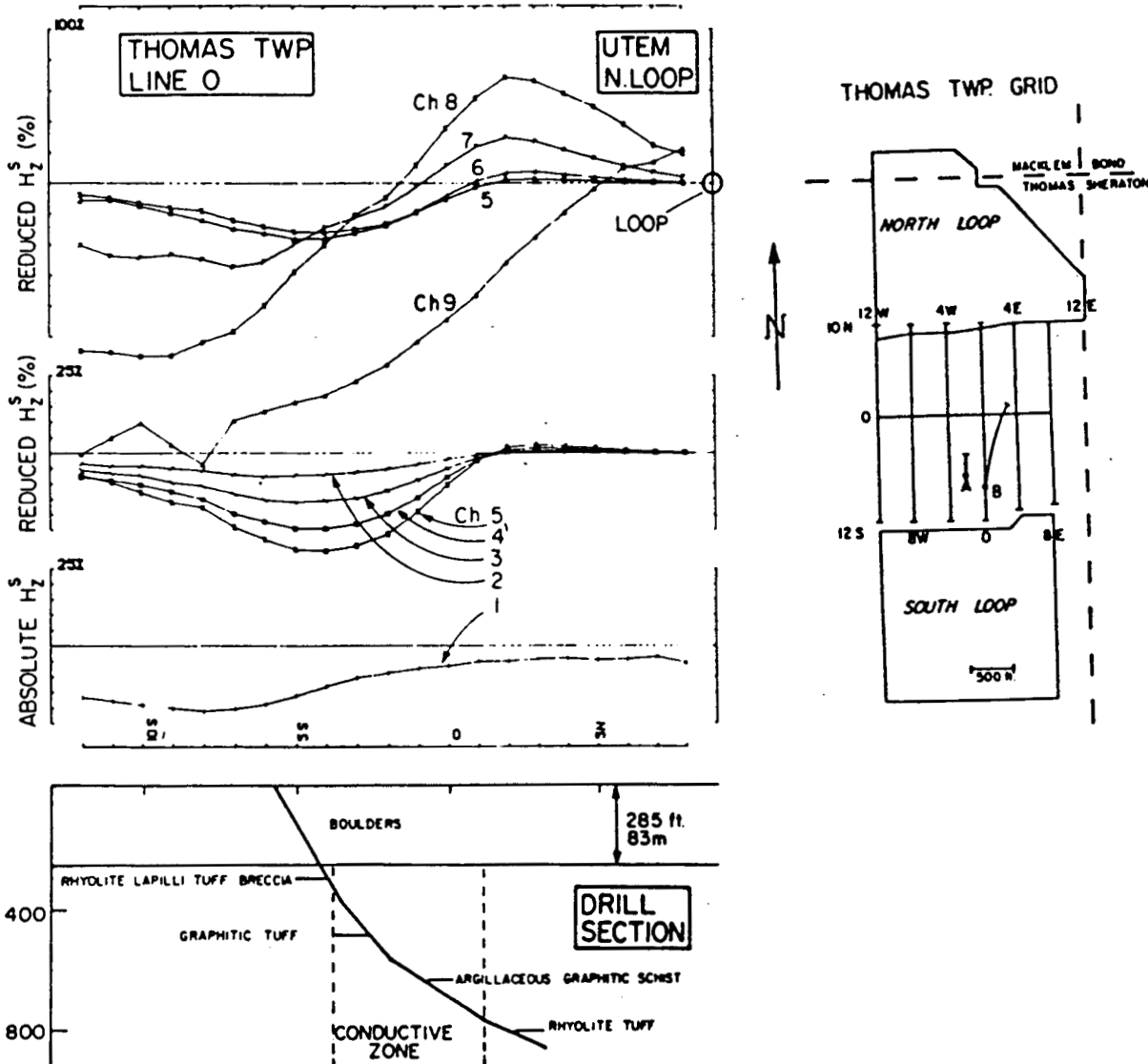


FIG. 18. A profile of  $H_z^s$  data from the north transmitter loop across the Thomas Twp test site. A map of the survey is included (different scale).



where and much less on average. It is mostly humus or thin glacial soil. Surface water is fresh, and likely quite resistive ( $> 100 \Omega\text{m}$ ). Figure 17 shows some of the data with a layer and half-space model fitted to it by iterative minimization of squared error. Also shown is a stratigraphic section from a well a few kilometers distant. The dolomite layer is too resistive for its conductivity to be determined by data whose earliest time sample is at  $100 \mu\text{s}$ . (The survey was done with UTEM I.) At first glance, the data look just like that for any conductive earth, as the early-time data at the end of profiles have the usual strong negative anomaly, and there is a regular outward progression of crossovers as time progresses (decreasing channel number). However, the resistive surface layer does reveal itself in the limited approach of the early time curves to  $-200$  percent anomaly. The convergence of  $E_z$  at late time to 100 percent of the primary field confirms the excellent lateral homogeneity of the site.

#### Thomas Township, Northern Ontario

This site has become an interesting test range for electrical methods, and a new grid has been cut and named the Night-hawk Lake geophysical test range. It is a graphitic zone that has many of the geometrical and electrical characteristics of a massive sulfide body. It is covered by 83 m of only moderately conductive overburden. It was found originally by airborne EM and has been intersected by two boreholes.

A UTEM II survey with 30 Hz base frequency was carried out on 6 lines of length 2200 ft and spacing 400 ft using transmitter loops to the north and south of the grid. Figure 18 shows a profile across the middle of the conductive zone.

At  $50 \mu\text{s}$  (Ch 9), the regionally induced (analogous) current is only 500 ft from the loop. The field has not penetrated the overburden at the target site. From  $100 \mu\text{s}$  to about  $500 \mu\text{s}$  (Ch 8-6), a crossover response is observed over the target. At about

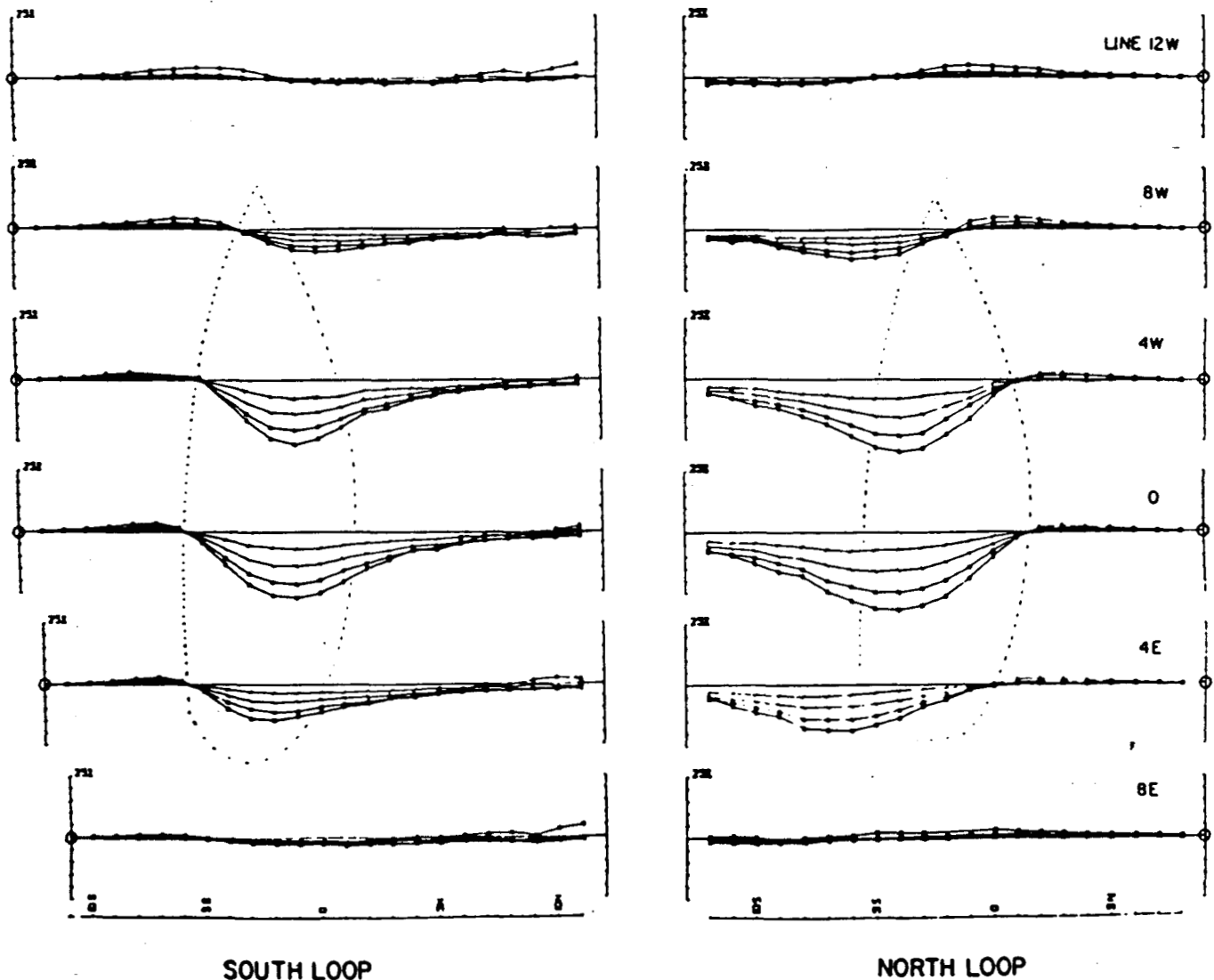


FIG. 19. Later time  $H_z$  profiles (Ch 5-2) outline the perimeter of the conductor.

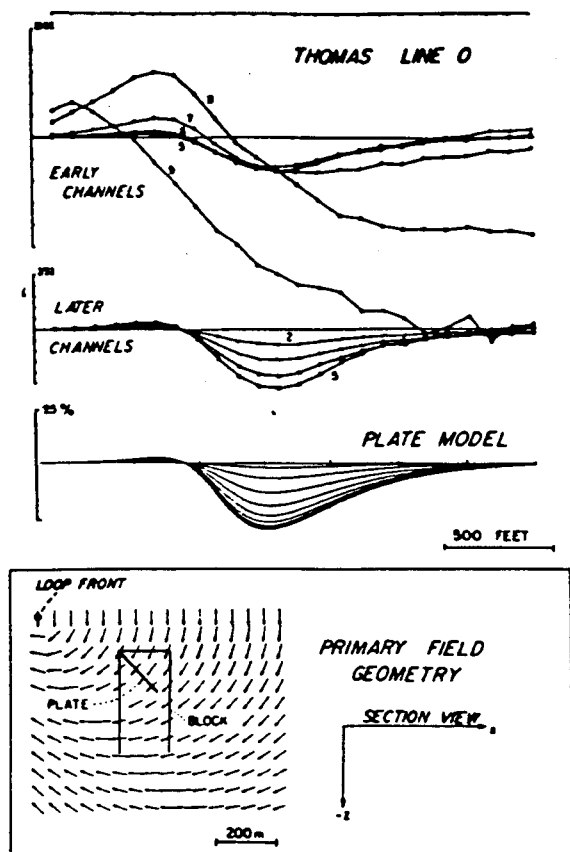


FIG. 20. Comparison of  $H_z$  data from the south transmitter loop with a free-space plate model. The configuration of the primary field is also shown.

500  $\mu$ s the response changes to an asymmetric negative anomaly which decays much more slowly than the crossover response. The early-time crossover response is a current gathering or channeling anomaly where the (analogous) anomalous current flows along the length of the zone, while the longer time constant response is a local induction anomaly, where induced currents flow in a vortex within the target conductor.

Figure 19 shows a map of all the late-time profiles. They clearly delineate the edge of the target body. Figure 20 shows how a rectangular plate model can be found which models the observed results from one transmitter loop quite accurately, but which has to be rotated in order to match the results from the other loop. The late-time induced (analogous) current system in the actual conductor appears to be a tightly defined normal current in the front upper (near-loop) edge of the conductor with a more diffuse, return current deep in the rear of the body. A survey with the transmitter loop located on the other side of the body was similarly fitted by a plate dipping away from that loop, indicating the conductor to be a thick zone in which currents can flow in a variety of directions.

Electric fields were measured at the Thomas site. The late time vector map is shown in Figure 21, along with a rough numerical model. The conductive zone shows very clearly, although its edge is ill defined. Figure 22 shows a profile of the longitudinal component of electric field over the body. The field

intensity is almost constant from channel 6 onward, and the main feature of the response is the aforementioned broad reduction in the field strength over the conductor. It is helpful, when looking at  $E$  field profiles, to imagine a plot on the same axes of the negative of the observed channel 1 response. This is the value the field starts from at the half-cycle transition. Even as early as 50  $\mu$ s (Ch 9), the electric field has made most of its polarity reversal. In fact, between the loop to the target body it has overshoot, while from the target body outwards it is changing relatively slowly. The time changes in  $E$  are actually very similar to those in  $H$ . There are two dominant decay times, a short one corresponding to the overburden and the channeling target response (Ch 8-6) and a long one corresponding to the local induction response (Ch 5-1). Also, these two  $E$ -field responses have a different geometrical form corresponding with the different forms of the magnetic anomalies. The scaled up version of the  $E$  data in Figure 22 shows the slowly decaying anomaly. Considerable noise is apparent in the data at this magnification.

#### Bedrock conductor beneath overburden

Figure 23 shows the measured secondary  $H_z$  fields at a site in Australia. The slow outward migration of the early-time channels and the -200 percent early-time limit away from the transmitter loop are characteristics of the response of a near-surface conductive weathered layer. This layer has a total conductance of about 4 S.

Around station 210W a more local superimposed crossover anomaly is evident which is fixed in location. This feature is evident over a great strike length. When the visually estimated overburden response is stripped from the anomaly and the peak-to-peak crossover response is plotted on a decay plot (Figure 26), the characteristics of early time blanking, time delay, and enhancement are clearly displayed. Corresponding to the model data of Figure 16, the early time blanking attenuates the local anomaly as the (analogous) magnetic field has not had time to penetrate the weathered layer. At intermediate times (Ch 5, 4) the response lies above a fitted free-space, half-plane conductor decay curve. This is partly an amplitude enhancement from current gathering and partly due to a small delay in time while the (analogous) magnetic field penetrates the near-surface conductor. It is not clear whether any of the L400S response can be identified as due to local induction. Nevertheless, the plotted induction curve for a half-plane in free space serves as a useful reference and establishes an upper limit on the conductance of the feature (7S in this case).

On two survey lines about 1 km away, the same local feature is observed, but the response has changed to one of longer time constant. As shown in Figure 24, a clear response persists through channels 2 and 1. These data are replotted with "point normalization" on Figure 25 to show the absolute secondary field. Absolute normalization preserves the true anomaly shape, but has the disadvantage of scaling up strongly those anomalies which lie near the transmitter. The stripped peak-to-peak response is plotted in decay form in Figure 26 and clearly shows the difference in time constant at the two locations.

The increase in time constant seen on line 600N is very significant, since little change is seen in the background response and only a lesser change in the blanking time. It indicates that the L600N late-time response is due to local induc-

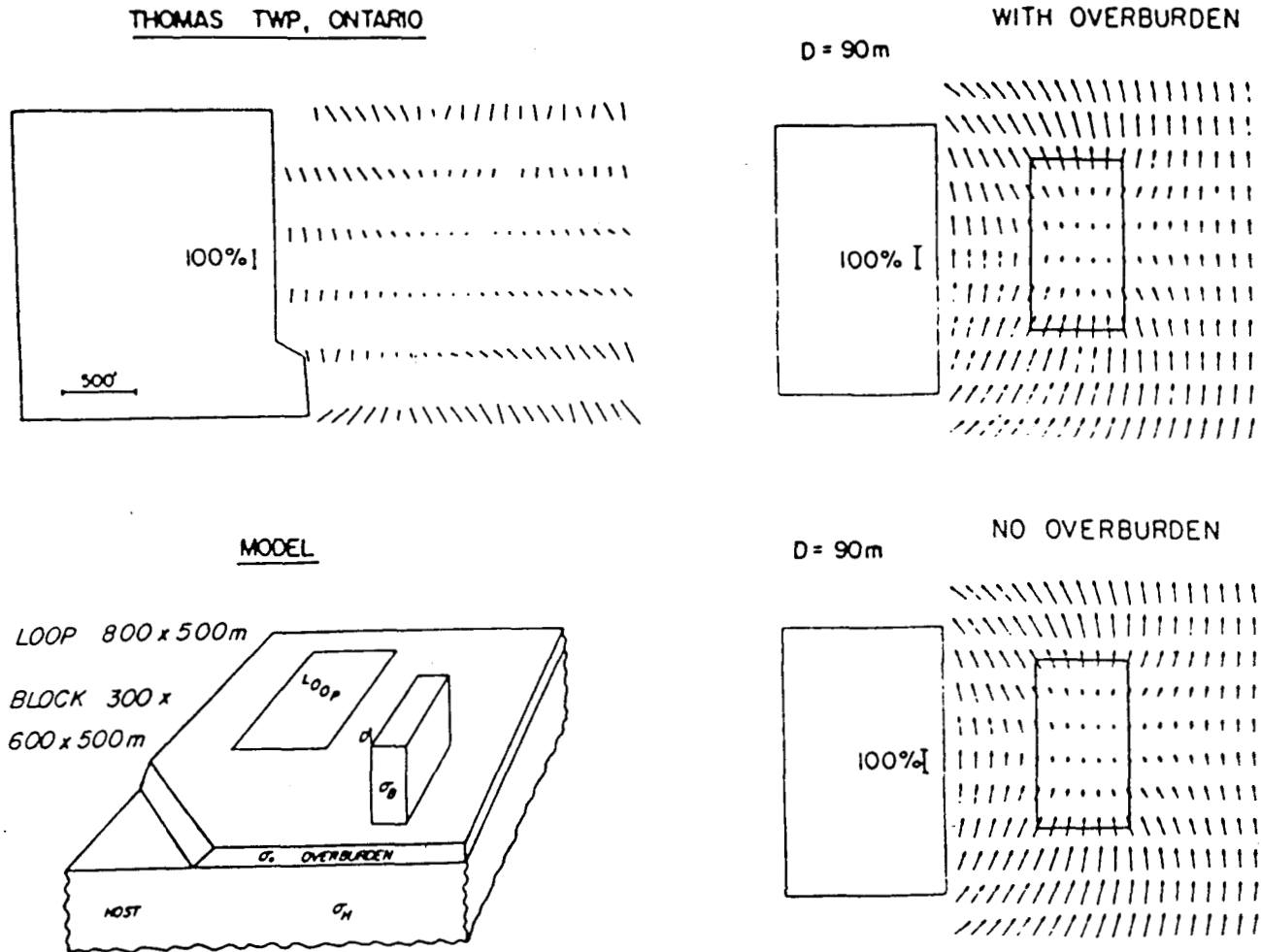


FIG. 21. Vector map of the late-time  $E$  field at Thomas Twp. A block model is included for comparison. The example is for a case where  $\sigma_B \gg \sigma_O \gg \sigma_H \gg \sigma_{AIR}$ .

tion. Model fitting of the decay, taking into account the limited strike extent of the long time constant response, leads to an interpretation of this feature as a local thickening of the half-plane conductor. The local conductance needed to produce the longer time constant is 120 S in contrast to the 7 S maximum of the rest of the bedrock conductor.

Drilling indicated that the extensive conductor was a 50 m thick calc-silicate zone containing both carbonates and sulfide lenses within a talc-sericite host. The locally more conductive part consisted chiefly of nearly massive noneconomic sulfides.

#### CONCLUSIONS

Experience with UTEM demonstrates that a wideband, time-domain EM system which measures the step response of the ground is electronically feasible and practical. Considerable field and modeling experience has shown that it is simple to use the amplitude information from such a system to aid significantly in interpretation. In our opinion the step response has a

significant advantage over the impulse response for detection and interpretation of good conductors in the presence of poorer ones. Electric field data measured with the system can provide independent information about lateral conductivity contrasts and may be a useful aid in interpretation.

#### ACKNOWLEDGMENTS

Development of the UTEM system and its interpretational capability was funded from a number of sources. UTEM I was developed with support from the National Research Council of Canada. UTEM II instrumentation was supported by UMEX Ltd., Texasgulf Inc., and Cominco Ltd., with interpretational studies funded by a consortium of companies consisting of Aquitaine, Asarco, Cominco, Geotrex, Gulf Minerals, Inco, Newmont, Noranda, Phelps Dodge, Selco, Shell Canada Resources, Texasgulf, and Umex. Graduate students, Y. Lamontagne, G. Lodha, J. Macnae, and M. Vallée, who worked on the project received stipendary and computing support from the

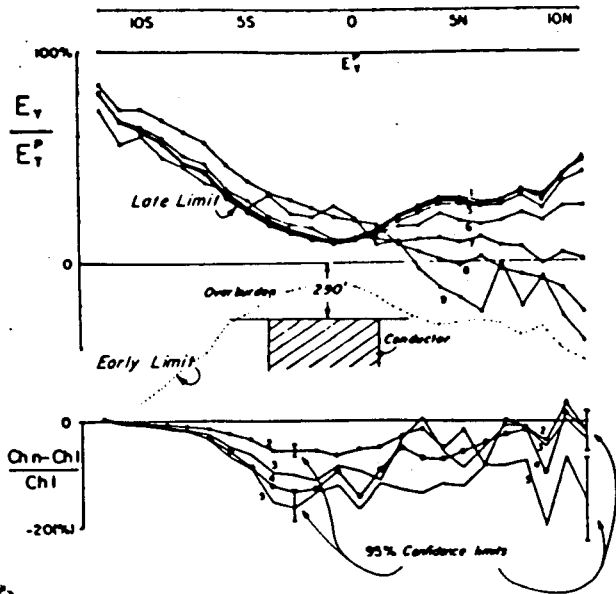


FIG. 22. Thomas Twp  $E_v$  data for line 0 from the south transmitter loop. The expanded scale data on the lower axes show that a very weak dynamic  $E$  field anomaly is associated with the main  $H_z^p$  late time response (Ch 5-1).

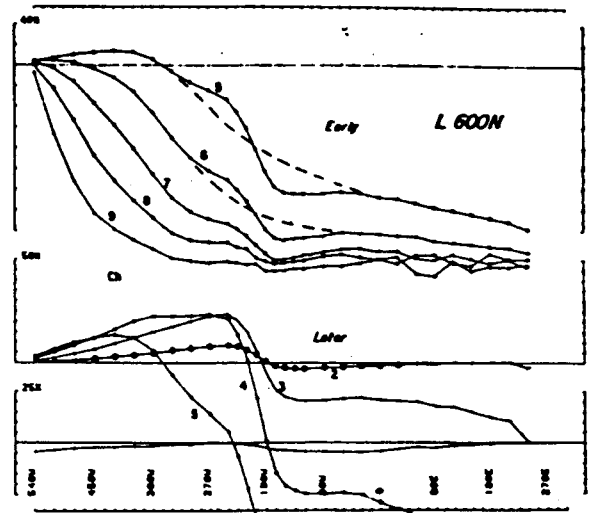


FIG. 24.  $H_z^p$  data on line 600N 1 km away from the previous figure showing a time decay of the local anomaly lasting to much later times. Re-measurement of the profile at 13 Hz gave virtually identical profiles (shifted one channel) with no visible Ch 1 anomaly.

Natural Sciences and Engineering Research Council of Canada and the University of Toronto. All this assistance is gratefully acknowledged. We also thank an anonymous reviewer for a very careful, helpful review.

REFERENCES

Annan, A. P., The equivalent source method for electromagnetic scattering analysis and its geophysical application: Ph.D. thesis, Memorial Univ. of Newfoundland.

Boschart, R. A., 1964, Analytical interpretation of fixed source electromagnetic data: Doctoral thesis, Univ. of Delft.  
 Dyck, A. V., Bloore, M., and Vallée, M. A., 1980, User manual for programs PLATE and SPHERE: Res. in Appl. Geophys. 14, Geophys. Lab. Dept. of Physics, Univ. of Toronto.  
 Kaufman, A., 1978, Frequency and transient responses of electromagnetic fields created by currents in confined conductors: Geophysics, v. 43, p. 1002-1010.  
 Lajoie, J., and West, G. F., 1976, The electromagnetic response of a conductive inhomogeneity in a layered earth: Geophysics, v. 41, p. 1133-1156.  
 Lamontagne, Y., 1975, Applications of wide-band, time domain EM

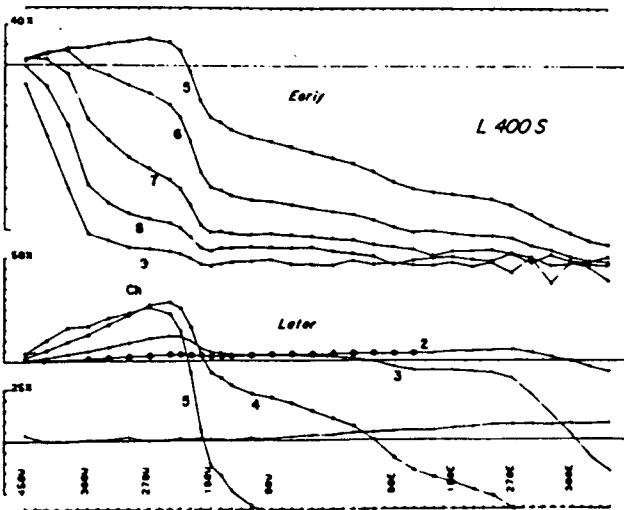


FIG. 23.  $H_z^p$  data from New South Wales showing the migrating crossovers of the overburden near the loop and a local anomaly around station 210 W. (Survey frequency 26 Hz.)

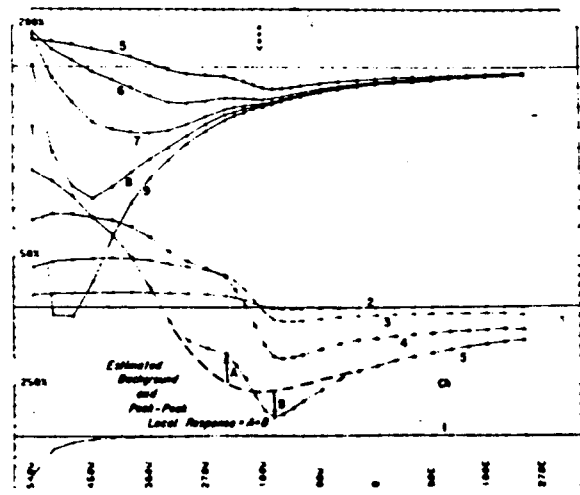


FIG. 25. Point normalized  $H_z^p$  from line 600N. The local secondary fields have been normalized to the constant primary field at station 210W and show how stripped peak-to-peak local anomaly amplitude is estimated.

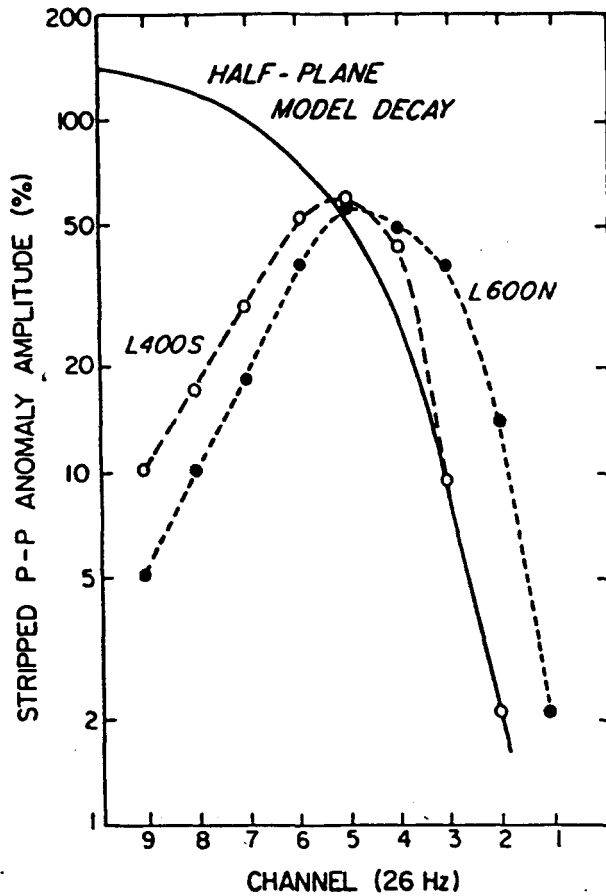
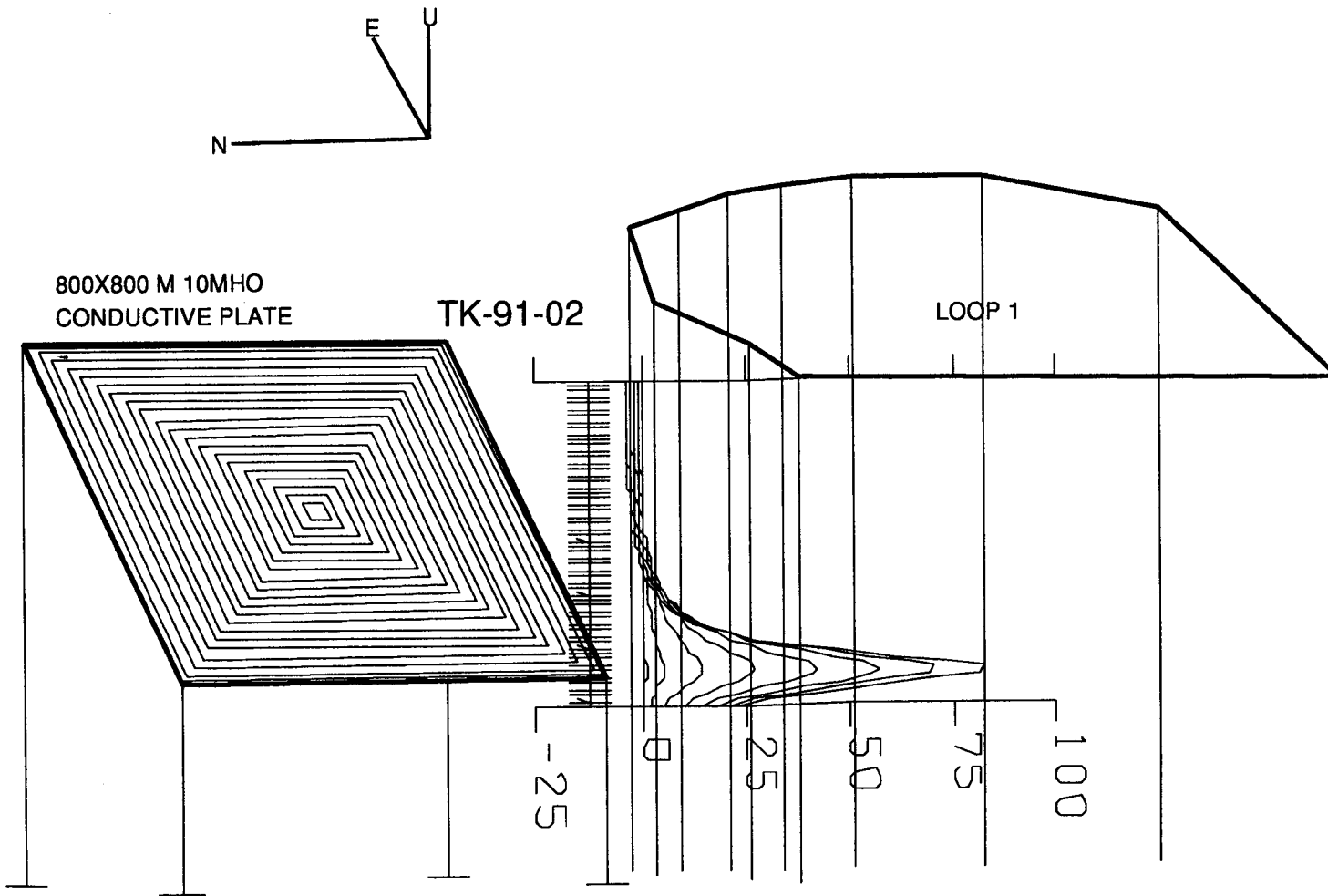


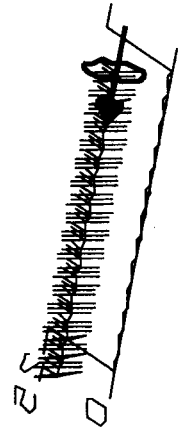
FIG. 26. Amplitude decay plot of stripped anomaly on lines 400S and 600N of the New South Wales survey.

- measurements in mineral exploration: Ph.D. thesis, Univ. of Toronto; available as Res. in Appl. Geophys. 7, Geophys. Lab., Univ. of Toronto.
- Lamontagne, Y., Lodha, G. L., Macnae, J. C., and West, G. F., 1977, Towards a deep penetration EM system: Paper presented at 79th annual meeting of the Can. Inst. of Min. and Metall., Ottawa, April; published in Bull. Austral. Soc. Expl. Geophys., v. 9, 1978.
- 1980, UTEM, "Wideband Time-domain EM Project 1976-8, Reports 1-5"; Res. in Appl. Geophys. 11, Geophys. Lab., Dept. of Physics, Univ. of Toronto.
- Lodha, G. L., 1977, Time domain and multifrequency electromagnetic responses in mineral prospecting: Ph.D. thesis, Univ. of Toronto; available as Res. in Appl. Geophys. 8, Geophys. Lab., Dept. of Physics, Univ. of Toronto.
- Macnae, J. C., 1977, The response of UTEM to a poorly conducting mineralized environment: M.Sc. thesis, Univ. of Toronto.
- 1980, The Cavendish test site: a UTEM survey plus a compilation of other ground geophysical data: Res. in Appl. Geophys. 12, Geophys. Lab., Dept. of Physics, Univ. of Toronto.
- 1981, Geophysical prospecting with electrical fields from an inductive source: Ph.D. thesis, Dept. of Physics, Univ. of Toronto, 279 p.; available as Res. in Appl. Geophys. 18, Geophys. Lab., Univ. of Toronto.
- Macnae, J. C., Lamontagne, Y., and West, G. F., 1984, Noise processing techniques for time-domain E.M. systems: Geophysics, v. 49, this issue, p. 934-948.
- Maxwell, J. C., 1891, A treatise on electricity and magnetism: London, Clarendon Press, v. 2, 500 p.
- Nabighian, M. N., 1979, Quasi-static transient response of a conducting half-space—An approximate representation: Geophysics, v. 44, p. 1700-1705.
- Podolsky, G., and Slankis, J., 1979, Izok Lake deposit, Northwest Territories, Canada. A geophysical case history: in Geophysics and Geochemistry in the search for metallic ores: P. J. Hood, ed., Econ. Geol. rep. 31, Geol. Survey of Canada.
- Wait, J. R., 1962, Electromagnetic waves in stratified media: New York, MacMillan Co.

APPENDIX IV



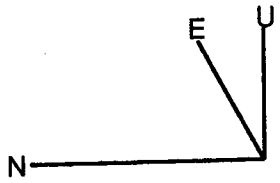
TK-91-04



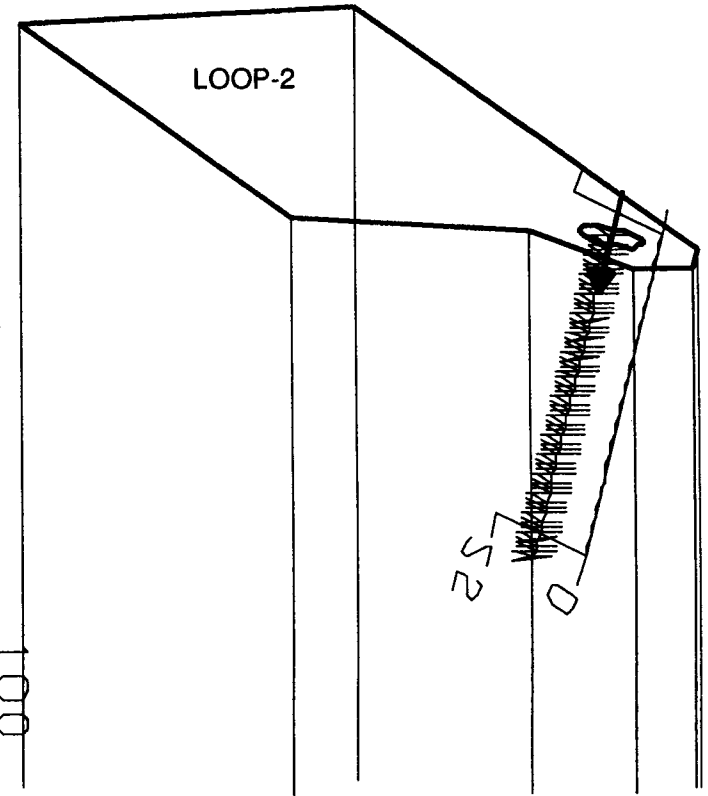
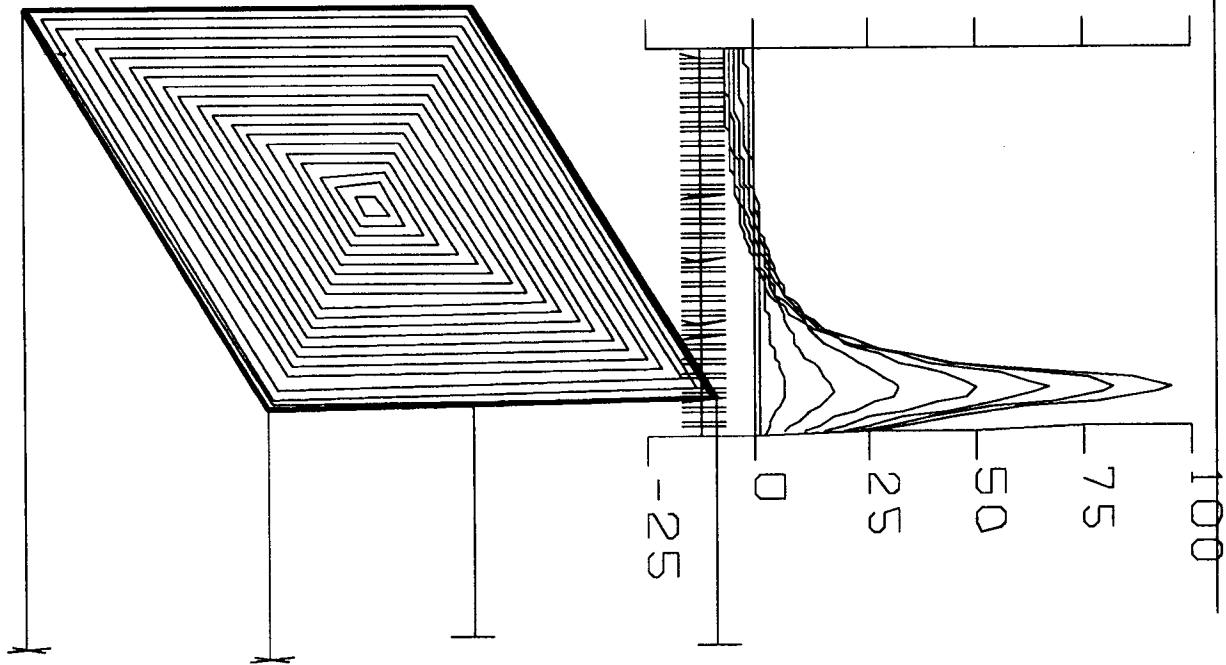
VIEW ANGLE 20DEG  
ELEVATION 900M  
VERTICAL SECTION

# MULTILOOP MODEL

FIG-1



800 X 800 M 10MHO  
CONDUCTIVE PLATE

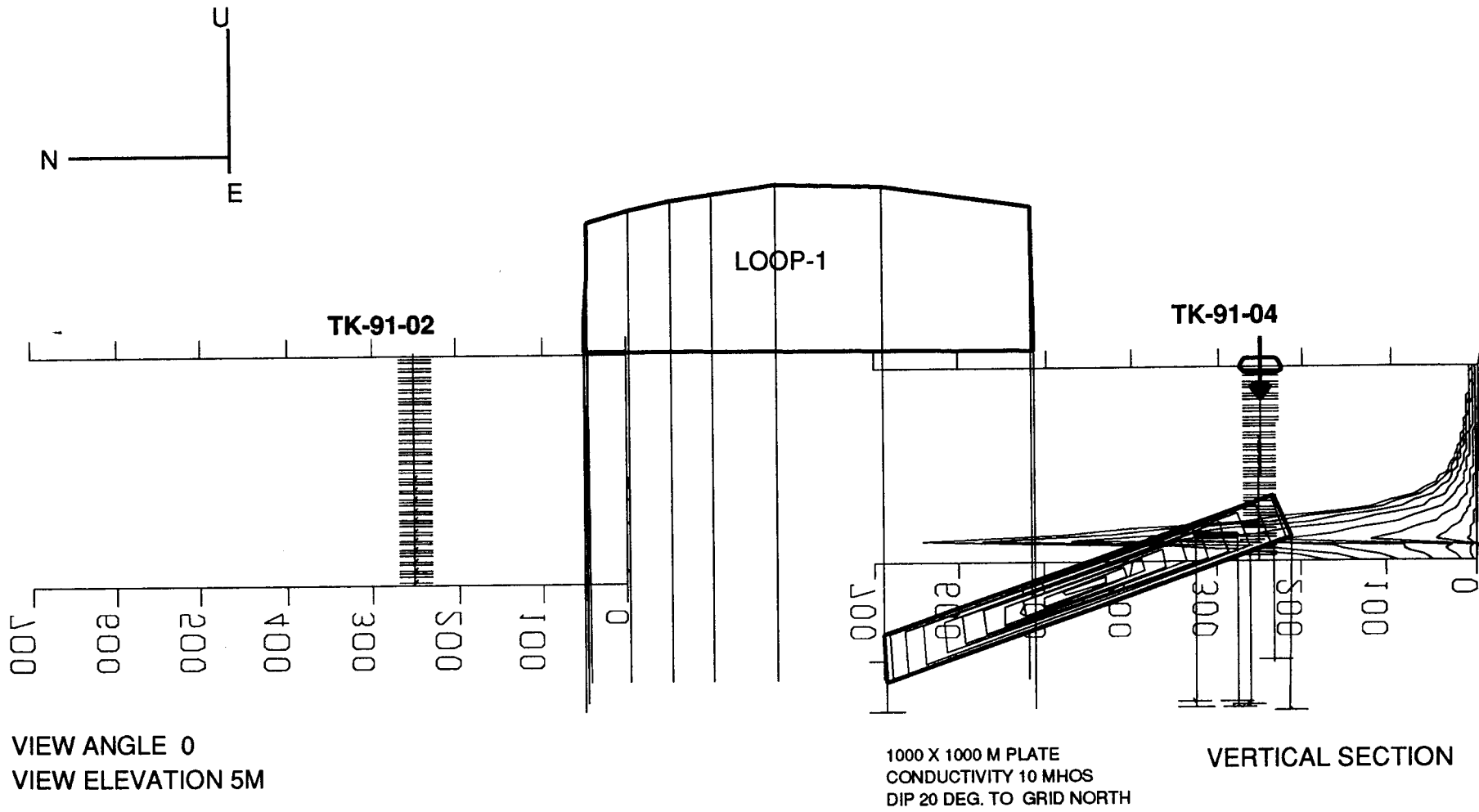


VIEW ANGLE 20 DEG  
ELEVATION 900M  
VERTICAL SECTION

# MULTILOOP MODEL

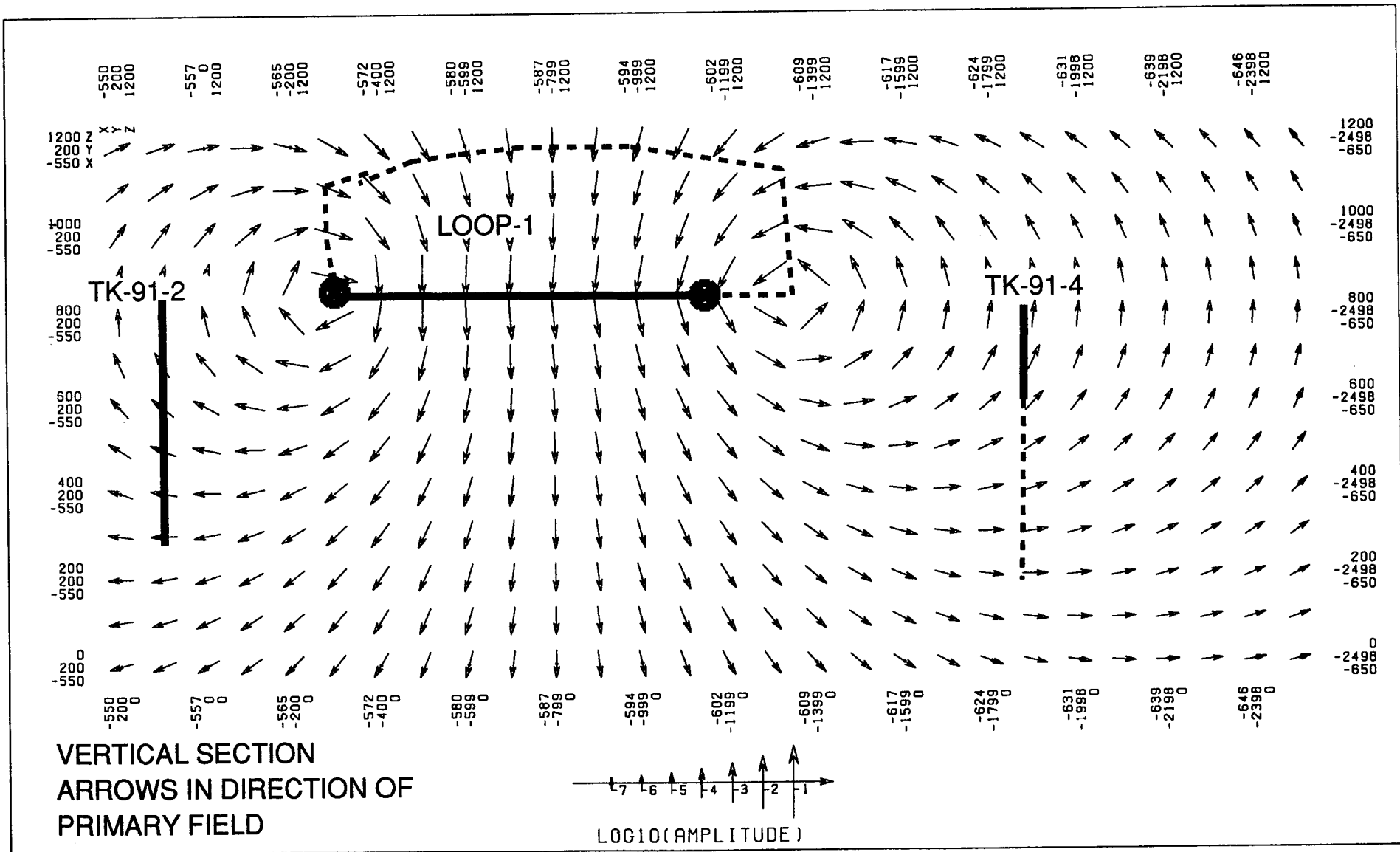
FIG-2





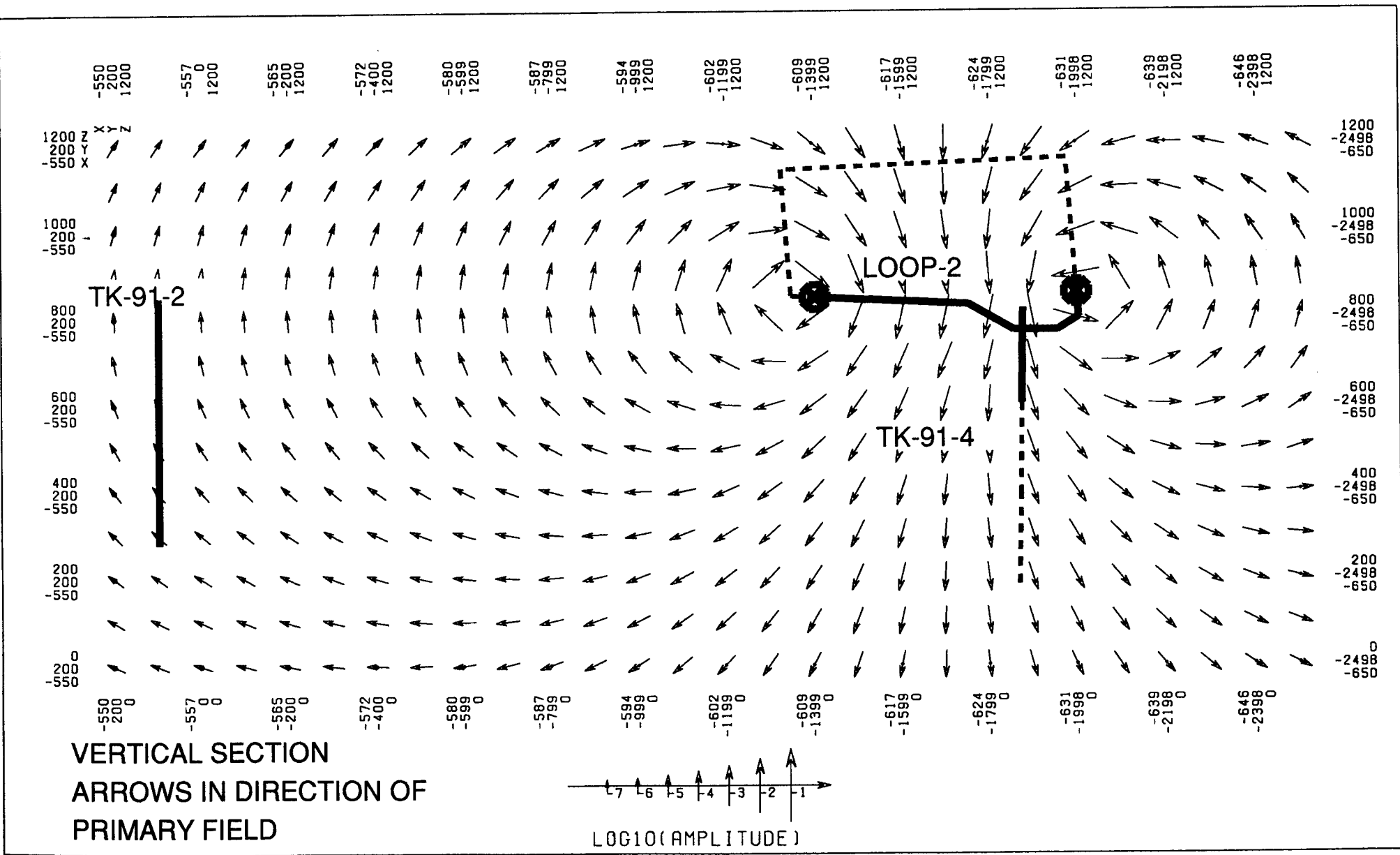
**MULTILOOP MODEL**

**FIG-3**



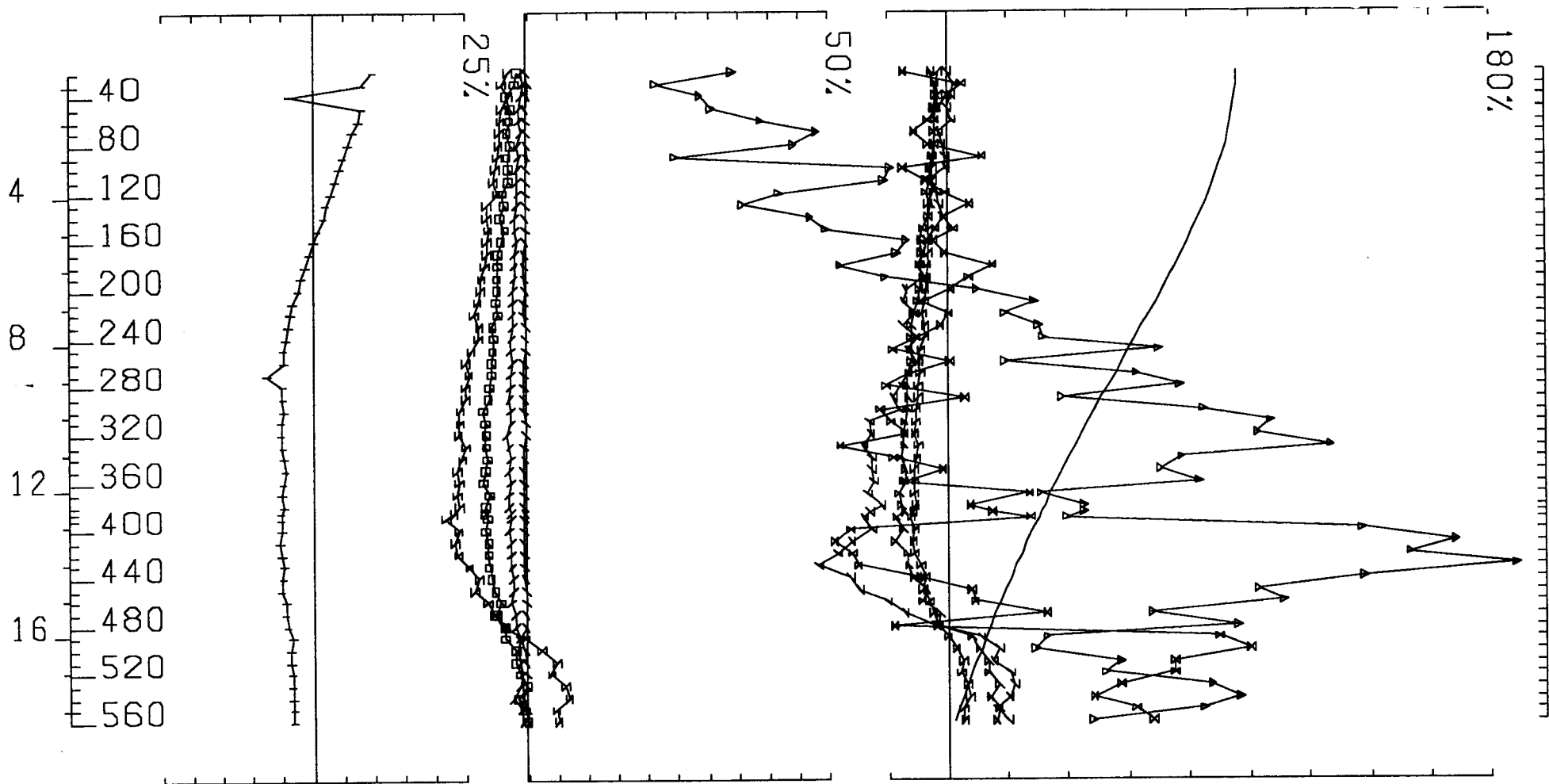
# VECTOR PLOT

FIG-4



**VECTOR PLOT**

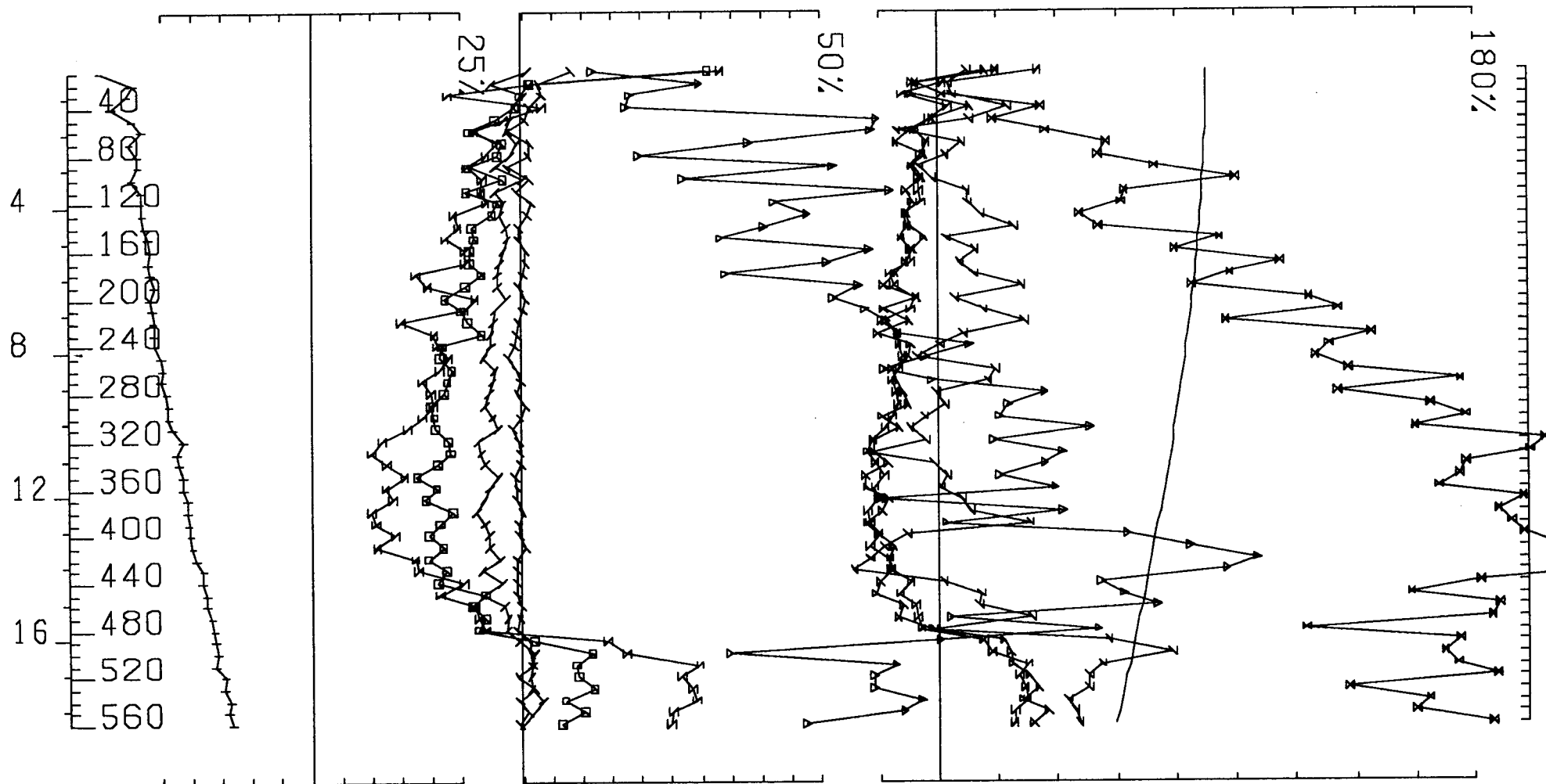
**FIG-5**



UTEM SURVEY AT MGM PROPERTY FOR TECK EXPLORATION LTD.

CONDUCTED BY SJ GEOPHYSICS LTD. JOB 9104 BASE FREQ (HZ) 30.96

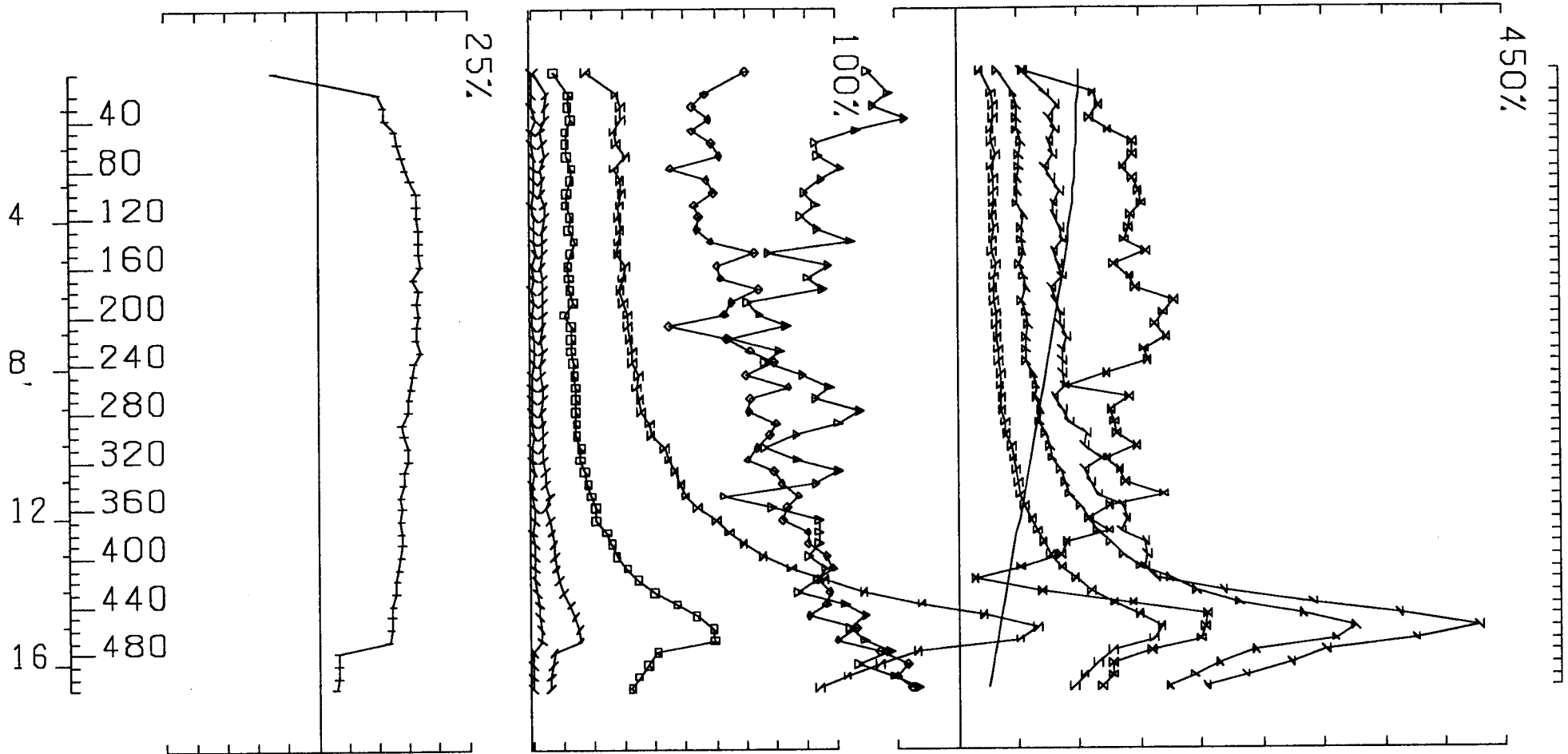
LOOP NO 1 HOLE TK-91-02 AXIAL COMPONENT SECONDARY FIELD CH1 CONTIN. NORM.



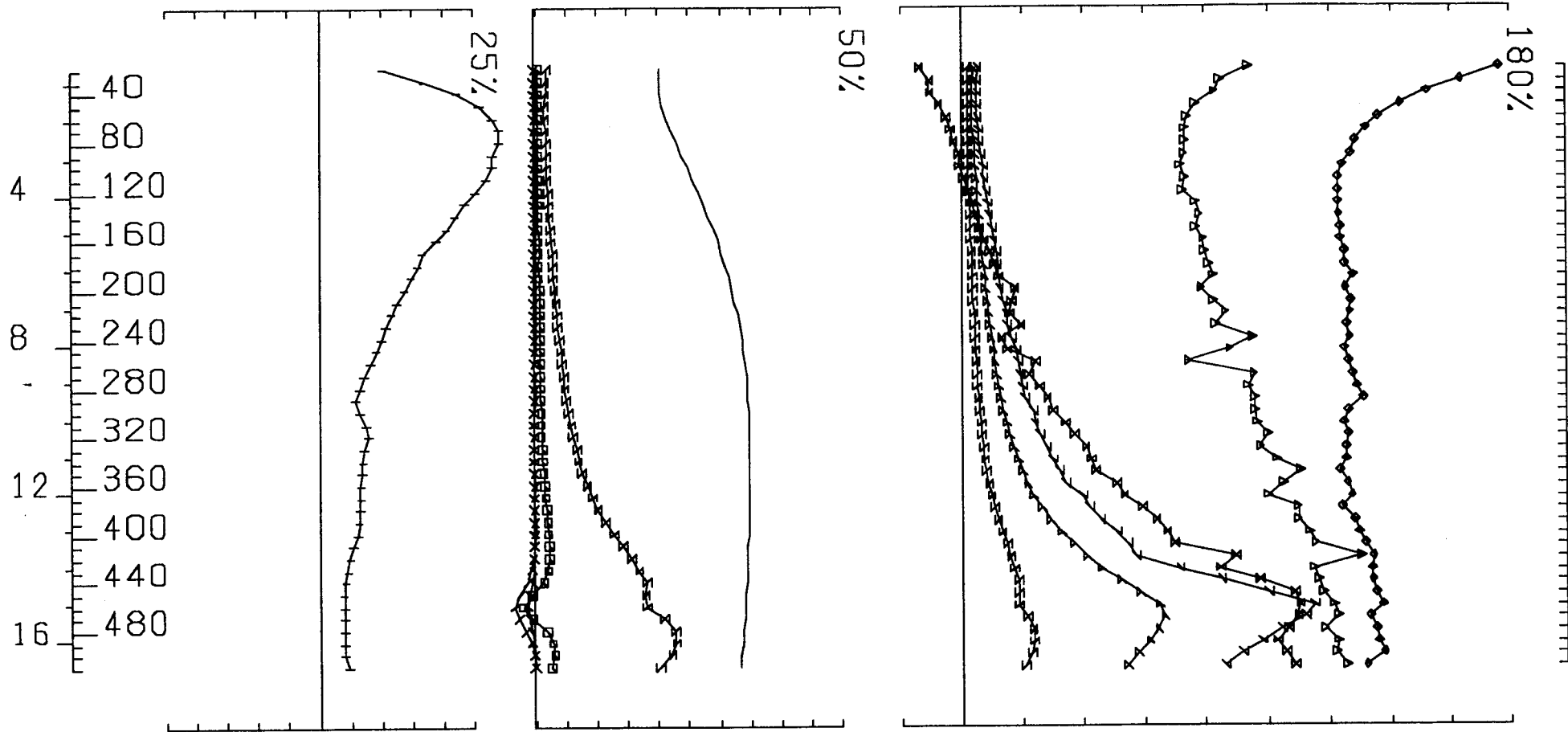
UTEM SURVEY AT MGM PROPERTY FOR TECK EXPLORATION LTD.

CONDUCTED BY SJ GEOPHYSICS LTD. JOB 9104 BASE FREQ (HZ) 30.96

LOOP NO 2 HOLE TK-91-02 AXIAL COMPONENT SECONDARY FIELD CH1 CONTIN. NORM.



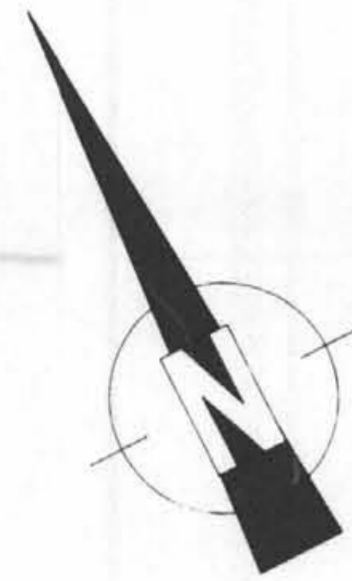
UTEM SURVEY AT MGM PROPERTY FOR TECK EXPLORATION LTD.  
 CONDUCTED BY SJ GEOPHYSICS LTD. JOB 9104 BASE FREQ (HZ) 30.96  
 LOOP NO 1 HOLE TK-91-04 AXIAL COMPONENT SECONDARY FIELD CH1 CONTIN. NORM.



UTEM SURVEY AT MGM PROPERTY FOR TECK EXPLORATION LTD.

CONDUCTED BY SJ GEOPHYSICS LTD. JOB 9104 BASE FREQ (HZ) 30.96

LOOP NO 2 HOLE TK-91-04 AXIAL COMPONENT SECONDARY FIELD CH1 CONTIN. NORM.



GEOLOGICAL BRANCH  
ASSESSMENT REPORT

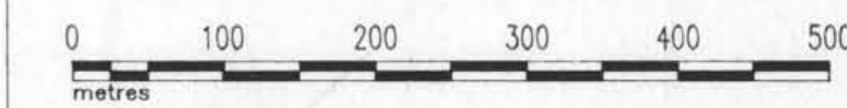
**22,149**

FIGURE 4

TECK EXPLORATION LTD.

MGM PROJECT

DRILL HOLE  
LOCATION MAP



DATE DRAWN: DEC. 18, 1991	SCALE: 1:5,000	DWG. NAME:
COMPILED BY: C.A.	JOB No: 1703	MGM-DDH
DRAWN BY: S.A.	NTS No: 83D/1	



3+00 W

2+00 W

1+00 W

Elev. 3410'

OVERBURDEN

BROKEN-RUBBLY MICA SCHIST

3b - MICACEOUS LIMESTONE

Lt. GREY LIMESTONE

MICACEOUS LIMESTONE

Lt. GREY LIMESTONE

Dk. GREY LIMESTONE  
Intercalated very fine grained Mudstone.

*Kinbasket  
Formation*

GREY LIMESTONE  
Qtz-Carb bands occur locally (originally chert?)

GARNETIFEROUS LIMESTONE

# GEOLOGICAL BRANCH ASSESSMENT REPORT

# 22,149

*Tsar Creek  
Formation*

>0.1,0.01,0.01  
Ba 3380 ppm

114201

GARNET SCHIST

SPOTTED SCHIST

Very Fine Grained GREY CHERT  
with interlayered Garnet Schist

8.6,0.76,2.24

114202

QUARTZ SERICITE SCHIST

1.1,0.09,0.52

114203

0.4,0.04,0.08

114204

Fine Grained SILICEOUS PYRITE UNIT (Chert?)

MINERALIZED DOLOMITE

0.1,0.03,0.28

114205

GARNET SCHIST (Argilliceous)

2.4,0.17,0.31

114206

CHERT LAYER (Formerly recognized as Quartzite)

0.1,0.03,0.05

114207

5.2,0.39,1.12

114208

GARNET-STAUROLITE SCHIST (Siliceous)

2.5,0.19,0.98

114209

2.6,0.13,0.71

114210

STAUROLITE GARNET SCHIST

65.6,4.22,9.36

114211

CHERT LAYERS with interbedded Garnet Schist

4.6,0.2,0.73

114212

GARNET STAUROLITE SCHIST

0.5,0.04,0.07

114213

<.1,0.01,0.01

114214

114215

End of Hole

VALUES ARE: g/t Ag, %Pb, %Zn

 TECK EXPLORATION LTD.

MGM PROJECT

HOLE TK-91-1

ELEVATION: 3410' AZIMUTH: 035° SCALE: 1:1000

FIGURE 5

6+00 W

5+00 W

4+00 W

Elev. 3120'

OVERBURDEN

MICACEOUS QUARTZOFELDSPATHIC SCHIST

GARNETIFEROUS BLACK BANDED ARGILLITE

ALTERNATING QUARTZOFELDSPATHIC SCHIST  
and GARNETIFEROUS SCHIST

CHERT

MUDDY CHERT

GARNET-STAUROLITE SCHIST

QUARTZOFELDSPATHIC SCHIST

GARNET-STAUROLITE SCHIST

CHERT with Interlayered pelitic schist

GARNET BEARING MICACEOUS ARGILLITE

INTERLAYERED CHERT/MICA SCHIST

Fault

LIMESTONE

*Kinbasket Formation*

BANDED GRAPHITE LIMESTONE

GARNET-MICA SCHIST

MICA SCHIST

INTERLAYERED LIMESTONE/MICA SCHIST

GARNET SCHIST

*Tsar Creek Formation*

QUARTZ-SERICITE SCHIST

MARBLE with MINOR Py

SILICEOUS GARNET SCHIST

INTERLAYERED CHERTY to SILICEOUS MICA SCHIST to QUARTZ-SERICITE SCHIST

GARNET SCHIST

End of Hole

**GEOLOGICAL BRANCH  
ASSESSMENT REPORT**

**22,149**

**TECK EXPLORATION LTD.**

MGM PROJECT

HOLE M-91-2

ELEVATION: 3120'

SCALE: 1:1000

**FIGURE 6**

7+00 W

6+00 W

5+00 W

OVERBURDEN

Banded Graphite Limestone

Grey to Micaceous Limestone

Garnet-Mica Schist

Limestone

Mica Limestone & Mica Schist interlayered and interbedded

*Kinbasket Formation*

Mica Schist

graphite limestone

spotted schist

interlayered garnet bearing mica schist and quartz-sericite schist

21.1,2.16,1.32  
3.3,0.41,1.54  
34.6,3.06,4.44

114225  
114227  
114228  
114229  
114230

Quartz-Sericite Schist

*Tsar Creek Formation*

114233 10.7,0.51,2.26  
114234 7.0,0.36,1.60  
114235  
114236 6.2,0.38,3.52  
114237 0.7,0.03,0.26

Folded Sequence

garnet-staurolite schist

grey chert

Lower Tsar Creek  
Garnet-Staurolite Schist

LEGEND



QUARTZ-SERICITE/MICA SCHIST



QUARTZ-SERICITE SCHIST



DOLOMITE



SILICEOUS PELITIC SCHIST



ARGILLACEOUS GARNET SCHIST

114236 6.2,0.38,3.52  
Sample Ag Pb Zn  
Number g/t % %

FIGURE 7

TECK EXPLORATION LTD.

MGM PROJECT

DDH TK-91-3

AZIMUTH 35

ELEVATION 3110'

DATE DRAWN: NOV. 22, 1991  
COMPILED BY: G.T./C.A.  
DRAWN BY: S.A.

SCALE: 1:1000  
JOB No: 1703  
NTS No: 830/1

DWG. NAME:  
MGM-91-3

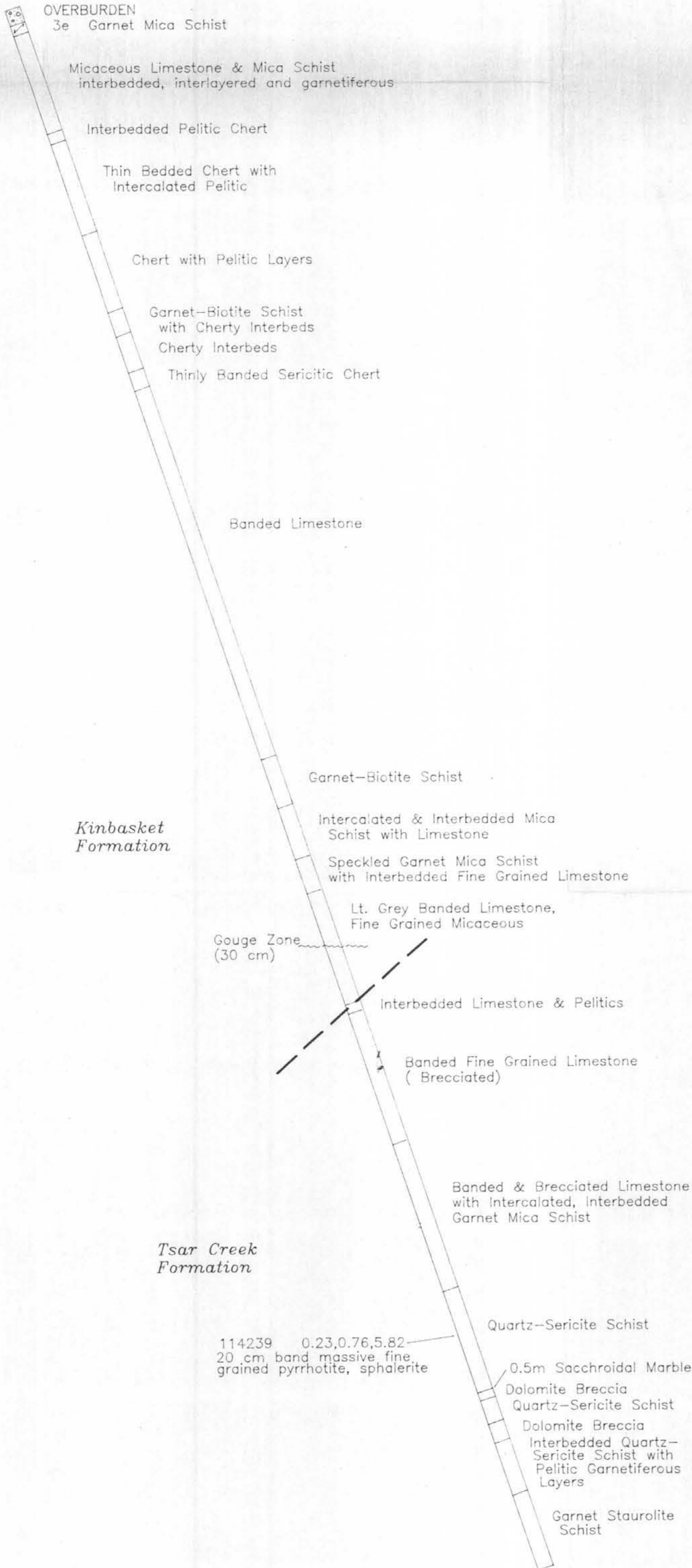
GEOLOGICAL BRANCH  
ASSESSMENT REPORT

22,149

7+00 W

6+00 W

5+00 W



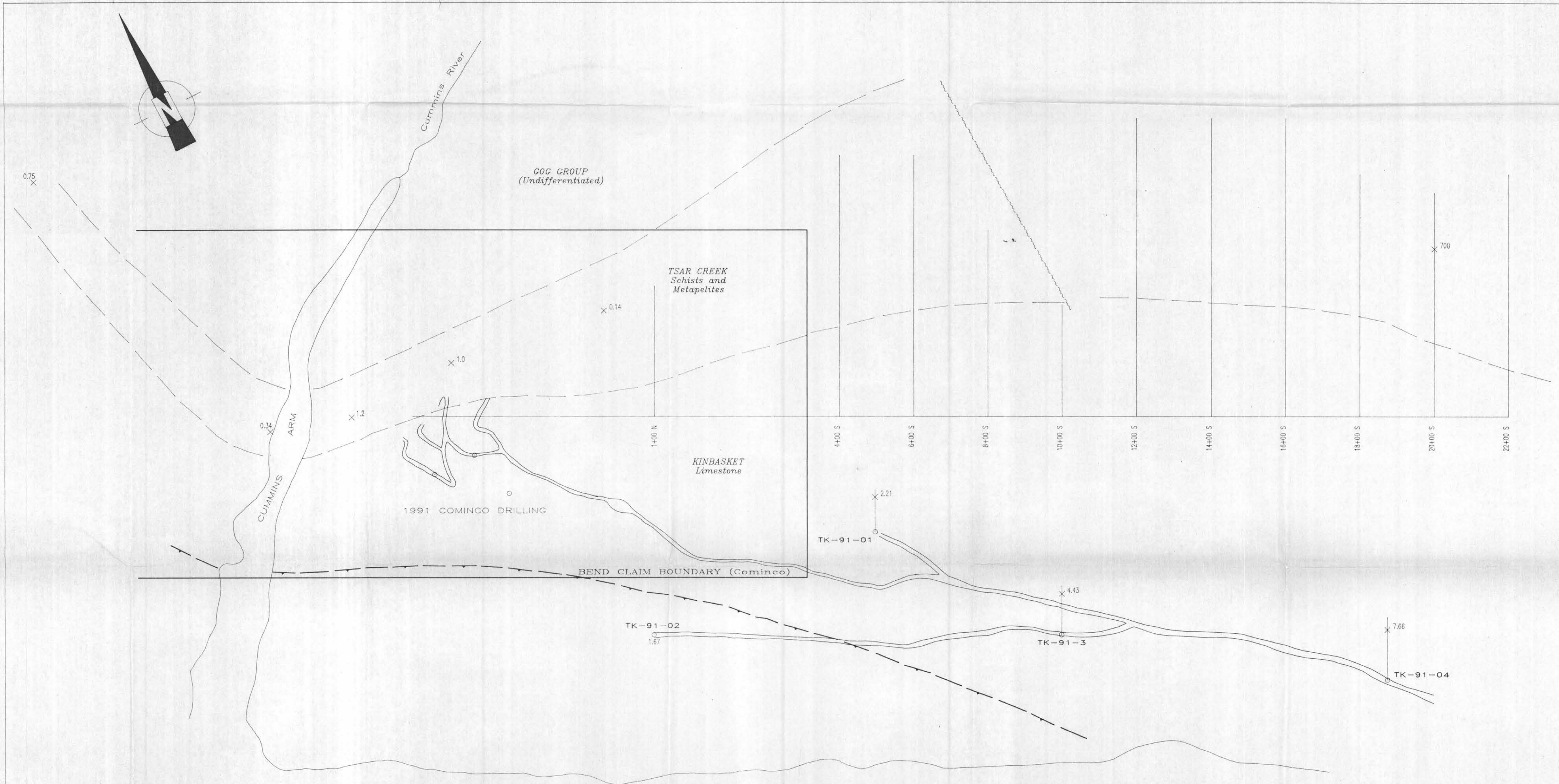
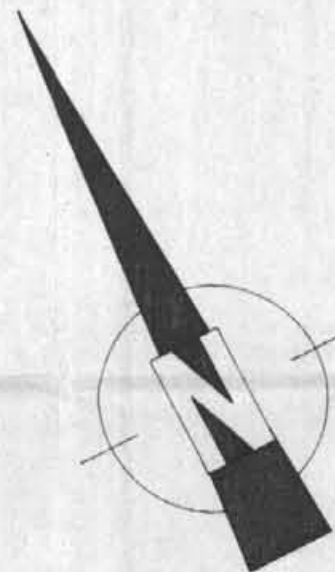
**GEOLOGICAL BRANCH ASSESSMENT REPORT**

**22,149**

114239	0.23, 0.76, 5.82
Sample Number	Ag Pb Zn g/t % %

**FIGURE 8**

MGM PROJECT		
<b>DDH TK-91-4</b>		
AZIMUTH 35°		ELEVATION 2990'
DATE DRAWN: NOV. 25, 1991	SCALE: 1:1000	DWG. NAME:
COMPILED BY: G.T./C.A.	JOB No: 1703	MGM-91-4
DRAWN BY: S.A.	NTS No: 83D/1	



C O L U M B I A R E A C H

GEOLOGICAL BRANCH  
ASSESSMENT REPORT

**22,149** FIGURE 9

TECK EXPLORATION LTD.

MGM PROJECT

Zn/Pb RATIOS



DATE DRAWN: DEC 17, 1991	SCALE: 1:5,000	DWG. NAME:
COMPILED BY: C.A.	JOB No: 1703	MGM-ZNPB
DRAWN BY: S.A.	NTS No: 830/1	

